

THE CITY COLLEGE
CITY UNIVERSITY OF NEW YORK
NEW YORK, N. Y. 10031

Technical Report

SPHERICAL HARMONIC ANALYSIS OF A SYNOPTIC
CLIMATOLOGY GENERATED WITH A GLOBAL
GENERAL CIRCULATION MODEL

Zaphiris D. Christidis

February 1980

(NASA-CR-162804) SPHERICAL HARMONIC
ANALYSIS OF A SYNOPTIC CLIMATOLOGY GENERATED
WITH A GLOBAL GENERAL CIRCULATION MODEL
(City Coll. of the City Univ. of New York.)
50 p HC A03/MF A01

N80-18607

Unclas

CSCL 04A G3/46

47327

NASA, Goddard Space Flight Center

Grant NGR 33-016-086

J. Spar, Principal Investigator



THE CITY COLLEGE
OF
THE CITY UNIVERSITY OF NEW YORK
NEW YORK, N. Y. 10031

DEPARTMENT OF EARTH AND PLANETARY SCIENCES

(212) 690- 6984

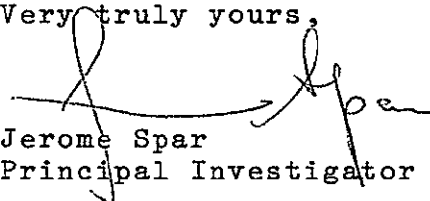
March 12, 1980

NASA Scientific and Technical Information Facility
P. O. Box 8757
Baltimore/Washington International Airport
Maryland 21240

Gentlemen:

Enclosed please find two (2) copies of a technical report by Z. D. Christidis ("Spherical Harmonic Analysis of a Synoptic Climatology Generated with a Global Circulation Model") which was prepared under Grant NGR 33-016-086 from the NASA Goddard Space Flight Center.

Very truly yours,



Jerome Spar
Principal Investigator

JS/ms
Encl.

Contents

	<u>Page</u>
Abstract	1
Introduction	2
Spherical Harmonic Functions	4
Examples and Tests of the Method	9
The Model Experiment	12
Results	14
Summary and conclusions	39
Acknowledgements	41
Appendix A.	42
Appendix B.	44
References	47

Abstract

Spherical harmonic analysis was used to analyze the observed climatological (C) fields of temperature at 850 mb, geopotential height at 500 mb, and sea level pressure. The spherical harmonic method was also applied to the corresponding "model climatological" fields (M) generated by a general circulation model, the "GISS climate model." The climate model was initialized with observed data for the first of December 1976 at 00. GMT and allowed to generate five years of meteorological history. Monthly means of the above fields for the five years were computed and subjected to spherical harmonic analysis.

It was found from the comparison of the spectral components of both sets, M and C, that the climate model generated reasonable 500 mb geopotential heights.

The model temperature field at 850 mb exhibited a generally correct structure. However, the meridional temperature gradient was overestimated and overheating of the continents was observed in summer.

The structure of the sea level pressure field was not correctly reproduced by the model. The four basic pressure systems of the Northern Hemisphere were found to be slightly misplaced, with incorrect intensities, and the mass distribution between the hemispheres was poorly simulated.

Introduction

During the past 20 years a number of global atmospheric general circulation models have been developed with the objective of simulating the large scale dynamics and physics of the atmosphere. In some cases the models were initialized with observed data and allowed to run, generating a forecast meteorological history. Runs for long time periods (years) may be used to compute model-generated climatologies.

In these experiments tests have been carried out to investigate how well the model simulates the real atmosphere. These tests may consist of diagnostics, such as energetics, transports, momenta, and vertical-meridional cross sections of various zonal mean atmospheric quantities. Forecast statistics and quantitative scalar measures of pattern agreement, such as correlation coefficients, root mean square errors, and gradient "skill-scores," provide additional information for verification, but they do not give detailed information on the quality of a model's simulations of nature. Another verification of model results can be done by comparing various horizontal model-generated synoptic patterns with the corresponding observed ones through the subjective inspection of maps.

Further information can be provided by comparing the spectral components of the above mentioned synoptic fields. These spectral components can be represented by the expansion coefficients of a series of certain orthogonal functions. In this study these functions will be the "surface spherical harmonics."

Spherical harmonic analysis as a quantitative and objective method of analyzing horizontal fields has been applied in the past to many geophysical problems (e.g. Spar, 1950; Chapman and Bartels, 1960; Leith, 1974; Blackmon, 1976; North, 1979). However, spherical harmonic analysis has not been widely adopted as a method for synoptic pattern verification.

Spherical harmonics will be used to analyze various horizontal fields generated by a general circulation model (GCM), the GISS "climate model" (Hansen et al., 1979), and to compare the model results with nature by analyzing the corresponding observed climatological horizontal fields in spherical harmonics. The comparison will be carried out in terms of the relative magnitudes of the spectral components for the model and for nature.

The model-generated horizontal fields are computed by initializing the model with global NMC¹ data, derived from operational analyses, for the first day of a month (at 00. GMT), and, for monthly simulation experiments, running the model until the end of a particular month, then computing the monthly means of various predicted horizontal fields. For climatology experiments the model is run continuously for a number of years, and the monthly mean fields of the predicted quantities are computed for all those years.

By expanding the above horizontal fields in finite series of spherical harmonics, the result will be a set of expansion coefficients or a set of magnitudes and phases of the spectral components for selected wave numbers, which may be shown in the form of vector diagrams (harmonic dials).

¹National Meteorological Center.

Spherical Harmonic Functions

The spherical harmonics are a complete orthonormal set of functions which are solutions of the Laplace equation in spherical coordinates, and satisfy the relationship

$$\int_{\mathcal{S}} Y_{n,m}^{\ell}(\phi, \lambda) \cdot Y_{n',m'}^{\ell'}(\phi, \lambda) \cdot d\Omega = \delta_{nn'} \cdot \delta_{mm'} \cdot \delta_{\ell\ell'} \quad (1)$$

where

$$\delta_{kk'} = \begin{cases} 1 & \text{if } k=k' \\ 0 & \text{if } k \neq k' \end{cases}$$

Ω is the solid angle which looks at the spherical surface, \mathcal{S} , where the spherical harmonic functions (SHF's) are defined ($d\Omega = \cos\phi d\phi \cdot d\lambda$ where ϕ is the latitude $[-\frac{\pi}{2}, \frac{\pi}{2}]$ and λ is the longitude $[0, 2\pi]$), m is the zonal (longitudinal) wave number of the n, m th harmonic, and $n - m$ is the number of nodal parallels, or twice the meridional wave number. Both n and m are integers with $0 \leq m \leq n$, while superscripts ℓ, ℓ' in (1) indicate the evenness or oddness of the spherical harmonic function under the substitution $\lambda \rightarrow -\lambda$.

The normalized SHF's (see Blackmon, 1976) can be written as follows:

$$\begin{cases} Y_{n,m}^{(\ominus)} \\ Y_{n,m}^{(\odot)} \end{cases} = \left[\frac{2n+1}{2\pi} \cdot \frac{(n-m)!}{(n+m)!} \right]^{\frac{1}{2}} \cdot \begin{cases} \cos m\lambda \\ \sin m\lambda \end{cases} \cdot P_{n,m}(\sin\phi) \quad , \quad n \geq m \geq 0$$

$$Y_{n,0} = \left[\frac{2n+1}{4\pi} \right]^{\frac{1}{2}} \cdot P_n(\sin\phi) \quad m = 0 \quad (2)$$

where $P_n(\sin\phi)$ are the Legendre polynomials (zonal harmonics), and

$P_{n,m}(\sin\phi)$ are the Legendre associated functions (tesseral harmonics). The superscripts (e) and (o) indicate the evenness and oddness of the SHF's, the eigenvalues n,m being the same as in (1). The normalization of the SHF's is done in such a way that the mean square value of the $Y_{n,m}$ over the surface of a sphere is $1/4\pi$ (see Appendix A).

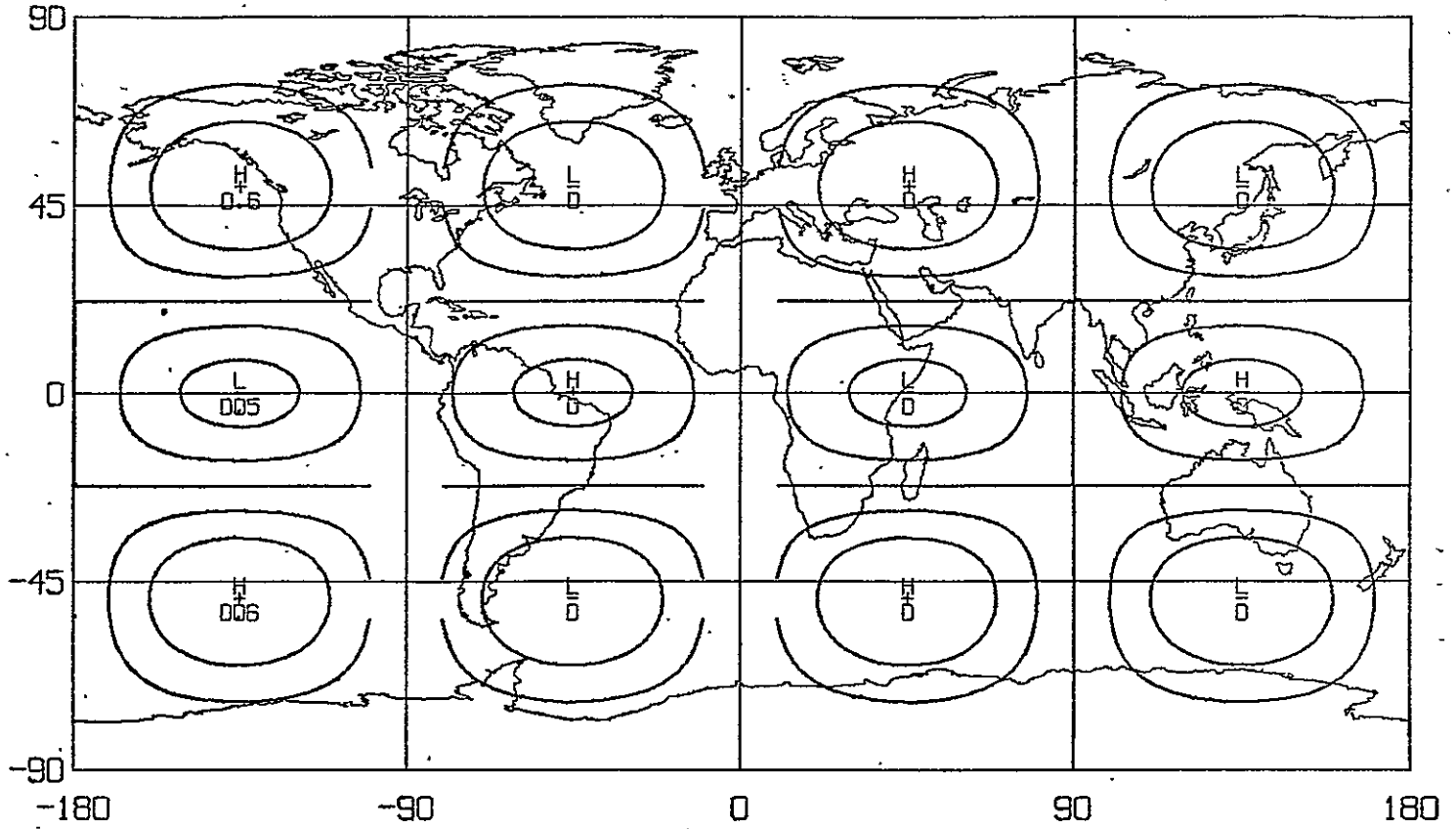
As an example, the distribution of $Y_{4,2}^{(e)}$ and $Y_{4,2}^{(o)}$ over the earth is shown in Figure 1. As we see, $Y_{4,2}$ is a meridional wave with two nodal parallels symmetric about the Equator ($n - m = 2$) and two complete waves in the zonal direction ($m = 2$). The distributions of $Y_{n,0}$ with latitude for $n \leq 6$ are shown in Figure 2. The $Y_{n,0}$ are zonally symmetric functions of latitude with n nodal parallels, and they are variable polynomials of degree n . Generally, if $n - m$ is an even number, the $Y_{n,m}$ is always symmetric about the Equator since the functions $P_{n,m}$ for $n - m$ even (odd) are even (odd) functions of latitude. (For more information, see Hobson (1955). Also, the practical advantages and limitations of Legendre polynomials and functions for latitudinal expansions as compared with Fourier modified series and Chebyshev polynomials, in general atmospheric problems on a sphere, are discussed by Boyd (1978).) Any horizontal field, Q , which is distributed on a sphere can be expanded as a function of latitude ϕ and longitude λ into finite series of SHF's as follows:

$$\hat{Q}(\phi, \lambda) = \sum_{n=0}^N \sum_{m=0}^n (C_{n,m} \cdot Y_{n,m}^{(e)} + S_{n,m} \cdot Y_{n,m}^{(o)}) \quad (3)$$

where $Y_{n,m}^{(e)}$, $Y_{n,m}^{(o)}$ are defined by (2), N is the truncation degree of the series, and $C_{n,m}$, $S_{n,m}$ are the normalized expansion coefficients of the series (3). These coefficients can be calculated from the data, Q , by using the orthonormality property (1) of the SHF's. (See Appendix B.)

Figure 1.

ODD HARMONIC FUNCTION Y N,M N=4 , M=2



ORIGINAL PAGE IS
OF POOR QUALITY

EVEN HARMONIC FUNCTION Y N,M N=4 , M=2

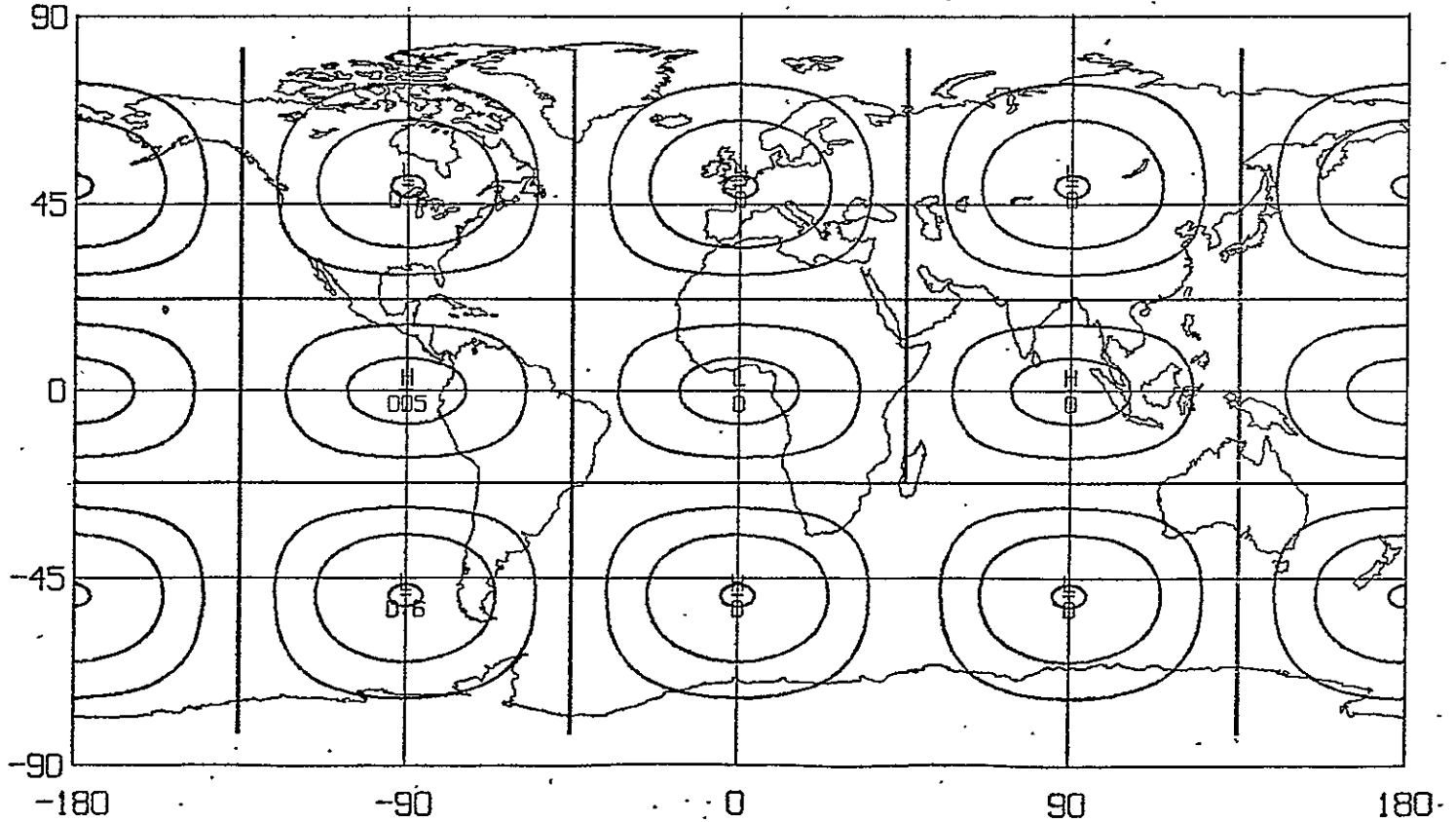
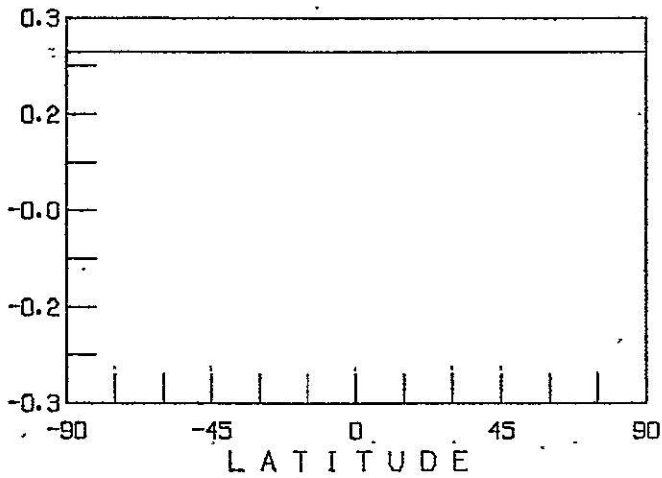


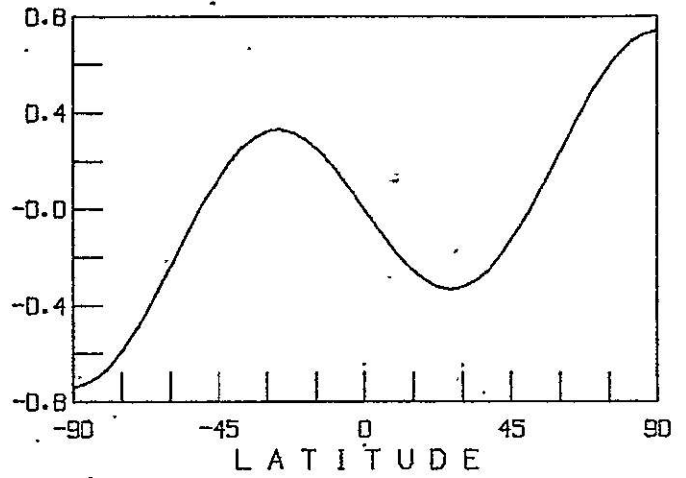
Figure 2.

ZONAL HARMONICS $Y_{n,0}$

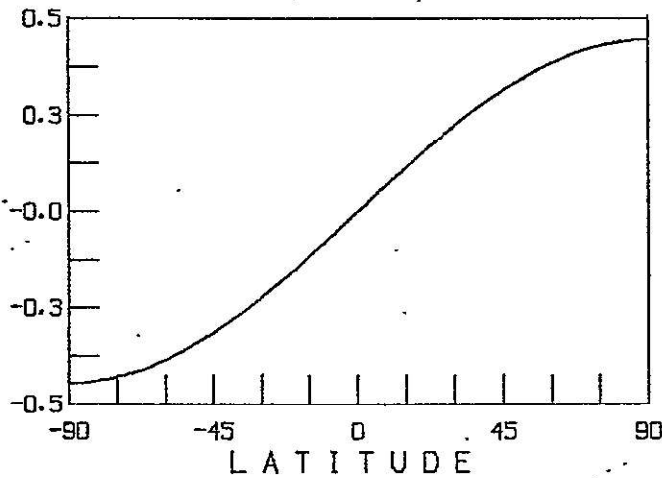
ZONAL HARMONIC $Y_{0,0}$ VS LATITUDE



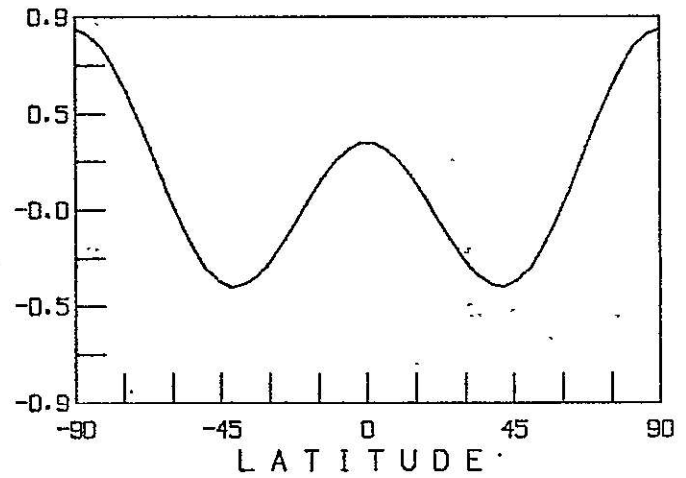
ZONAL HARMONIC $Y_{3,0}$ VS LATITUDE



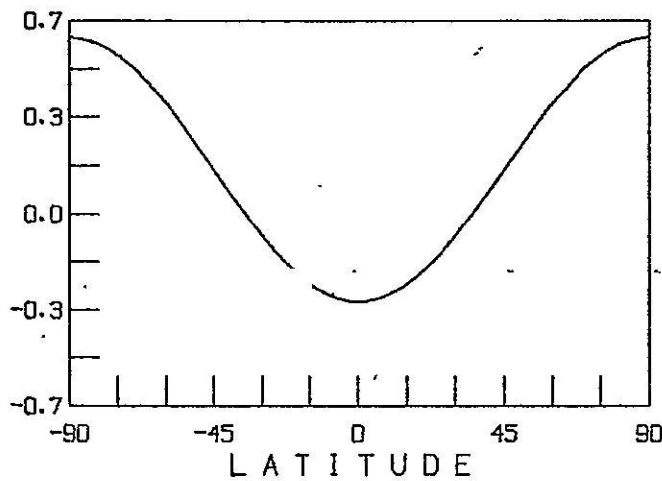
ZONAL HARMONIC $Y_{1,0}$ VS LATITUDE



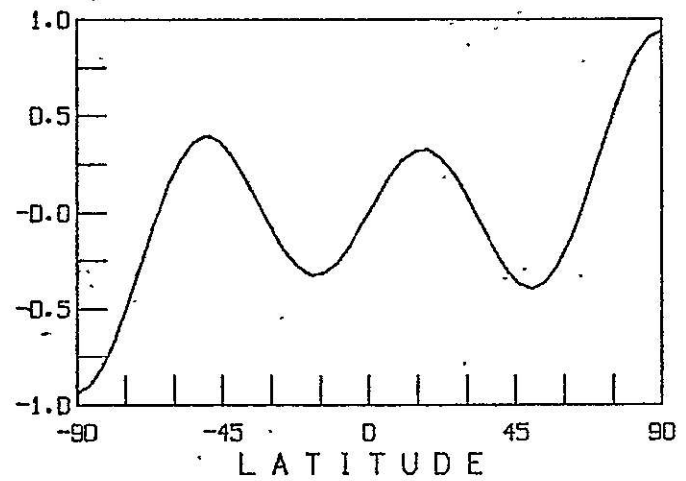
ZONAL HARMONIC $Y_{4,0}$ VS LATITUDE



ZONAL HARMONIC $Y_{2,0}$ VS LATITUDE



ZONAL HARMONIC $Y_{5,0}$ VS LATITUDE



Thus,

$$\begin{Bmatrix} C_{n,m} \\ S_{n,m} \end{Bmatrix} = \int_{-\pi/2}^{\pi/2} \int_0^{2\pi} Q(\phi, \lambda) \cdot \begin{Bmatrix} Y_{n,m}^{(\ominus)} \\ Y_{n,m}^{(\odot)} \end{Bmatrix} \cdot \cos\phi \cdot d\phi d\lambda \quad (4)$$

The normalization makes it possible to compare coefficients of different order m and degree n in the same series or among different series.

As we see from (4), the truncation of the series at $N = k$ does not affect the calculations of the coefficients $C_{n,m}$, $S_{n,m}$ for $m \leq n = k$ because in the above integrals the independent variables are not the n, m but ϕ, λ .

We can calculate the amplitude $A_{n,m}$ and the phase angle $\beta_{n,m}$ of any harmonic from

$$\begin{aligned} A_{n,m} &= \left[C_{n,m}^2 + S_{n,m}^2 \right]^{1/2} \\ \beta_{n,m} &= \tan^{-1} \left[S_{n,m} / C_{n,m} \right] \end{aligned} \quad (5)$$

The above relations are as indicated in the harmonic dial in Figure 3.

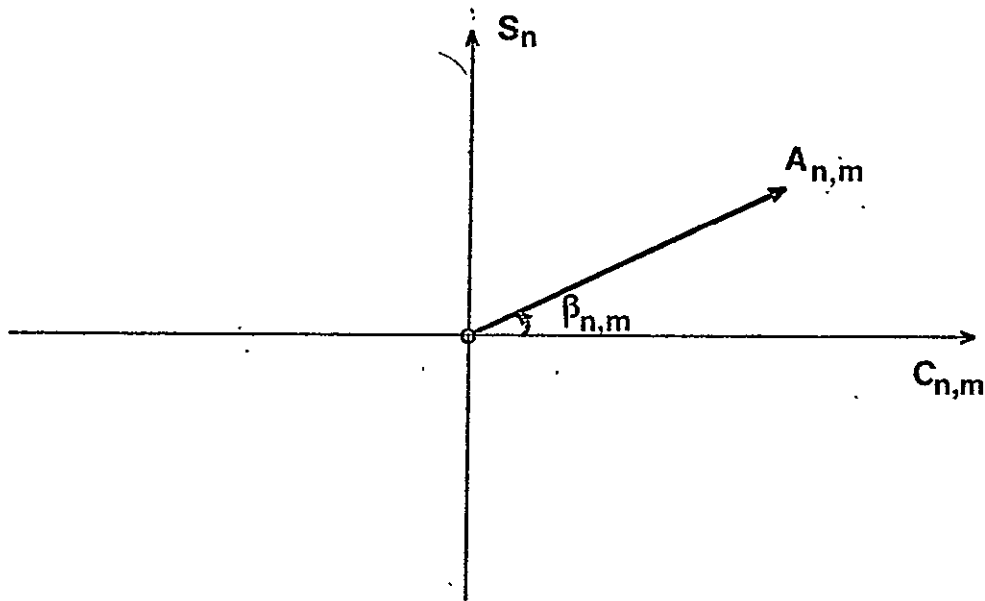


Fig. 3.

For calculating the expansion coefficients $C_{n,m}$, $S_{n,m}$, a closed-form numerical integration scheme is required to approximate the integrals (4). Since the data, Q , are given on grid points (discrete function of ϕ, λ), this makes necessary the discretization of the $Y_{n,m}$ at the same grid points, which leads to the evaluation of the Legendre and Fourier sine-cosine functions on the above grids.

Generally tables of normalized associated Legendre polynomials are available (e.g. Belousov, 1962) but they do not correspond to the GISS grid spacing ($8^\circ \times 10^\circ$ latitude-longitude grid). So, following the instructions of Belousov (1962) and Hobson (1955), the Legendre polynomials and associated functions were computed by means of Rodrigues' formula (6),

$$P_{n,m}(\sin\phi) = (\cos\phi)^m \cdot \frac{d^m P_n(\sin\phi)}{d(\sin\phi)^m} = (\cos\phi)^m \cdot \sum_k (b_k(n,m) \cdot (\sin\phi)^k) \quad (6)$$

up to $n = m = 18$, for the appropriate latitudes ϕ , and stored on disk for use as required. The calculations were done by extended precision (28 significant figures) on an IBM 360/95 computer.

An attempt to recreate Belousov's tables by using the algorithm (6), for the same latitudes up to $n = m = 18$, showed perfect agreement. (Alternative numerical methods for computing Legendre functions and polynomials are discussed by Merilees (1973).)

Various numerical integration schemes for the calculation of the integrals (4) were tested by checking the orthonormality property (1) of the SHF's. This was done by substituting $Q(\phi, \lambda)$ in (4) for one of the $Y_{n,m}^{(e)}$, $Y_{n,m}^{(o)}$.

Finally, the method that has been adopted was a combination of the Simpson and "three-eighths" rule (Krulov, 1962) for the ϕ integration and Filont's rule (Davis and Rabinowitz, 1967) for the λ -integrals. The integration was carried out in two steps:

$$\text{a) } \phi\text{-integration} \quad F_{n,m}(\lambda) = R_{n,m} \cdot \int_{-\pi/2}^{\pi/2} Q(\phi, \lambda) \cdot P_{n,m}(\sin\phi) \cdot \cos\phi d\phi \quad (7)$$

$$\text{b) } \lambda\text{-integration} \quad \begin{Bmatrix} C_{n,m} \\ S_{n,m} \end{Bmatrix} = T_m \int_0^{2\pi} F_{n,m}(\lambda) \cdot \begin{Bmatrix} \cos m\lambda \\ \sin m\lambda \end{Bmatrix} d\lambda \quad (8)$$

$$\text{where } R_{n,m} = \left[\frac{2n+1}{2} \cdot \frac{(n-m)!}{(n+m)!} \right]^{\frac{1}{2}}, \quad T_m = \left[\frac{1}{\delta_m \pi} \right]^{\frac{1}{2}}, \quad \delta_m = \begin{cases} 1 & \text{if } m \neq 0 \\ 2 & \text{if } m = 0 \end{cases}$$

With the above method, equation (1) was satisfied up to the sixth decimal place.

Examples and Tests of the Method

The area-weighted mean value, \tilde{Q} , of any synoptic field, Q , is

$$\tilde{Q} = \frac{1}{4\pi} \int_S Q(\phi, \lambda) \cdot d\Omega .$$

From (2) we have $Y_{0,0} = (4\pi)^{-\frac{1}{2}}$; so

$$\tilde{Q} = Y_{0,0} \int_S Q(\phi, \lambda) \cdot d\Omega \rightarrow$$

$$\tilde{Q} = Y_{0,0} \int_S Q(\phi, \lambda) \cdot Y_{0,0} d\Omega = Y_{0,0} \cdot C_{0,0} . \text{ Therefore}$$

$$\tilde{Q} = \sqrt{\frac{1}{4\pi}} \cdot C_{0,0} \tag{9}$$

A coefficient $C_{n,0}$ represents the amplitude of a zonally symmetric function of latitude only. For example, $Y_{1,0} = (4/3 \cdot \pi)^{-\frac{1}{2}} \cdot \sin \phi$, $Y_{2,0} = (3 \cdot 2 \cdot \pi)^{-\frac{1}{2}} \cdot (3 \cdot \sin^2 \phi - 1)$. Then we may say that the amplitude of the mean meridional difference between values of Q at the North and South Poles is approximately represented by $C_{1,0}$. Also, $C_{2,0}$ is a rough measurement of the mean meridional Pole-to-Equator Q -field difference.

By using the already described numerical methods, the observed climatological fields of temperature at 850 mb (T850), 500 mb geopotential height (G500), and sea level pressure (SLP)² were analyzed in spherical harmonics. Each field is represented by a set of 361 nontrivial expansion coefficients. From the series (3) the fields Q were reproduced for different truncations N , up to $N = 18$.

²The observed climatological fields were obtained from NCAR, the National Center for Atmospheric Research, in Boulder, Colorado.

Figures 4, 5, and 6 indicate three climatological fields for the month of December which were subjected to harmonic analysis.

An area-weighted root-mean-square (rms) error test (10) was carried out between the initial fields, Q , and the reproduced ones, Q_N , as follows:

$$\epsilon_N = \left[\frac{1}{4\pi} \int_S \{Q - Q_N\}^2 \cdot d\Omega \right]^{\frac{1}{2}} \quad (10)$$

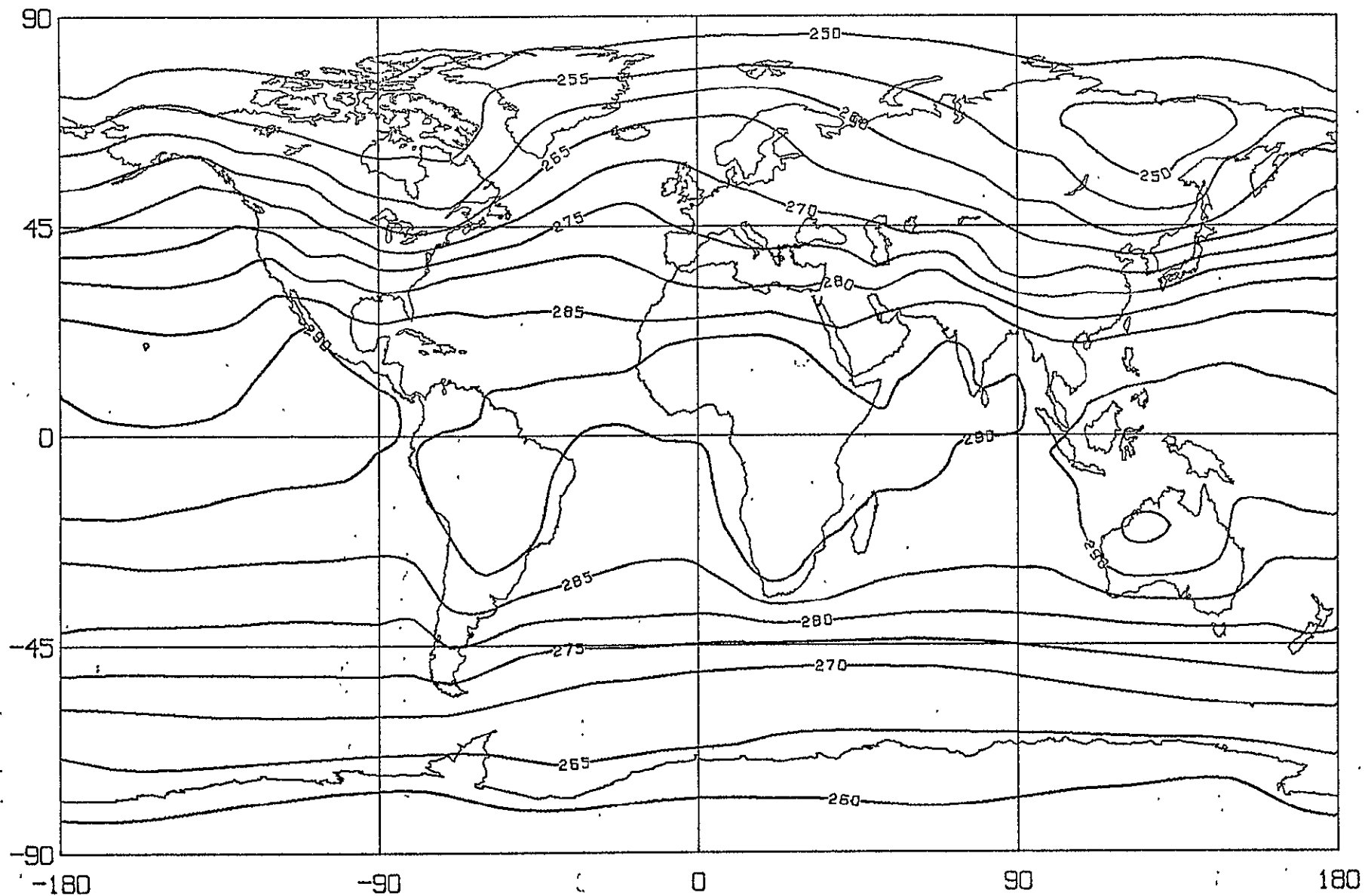
In Figure 7 a, b, c are plotted the rms errors of the reproduced December climatology for T850 in degrees C^o, G500 in meters, and SLP in millibars, as a function of the truncation N .³ As we see in Figure 7 a, b, there is a big reduction of the rms for $1 < N \leq 2$ due to the symmetrical zonal structure of T850 and particularly G500. By truncating the series at $N = 2$, the hemispheric and the zonal structure ($Y_{2,0}$, $Y_{2,0}$) of those fields has been captured. Therefore, the $Y_{2,0}$ harmonic accounts for a large percentage of the total variance of T850 and G500. The small scale features of the three fields can be captured with truncations $N \geq 8$. We observe that for these truncations (Figure 7) the rms error does not diminish at the same rate as for $N \geq 7$. This leads to the conclusion that only a small portion of the variance in these fields can be explained by using harmonics up to $n = m = 18$.

The existence of a non-zero rms error for $N = 18$ is characteristic of the integration "noise." The noise can be reduced by reproducing the fields, Q , from only the leading harmonics. This was done by ranking the coefficients in descending order and reproducing the field using

³The number of harmonics which is used each time for the reproduction of Q_N is $(N + 1)^2$.

Figure 4.

DECEMBER CLIMATOLOGY TEMPERATURE AT 850 MB



ORIGINAL PAGE IS
OF POOR QUALITY

Figure 5. DECEMBER CLIMATOLOGY GEOPOTENTIAL HEIGHT 500 MB

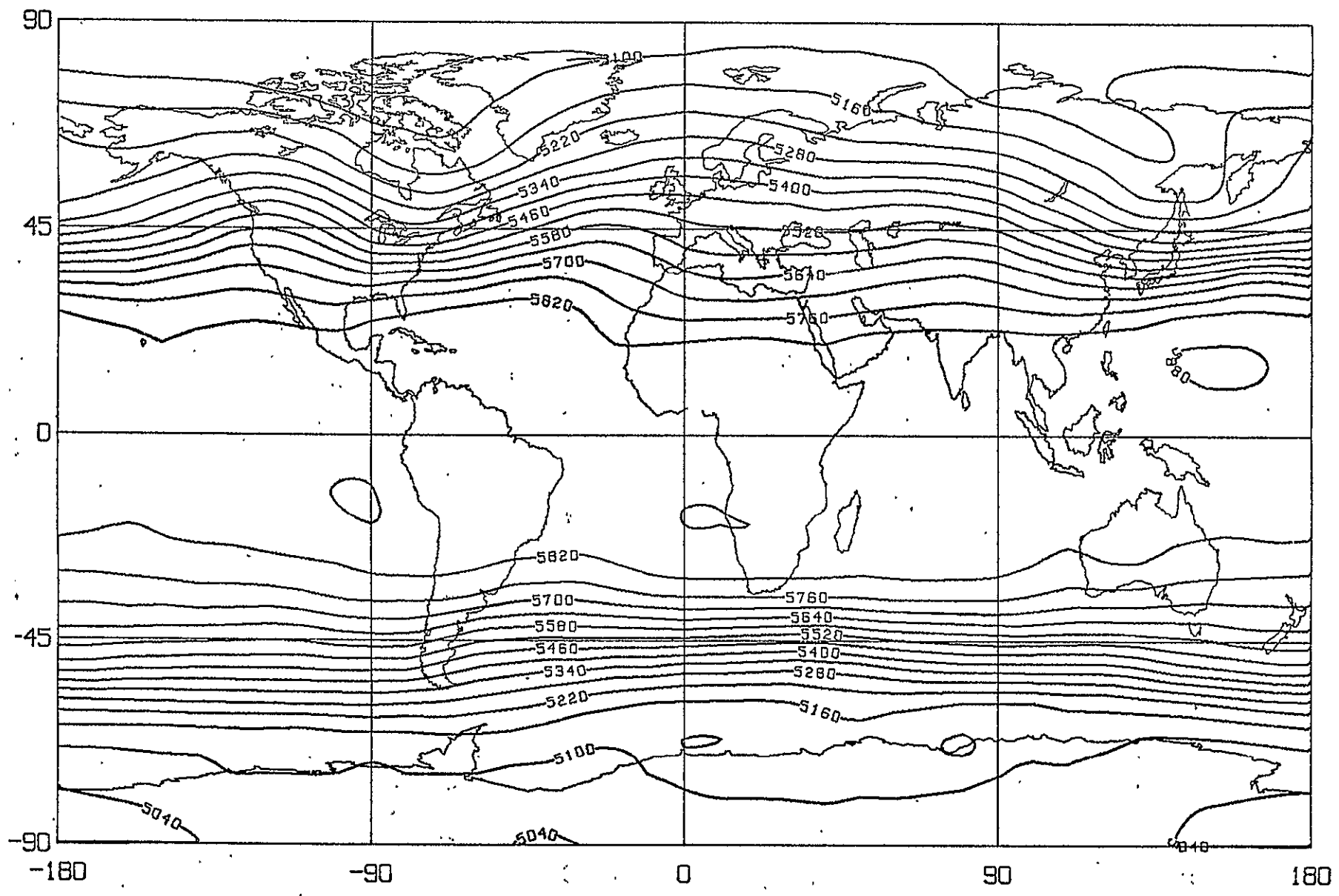


Figure 6.

DECEMBER CLIMATOLOGY SEA LEVEL PRESSURE

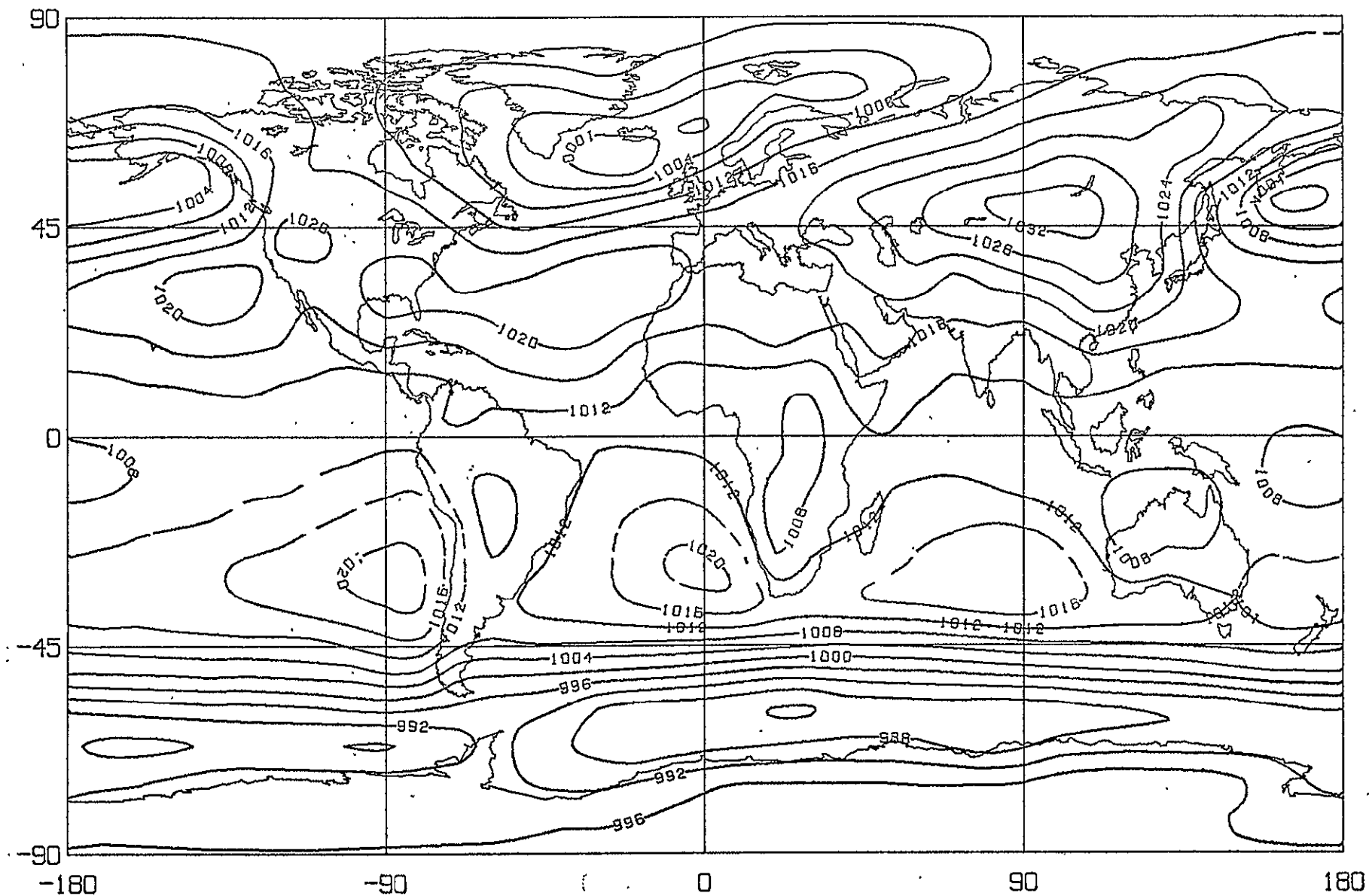
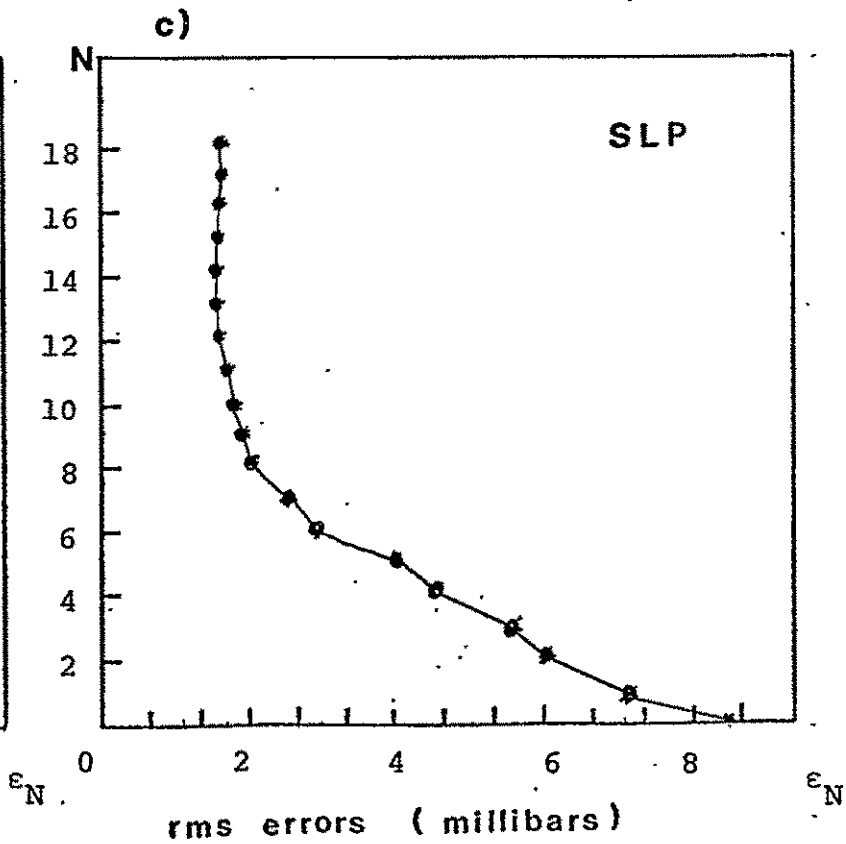
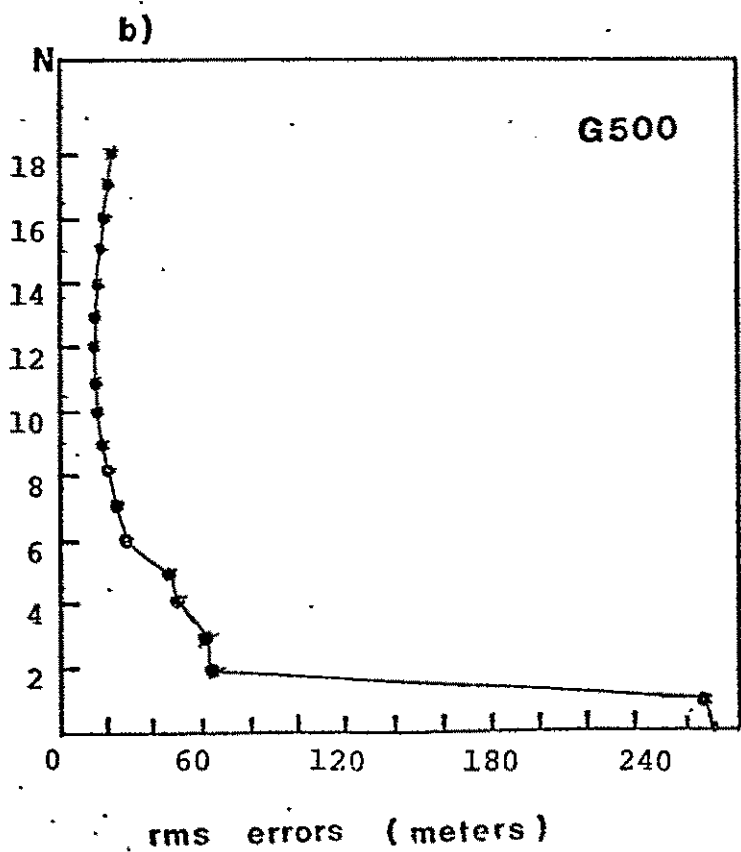
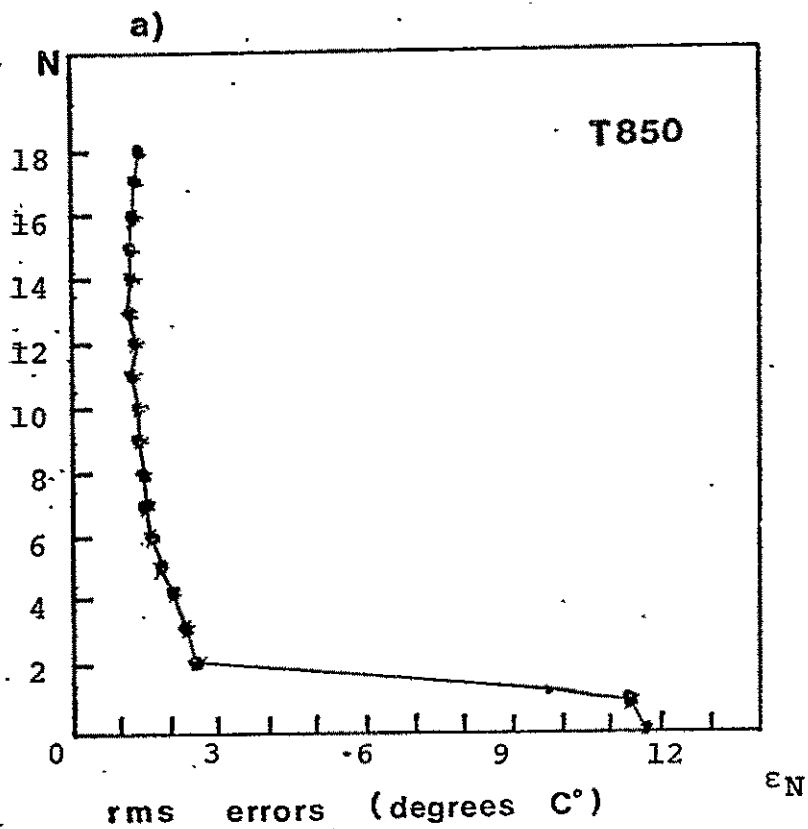


Figure 7 . rms errors (ϵ_N) versus truncation (N) for the fields T850, G500 and SLP.



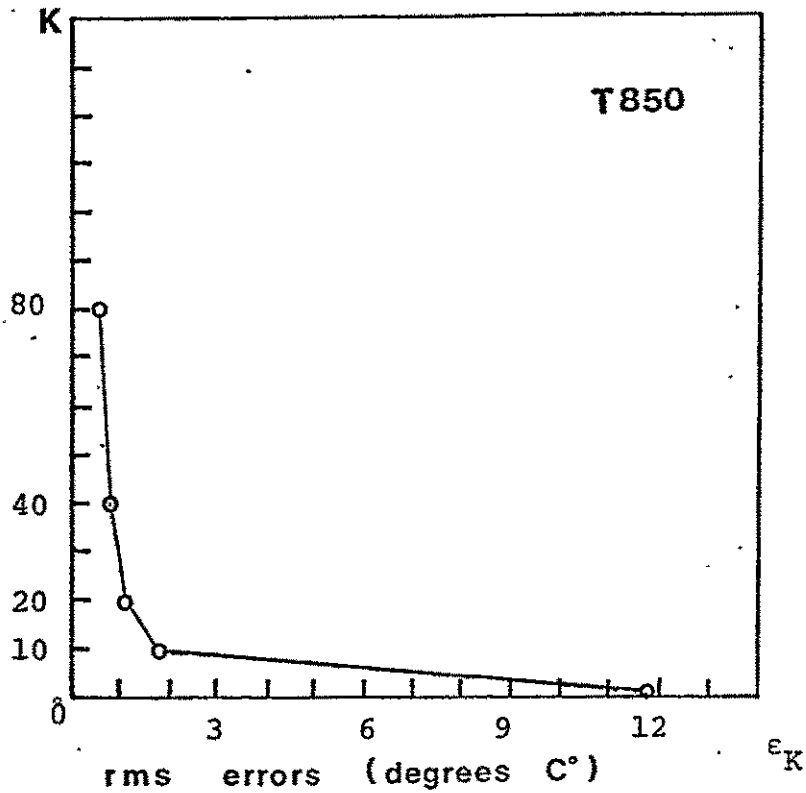
only the first 10, 20, 40, 80 dominant harmonics. As before, an rms error test was carried out and the results are illustrated in Figure 8 a, b, c.

For the above reasons it will be instructive in the course of this study to represent the fields by a small set of coefficients, corresponding to their leading harmonics.

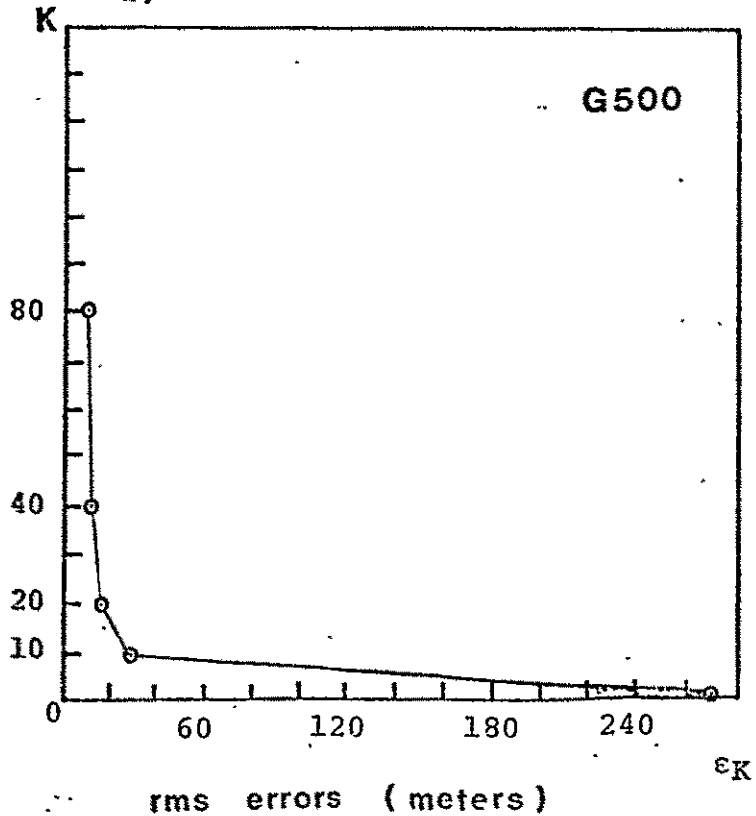
Figures 9 a; b, c, d - 11 a, b, c, d show how the fields are simulated when reproduced from 10, 20, or 40 leading harmonics, and all the harmonics. Note that by adding more harmonics, small wave length disturbances become apparent in the synoptic maps.

Figure 8 . rms errors (ϵ_K) versus number of the leading harmonics (K) for the fields T850, G500 and SLP

a)



b)



c)

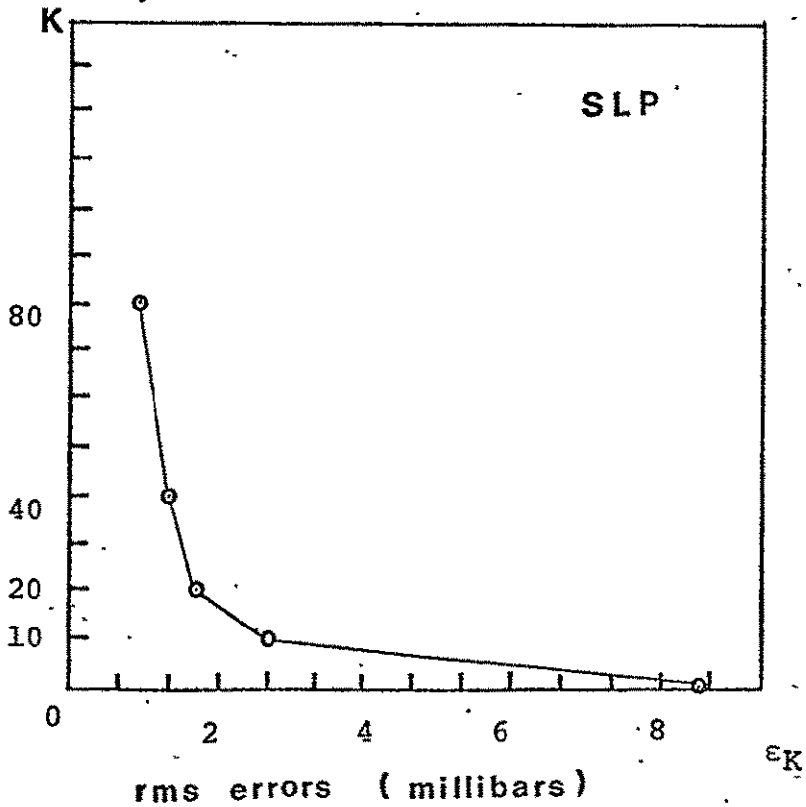
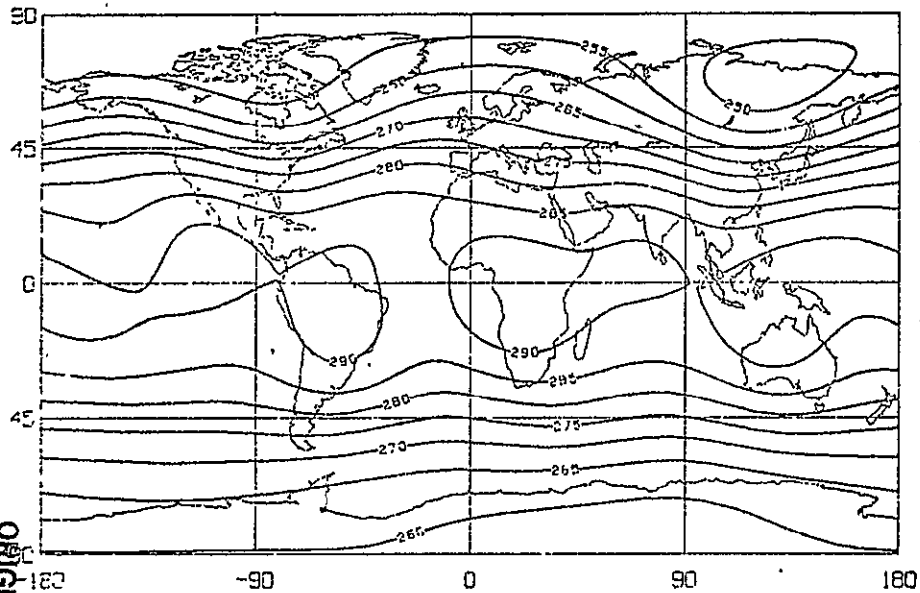
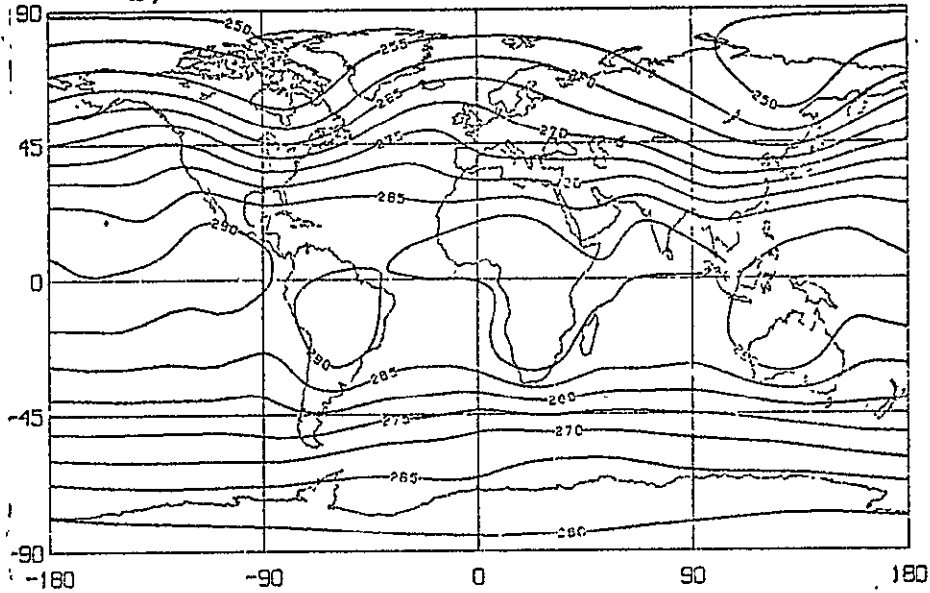


Figure 9

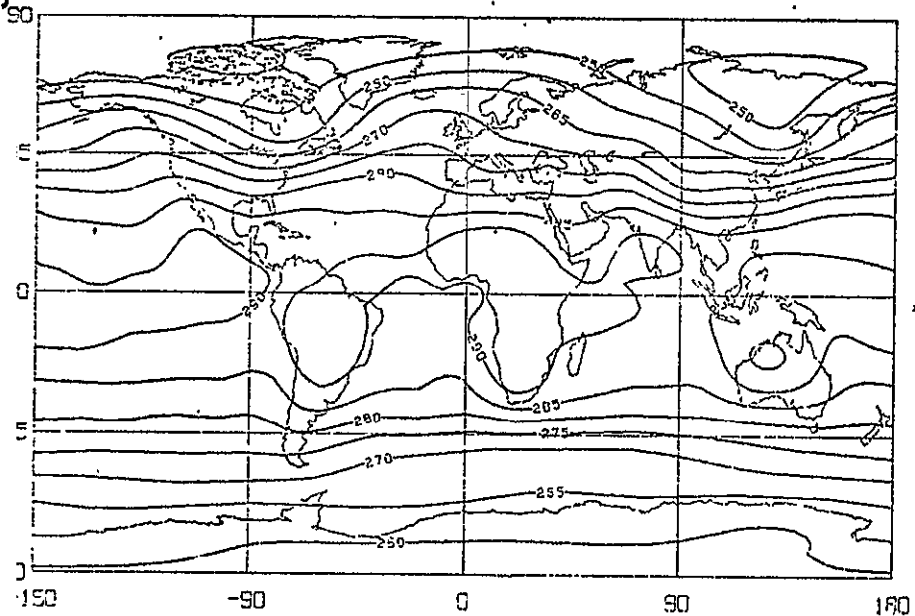
a) DECEMBER CLIMATOLOGY TEMPERATURE AT 650 MBS REPRODUC



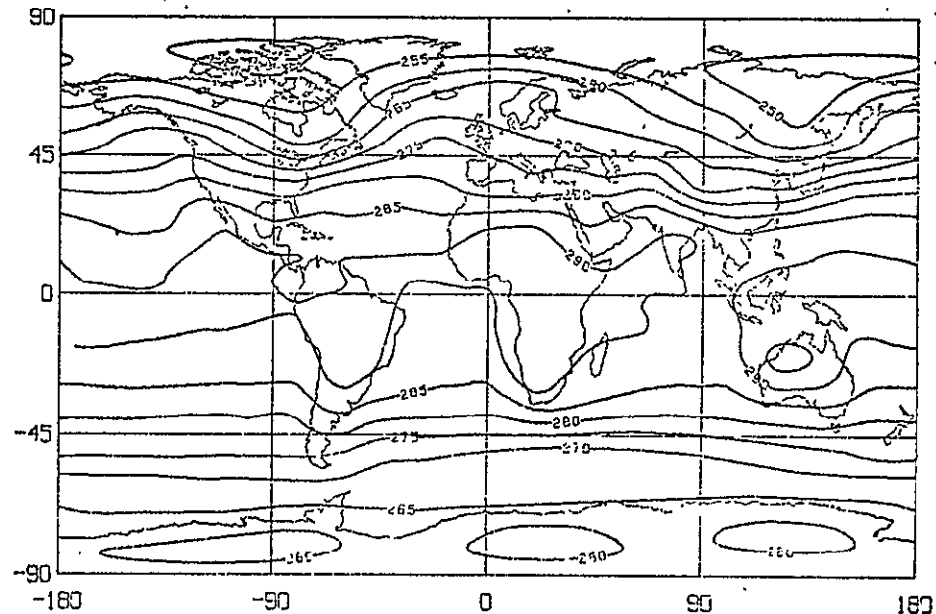
b) DECEMBER CLIMATOLOGY TEMPERATURE AT 650 MBS REPRODUC



c) DECEMBER CLIMATOLOGY TEMPERATURE AT 650 MBS REPRODUC



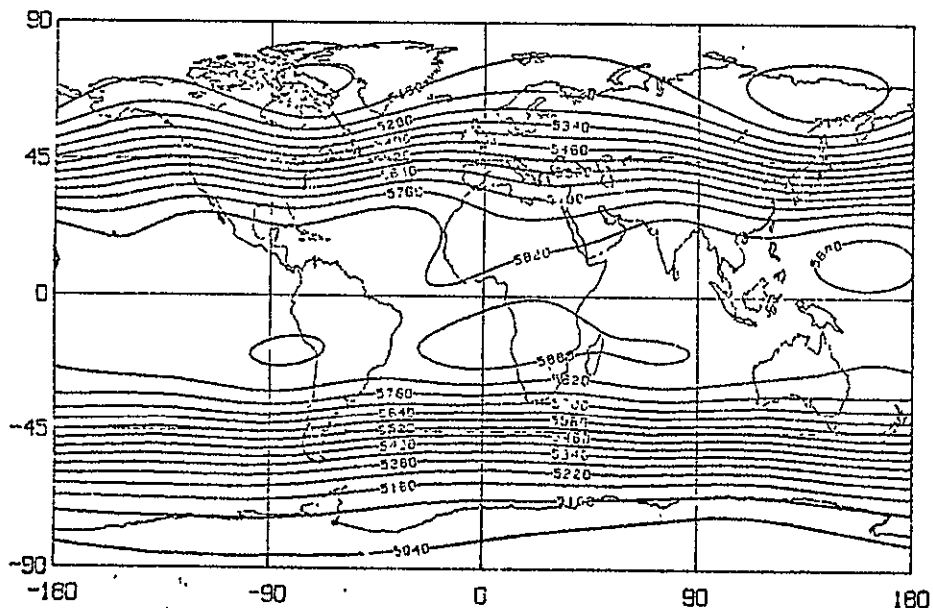
d) DECEMBER CLIMATOLOGY TEMPERATURE AT 650 MBS REPRODUC



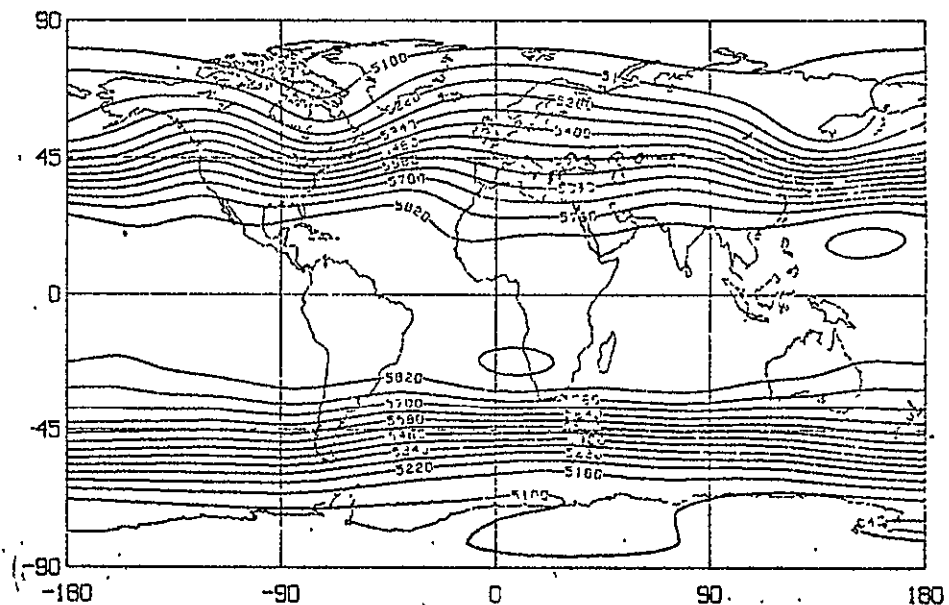
ORIGINAL PAGE IS
OF POOR QUALITY

Figure 10.

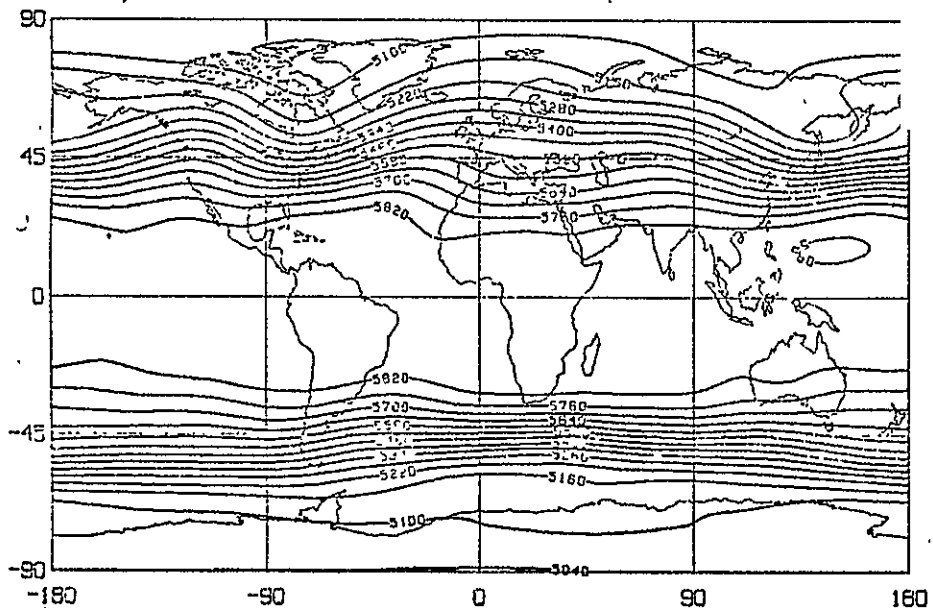
a) DECEMBER CLIMATOLOGY GEOPOTENTIAL HEIGHT 500 MBS REPRODUC



b) DECEMBER CLIMATOLOGY GEOPOTENTIAL HEIGHT 500 MBS REPRODUC



c) DECEMBER CLIMATOLOGY GEOPOTENTIAL HEIGHT 500 MBS REPRODUC



d) DECEMBER CLIMATOLOGY GEOPOTENTIAL HEIGHT 500 MBS REPRODUC

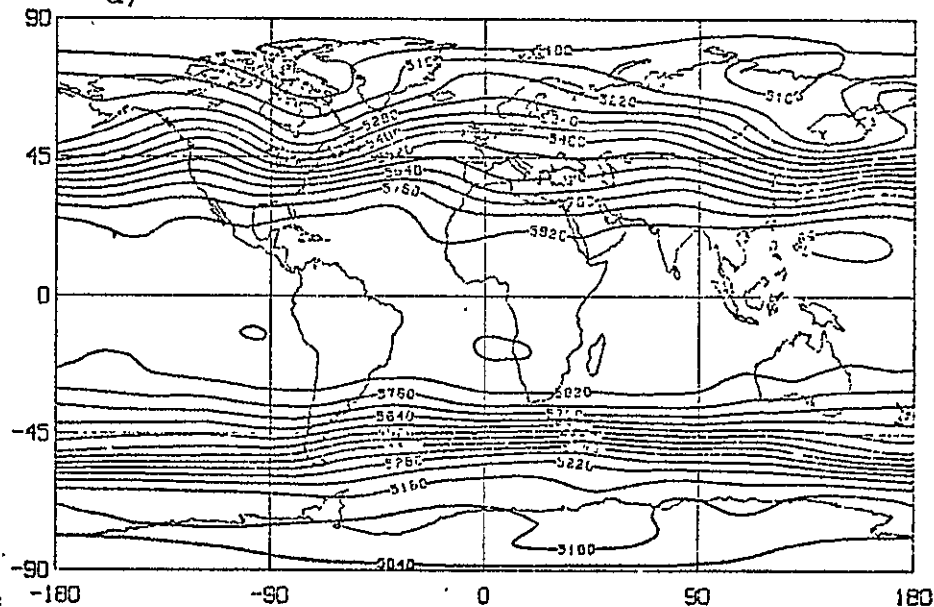
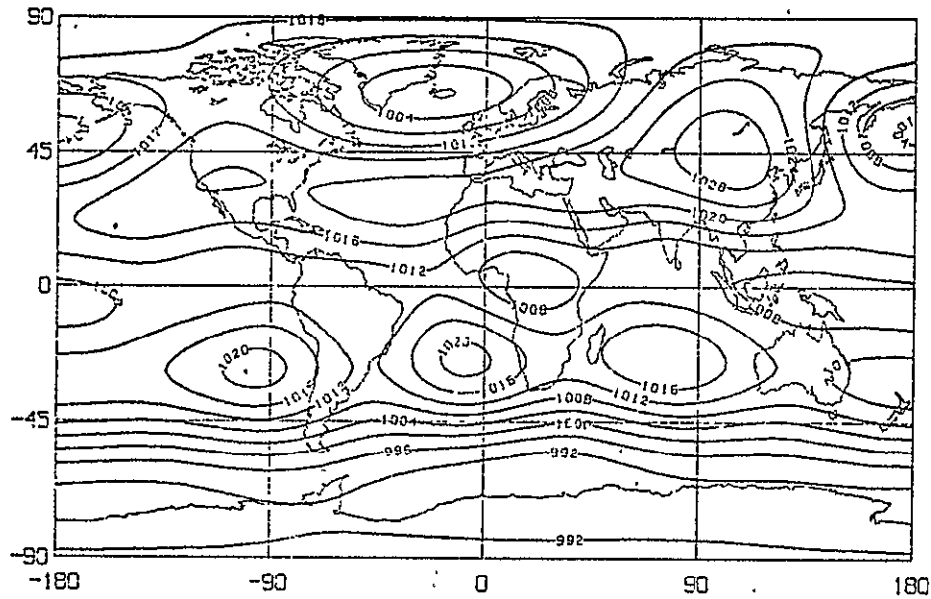
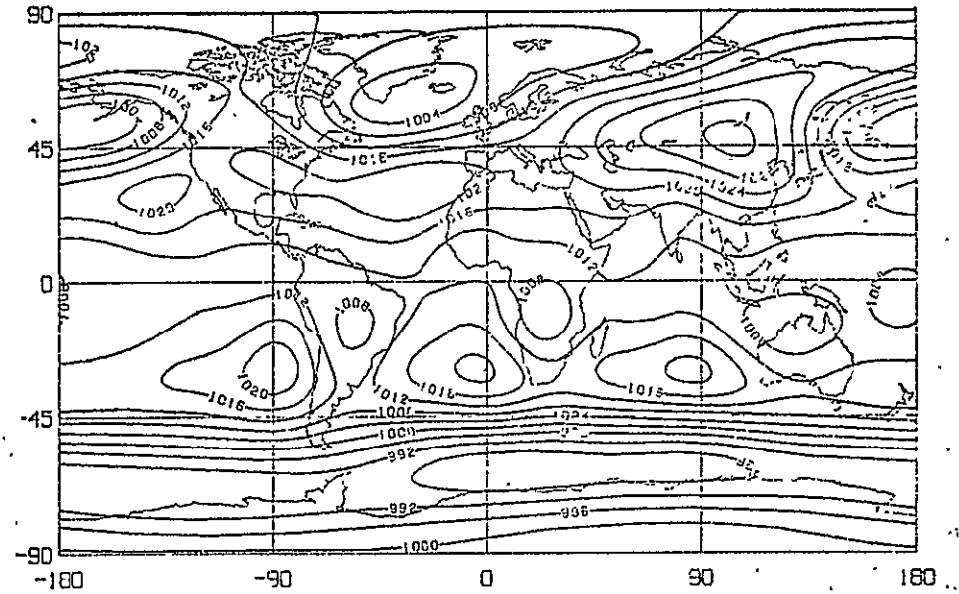


Figure 11.

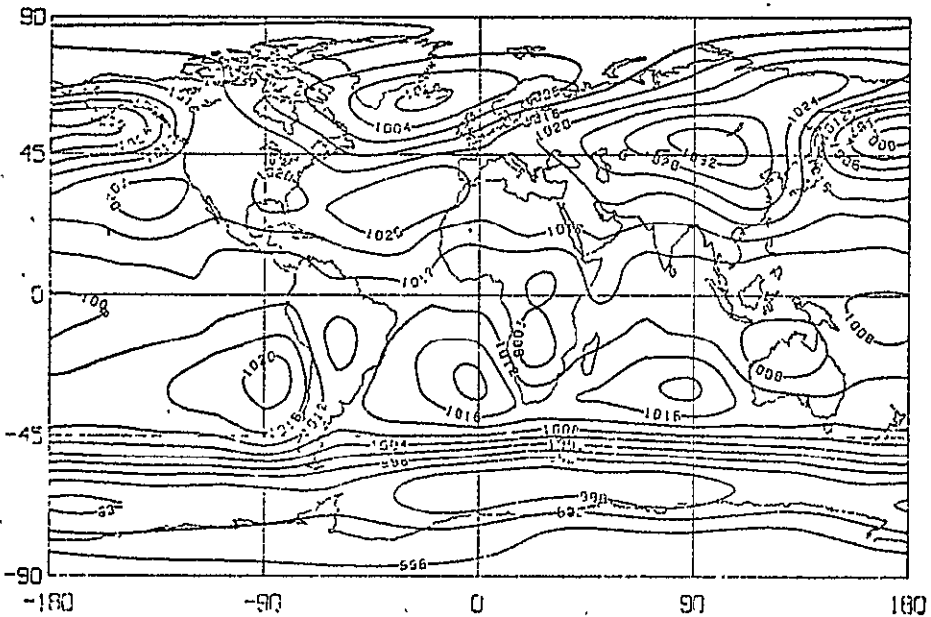
a) DECEMBER CLIMATOLOGY SEA LEVEL PRESSURE REPRODUCED



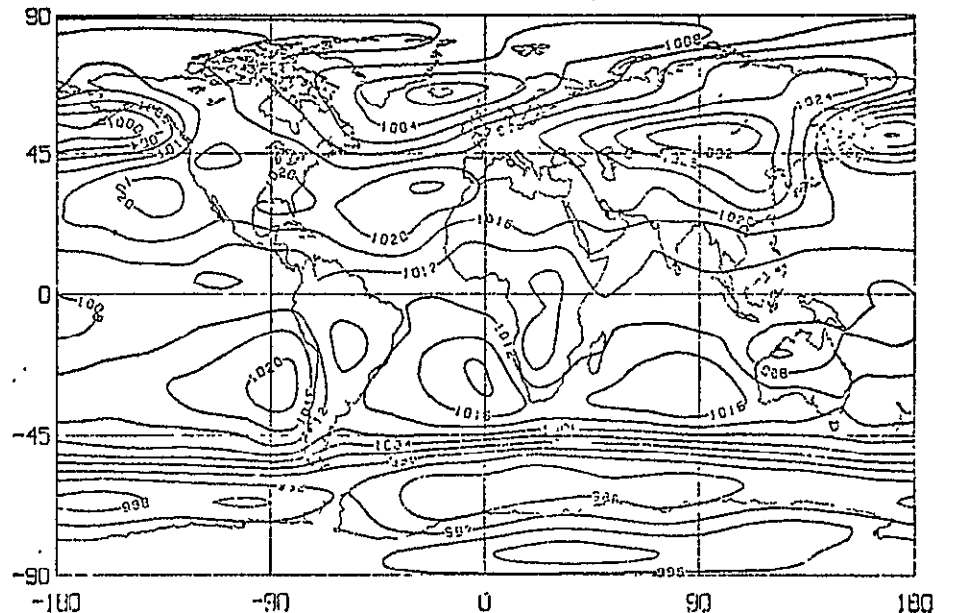
b) DECEMBER CLIMATOLOGY SEA LEVEL PRESSURE REPRODUCED



c) DECEMBER CLIMATOLOGY SEA LEVEL PRESSURE REPRODUCED



d) DECEMBER CLIMATOLOGY SEA LEVEL PRESSURE REPRODUCED



The Model Experiment

A global general circulation model has been developed for climate circulation studies by a group under J. Hansen at the Goddard Institute for Space Studies (GISS) in New York. This model can be operated with a horizontal grid of 8° of latitude, ϕ , by 10° of longitude, λ , and seven sigma (σ) layers in the vertical. With this resolution one simulated month takes about two hours on an IBM 360/95 computer. (See Hansen et al., 1979 for further details of the climate model and Somerville et al., 1974 for a description of the first GISS model from which it was developed.)

In order to generate a climatology history, the GISS climate model was initialized with observed global data derived from operational NMC analyses and interpolated to the GISS grid. The initial conditions were for the first day of December 1976 at 00. GMT. Then the model was allowed to run for five simulated years until the end of January 1982 and the monthly outputs were averaged to obtain a five-year model climatology.

The model-generated (M) global fields of sea level pressure (SLP), geopotential height at 500 mb (G500) and 850 mb temperature were selected for verification. The monthly means of these fields for all five years were analyzed in series of spherical harmonics.

Global observed climatological data (C) of the same horizontal fields provided by NCAR and interpolated to the GISS grid were also subjected to spherical harmonic analysis. Each field was represented this way by 361 expansion coefficients for the "global" harmonic analysis.

In addition, by assuming that the data, M and C, are even functions of latitude about the Equator (reflecting the Northern Hemisphere data into the Southern Hemisphere), we can eliminate possibly incorrect data

due to the lack of observations in the Southern Hemisphere, and apply the spherical harmonic analysis by calculating the integrals (4) and the relations (5). This time, since we have assumed that the data are even about the Equator, only coefficients with even $n - m$ will be non-zero (see Appendix B), and each field will be represented by 190 expansion coefficients. This will be called a Northern Hemisphere analysis.

Results

In order to be able to compare the model-generated climatology (M) with the actual climatology (C), it was assumed that the actual climatology remains in steady state for the next five years.

Interpretation of the results will be done:

- a) by tabulating and ranking the leading harmonics of each field in descending order of the magnitudes of the amplitude coefficients, $A_{n,m}$;
- b) for a particular field, by comparing the annual cycle of each component (amplitude and phase of the harmonic) for M with the cycle of the same component for C.

The annual cycles of only the leading components for the three synoptic fields will be examined. Also, seasonal climatologies for M and C were obtained by averaging the amplitudes of the harmonics over a three-month period (see Appendix B). The seasons were defined as follows:

Spring: March, April, May; Summer: June, July, August;

Fall: September, October, November; Winter: December, January, February

For the above seasons the eight leading harmonics with their magnitudes, $A_{n,m}$, and their phases, $\beta_{n,m}$, will be tabulated. For the case where $m = 0$, the phase angle $\beta_{n,0}$ is defined as follows:

$$\beta_{n,0} = \begin{cases} 180^\circ & \text{if } C_{n,0} < 0 \\ 0^\circ & \text{if } C_{n,0} > 0 \end{cases} \quad (11)$$

The synoptic fields may then be represented in terms of the amplitudes and phases of the dominant components of each field.

Table 1 contains the eight leading harmonics, not including $A_{0,0}$.

Table 1. Global mean values and the 8 largest harmonics $A_{n,m}$ for each field (T850, G500, SLP) for winter actual climatology (C) and winter model generated climatology (M) (global sph. harm. analysis) Code: $\frac{A_{n,m}}{\beta_{n,m}}$

T850	MEAN	1	2	3	4	5	6	7	8
C	279.7	2,0 40.1/180	1,0 11.4/180	3,2 3.6/ 73	2,1 3.4/341	3,1 3.1/306	4,2 3.0/ 53	5,2 2.8/ 43	5,4 2.6/333
M	279.2	2,0 43.8/180	1,0 13.1/180	6,0 5.2/ 0	3,1 4.1/302	3,2 3.9/ 77	2,1 3.5/340	8,0 3.4/180	6,2 2.8/ 43
G500	MEAN	1	2	3	4	5	6	7	8
C	5636.0	2,0 916.4/180	6,0 112.1/ 0	4,0 111.0/180	1,0 83.9/180	3,0 76.4/ 0	7,0 59.5/180	2,1 51.9/ 10	4,1 49.5/ 35
M	5605.2	2,0 843.0/180	1,0 191.2/180	6,0 94.3/ 0	4,0 85.3/180	4,1 53.0/ 10	2,1 47.0/358	3,1 46.5/336	5,0 42.2/ 0
SLP	MEAN	1	2	3	4	5	6	7	8
C	1011.2	1,0 18.5/ 0	2,0 10.7/180	4,0 10.3/180	6,0 8.5/ 0	3,0 7.2/ 0	7,0 4.8/180	4,2 4.7/192	2,1 4.4/ 88.
M	1010.7	4,0 9.4/180	1,0 9.3/ 0	2,0 6.6/ 0	3,1 4.9/109	8,0 4.6/ 0	3,2 4.6/241	2,1 4.5/ 97	4,1 3.9/ 85

for the winter C and M fields. Included in Table 1 are the harmonic indices, n,m , and amplitudes, $A_{n,m}$, and the phase angles for the eight leading harmonics. Also tabulated are the global mean values of each field, computed from $A_{0,0}$ using equation (9). Reasonable global means were generated by the model for T850, SLP and G500. The same dominant harmonics, 2,0, for G500 and T850 appear in M and C. However, the model has overestimated the polar equatorial difference, 2,0, in T850 and underestimated it in G500 and SLP, with a phase difference of 180° in the last field. The difference between the poles, 1,0, is grossly underestimated by the model in SLP (18.5 vs 9.3) and overestimated in G500. The 1,0 in the case of SLP indicates an excess of mass in the Northern Hemisphere during winter.

The differences between the eight leading harmonics for C and M indicate the character of the predicted climatology error which is dominated by the 6,0 harmonic in T850 (not found in the C list) and in SLP (not found in the M list). Also in SLP the error is in the 3,0 and 7,0 terms (contributions to the asymmetry of the two hemispheres) which do not appear among the eight leading M harmonics.

The data listed in Table 2 are for the spring. Again the global means for T850, SLP and G500 were correctly estimated by the model. The polar equatorial difference is still dominant and 4,0 is the second dominant harmonic for T850 and G500. The 2,0 is again overestimated by the model in T850 but is well estimated in G500. Also the 4,0 is well estimated for T850 and G500. In SLP the 2,0 is overestimated by the model with a phase difference of 180° . Also overestimated are the 7,0 and 8,0 terms. Additionally, the 1,0 and 3,0, which are the dominant harmonics in C, do not appear among the eight leading harmonics in M. Generally the M error in SLP is dominated by the 5,0 and by 1,0, 3,0, 4,0, which are not found in the M list.

Table 3 contains information as in Table 2 but for the summer

Table 2. Global mean values and the 8 largest harmonics $A_{n,m}$ for each field (T850, G500, SLP) for spring actual climatology (C) and spring model generated climatology (M) (global sph. harm. analysis)

Code: $\frac{A_{n,m}}{\beta_{n,m}}$

T850	MEAN	1	2	3	4	5	6	7	8
C	280.7	2,0 40.5/180	4,0 4.7/180	2,1 3.5/42	5,0 3.4/0	1,1 2.8/27	5,4 2.3/340	8,0 2.0/180	3,2 1.9/127
M	280.0	2,0 46.1/180	4,0 4.8/180	5,0 4.3/0	2,1 4.1/34	8,0 3.7/180	7,0 3.6/0	1,1 3.5/39	6,2 3.3/20
G500	MEAN	1	2	3	4	5	6	7	8
C	5651.2	2,0 889.0/180	4,0 132.2/180	3,0 123.3/0	1,0 119.1/0	6,0 77.0/0	4,1 44.9/31	5,0 37.6/0	2,1 37.5/38
M	5618.6	2,0 851.8/180	4,0 137.6/180	6,0 66.2/0	6,2 37.2/50	7,2 36.2/65	5,1 33.3/323	5,2 33.2/61	5,0 33.0/0
SLP	MEAN	1	2	3	4	5	6	7	8
C	1011.0	1,0 15.8/0	3,0 12.5/0	2,0 10.2/180	4,0 9.3/180	6,0 8.6/0	7,0 4.8/180	8,0 3.9/0	8,1 3.5/244
M	1011.0	2,0 12.4/0	8,0 7.8/0	7,0 7.5/180	5,0 6.0/180	8,1 5.1/255	6,0 5.1/0	5,1 4.6/79	1,1 4.1/238

Table 3. Global mean values and the 8 largest harmonics $A_{n,m}$ for each field (T850, G500, SLP) for summer actual climatology (C) and summer model generated climatology (M) (global sph. harm. analysis)

Code: n, m
 $A_{n,m} / \beta_{n,m}$

T850	MEAN	1	2	3	4	5	6	7	8
C	282.4	2,0 32.4/180	1,0 21.2/ 0	4,0 6.3/180	2,1 4.3/ 73	5,1 2.6/218	5,0 2.6/ 0	7,0 2.3/ 0	2,2 2.1/143
M	283.0	2,0 35.0/180	1,0 25.6/ 0	4,0 10.0/180	2,1 6.3/ 68	7,0 4.7/ 0	4,2 4.7/166	3,2 4.7/165	1,1 3.4/ 55
G500	MEAN	1	2	3	4	5	6	7	8
C	5680.3	2,0 769.1/180	1,0 478.5/ 0	4,0 132.8/180	3,0 129.5/ 0	6,0 74.4/ 0	9,0 37.1/180	4,1 37.1/ 71	8,1 35.3/219
M	5665.6	2,0 706.3/180	1,0 462.4/ 0	4,0 155.3/180	5,0 52.9/180	3,0 46.3/ 0	7,0 38.0/ 0	4,1 29.2/ 89	9,0 29.2/180
SLP	MEAN	1	2	3	4	5	6	7	8
C	1010.7	2,0 14.5/180	3,0 14.2/ 0	1,0 10.0/ 0	6,0 8.1/ 0	4,0 8.1/180	1,1 6.3/293	2,1 6.1/262	4,1 4.4/ 61
M	1010.6	2,1 9.8/254	7,0 8.7/180	6,0 8.6/ 0	2,0 8.3/ 0	5,1 6.9/ 72	5,0 6.8/180	3,2 6.8/ 1	1,0 6.7/180

period. The global means were very well estimated by the model for the three fields. Again the dominant harmonic for T850 and G500 is the 2,0, due to the strong meridional gradient of these fields. In G500 the amplitude of this gradient is underestimated by the model. The other dominant components for the G500 and T850 are the 1,0 and 4,0. All of them except the 4,0 in G500, and especially in T850, are overestimated.

From winter to summer we find, comparing Tables 1 and 3, an increase in the relative magnitude of the 4,0 harmonic, notably in T850. This appears to reflect the heating of the mid-latitude continents in the Northern Hemisphere summer, as a result of which high temperature and geopotential values are observed north of the geographical Equator. This meridional pattern is represented by the zonal harmonic 4,0 with the phase angle of 180° , indicating relatively high temperatures and geopotential in middle latitudes. The 3,0 term which contributes to the asymmetry of G500 in both hemispheres is badly estimated by the model. The M error in this case is dominated by the 4,2 in T850 and by 6,0 and 5,0 terms in G500. In SLP the 2,0 harmonic is significantly underestimated with opposite phase as is the 1,0 term. The M error is dominated by the asymmetric term 3,0 and by 4,0. The other harmonics, 6,0 and 2,1, are found in both the C and M sets with about the same amplitudes and phases.

Fall results are indicated in Table 4, which shows that nearly perfect global mean values were estimated by the model for all fields. The 2,0 term is dominant in T850 (overestimated) and G500 (underestimated). The 1,0 and 4,0 are the next dominant components in T850 and G500. Beyond the third dominant harmonic 4,0 there is little correspondence in T850 between the C and M harmonics. In SLP the 1,0, 2,0 and 3,0 terms are grossly underestimated with opposite phase in 2,0. The 4,0 harmonic is not found in the M list while the 7,0 and 5,0 are not found in the C list.

Table Global mean values and the 8 largest harmonics $A_{n,m}$ for each field (T850, G500, SLP) for fall actual climatology (C) and fall model generated climatology (M) (global sph. harm. analysis)

Code: $A_{n,m} / \beta_{n,m}$

T850	MEAN	1	2	3	4	5	6	7	8
C	280.7	2.0 38.0/180	1.0 7.3/ 0	4.0 4.6/180	2.1 3.1/ 29	5.4 2.5/327	3.1 2.4/298	5.0 2.2/ 0	3.3 2.0/109
M	280.7	2.0 41.9/180	1.0 6.7/ 0	4.0 5.5/180	7.0 3.8/ 0	3.0 2.9/180	5.4 2.8/351	6.0 2.7/ 0	8.0 2.7/180
G500	MEAN	1	2	3	4	5	6	7	8
C	5653.1	2.0 895.1/180	1.0 259.2/ 0	4.0 166.9/180	6.0 89.4/ 0	3.0 88.5/ 0	4.1 53.4/ 44	2.1 38.4/ 43	8.1 37.3/215
M	5631.8	2.0 804.4/180	1.0 205.3/ 0	4.0 133.7/180	6.0 58.2/ 0	7.0 33.0/ 0	7.2 31.9/ 88	7.3 30.2/305	6.2 29.7/ 39
SLP	MEAN	1	2	3	4	5	6	7	8
C	1011.0	1.0 15.4/ 0	2.0 14.7/180	3.0 12.5/ 0	4.0 12.4/180	6.0 7.6/ 0	8.0 4.8/ 0	8.1 3.8/249	4.1 3.5/ 83
M	1010.7	2.0 9.4/ 0	1.0 7.5/ 0	7.0 5.8/180	8.0 5.7/ 0	3.0 5.4/ 0	5.0 4.8/180	8.1 4.3/247	6.0 4.1/ 0

In the spherical harmonic analysis for the Northern Hemisphere alone, the asymmetries between the two hemispheres are eliminated and the effects of oceans and continents in T850 and SLP are more pronounced. The ocean-continent distribution in the Northern Hemisphere corresponds to zonal wavenumber $m = 2$. For example, during the Northern Hemisphere winter the oceans are warmer than the continents (continentality) and zonally the temperature distribution consists of two alternating high and low values due to the two large continental areas (North America, Eurasia) and two oceans (Atlantic, Pacific). The above pattern corresponds to the harmonic 4,2 as indicated in Figure 1. The same pattern, with a small phase shift, fits the SLP field due to the longitudinal distribution of the four basic pressure cells in the Northern Hemisphere (Aleutian low, Canadian high, Icelandic low, and Siberian high).

Table 5 contains the leading harmonics of the three Northern Hemisphere fields for winter. The model has generated a reasonable hemisphere mean value for T850, with a slight cold bias. The area-weighted means of G500 and SLP are underestimated. Differences between the North Pole and Equator, 2,0, are overestimated by the model, especially in SLP, for which 2,0 is not even found among the eight dominant harmonics in the observed climatology (C). Although the model generates a 2,0 harmonic as the leading component of SLP, in nature this term does not even appear among the eight leading harmonics. The 4,2 is the dominant SLP harmonic in C and the second dominant term in T850. The model generates a reasonable 4,2 harmonic in SLP and T850, although it is not the leading term in M. This means that the locations and the intensities of the above pressure cells were not correctly simulated by the model. Also, the 4,2 in T850 was underestimated. The M error in the T850 is dominated by the 6,0. The harmonics 6,0, 3,1 appear among the dominant terms in the M G500 but in different order. The 7,1 and 6,0 represent model climatology errors in SLP.

Table 5. Global mean values and the 8 largest harmonics $A_{n,m}$ for each field (T850, G500, SLP) for winter actual climatology (C) and winter model generated climatology (M) (Northern Hemisphere analysis) Code: n,m

$$\frac{A_{n,m}}{\beta_{n,m}}$$

T850	MEAN	1	2	3	4	5	6	7	8
C	277.0	2.0 46.0/180	4.2 6.6/ 57	3.1 5.2/329	1.1 4.6/331	6.2 4.0/ 40	2.2 3.8/ 68	5.3 3.3/276	5.1 2.7/ 58
M	276.3	2.0 52.1/180	3.1 7.5/312	6.0 6.3/ 0	5.3 5.6/274	4.2 5.6/ 55	6.2 5.0/ 31	1.1 4.7/ 2	7.1 4.4/ 70
G500	MEAN	1	2	3	4	5	6	7	8
C	5612.4	2.0 919.6/180	6.0 85.8/ 0	3.1 82.2/358	5.3 78.9/315	4.2 74.7/ 96	6.2 64.3/ 69	8.0 58.5/180	1.1 53.8/339
M	5561.4	2.0 948.5/180	3.1 100.0/351	6.0 93.4/ 0	6.2 78.5/ 75	5.1 77.1/ 14	5.3 64.7/283	4.2 55.7/ 79	7.3 54.1/323
SLP	MEAN	1	2	3	4	5	6	7	8
C	1015.2	4.2 8.7/193	4.0 7.4/180	3.1 7.2/106	7.1 6.3/226	6.0 5.7/ 0	5.1 4.9/177	6.2 4.7/186	2.2 4.7/208
M	1012.7	2.0 13.4/ 0	3.1 9.8/100	4.0 8.3/180	4.2 7.2/207	2.2 5.4/222	6.2 5.4/173	1.1 3.7/122	7.1 3.6/267

Table 6 contains the data for the spring. The same dominant harmonic 2,0 appears for all fields, and it is grossly overestimated by the model, especially in SLP. All the area-weighted means are underestimated as well as the majority of dominant harmonics in T850. The M T850 error is dominated as before by the 6,0 and 3,1 terms. In the G500 the 4,0 and 6,0 are overestimated. In SLP the 7,1 and 6,0 are underestimated as in winter. The 6,0 is not found among the first eight harmonics in M. This is considered to be an M structure error in SLP because the 6,0 corresponds to the C meridional pressure distribution shown in Figure 12.

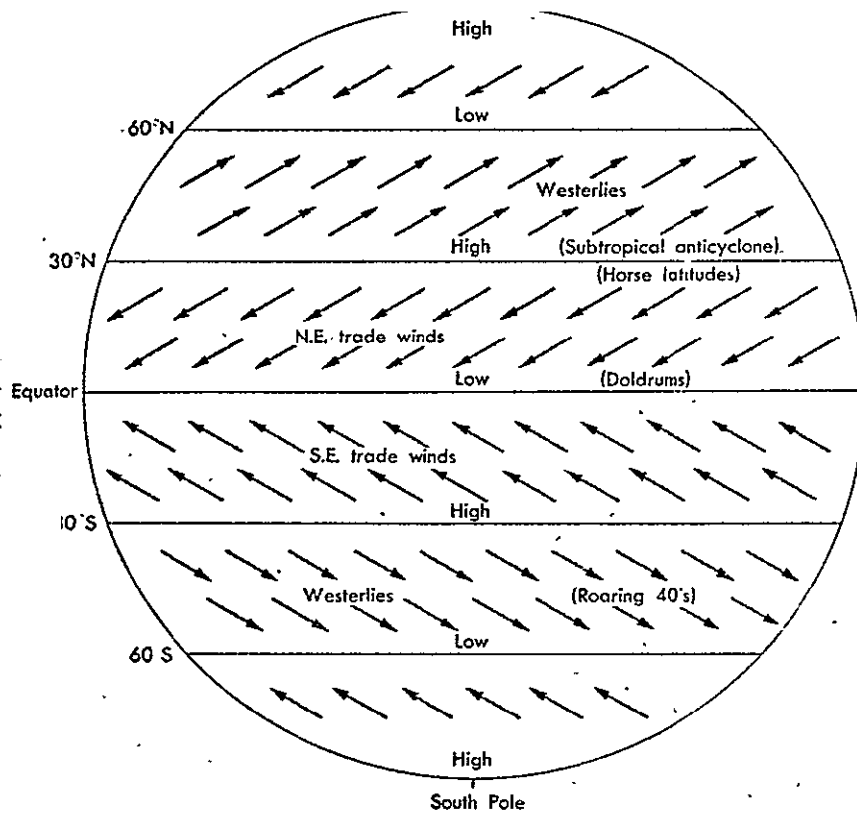


Figure 12: Meridional pressure pattern at sea level
(From J. Spar, Earth, Sea and Air, 1962)

Table 6. Global mean values and the 8 largest harmonics $A_{n,m}$ for each field (T850, G500, SLP) for spring actual climatology (C) and spring model generated climatology (M) (Northern Hemisphere analysis)

Code: n,m
 $A_{n,m} / B_{n,m}$

T850	MEAN	1	2	3	4	5	6	7	8
C	281.1	2,0 39.4/180	1,1 6.1/ 36	2,2 3.2/125	6,2 2.8/ 28	4,4 2.2/352	4,2 2.0/101	8,0 1.9/180	9,1 1.9/217
M	280.2	2,0 47.4/180	6,0 8.1/ 0	1,1 7.1/ 41	6,2 6.6/ 13	2,2 4.3/120	3,1 4.2/334	5,1 3.8/285	4,2 3.7/ 93
G500	MEAN	1	2	3	4	5	6	7	8
C	5671.1	2,0 752.0/180	6,0 70.7/ 0	3,1 52.4/ 5	4,2 50.1/102	4,0 47.6/180	8,0 46.5/180	6,2 44.2/ 75	1,1 33.4/ 9
M	5620.9	2,0 827.4/180	4,0 101.9/180	6,0 89.0/ 0	6,2 77.0/ 56	3,1 47.0/351	7,3 43.9/336	5,1 42.4/346	4,2 39.8/ 67
SLP	MEAN	1	2	3	4	5	6	7	8
C	1013.8	2,0 6.1/ 0	7,1 5.4/241	6,2 4.6/177	6,0 4.6/ 0	1,1 4.4/257	4,0 3.2/180	8,4 2.4/ 28	3,3 2.4/272
M	1010.7	2,0 14.7/ 0	1,1 7.6/240	6,2 6.4/163	5,1 5.2/ 84	4,0 4.4/180	2,2 4.1/306	3,1 3.8/143	7,1 3.4/247

For the summer (Table 7), the mean T850 is warm-biased and there is a deficit of mass in the Northern Hemisphere, indicated by the underestimation of the mean SLP, while the mean G500 is well simulated.

The dominant harmonics for T850 and G500 are the 2,0, which were correctly simulated by the model, and the 4,0, due to the insolation, which is grossly overestimated in both M fields. The same tendency of 4,0 in the summer was observed in the global analysis.

The 4,2 is overestimated by the model in T850 and SLP with a phase shift in SLP. This indicates that during summer there is an opposite continentality effect which also results in an opposite zonal pressure distribution than the one in the winter. The above is clearly indicated by the increase of 4,2 in SLP, with 180° phase shift from winter to summer. A monsoonal pressure distribution term, 1,1, appears in both M and C as the leading harmonic for SLP. The 3,1 and the 2,2 which represent, together with 4,2, the continentality effects are overestimated by the model in both T850 and SLP. The M error in SLP is dominated by 2,0 (not in the M list).

For fall (Table 8), we have reasonable means for T850 and G500. The same components, 2,0 and 4,0, as in the summer are dominant in the above fields. In T850 there is an overestimation of the 2,0, 4,0 and 6,0, while the 1,1 and 3,1 are correctly estimated. The M error is dominated by 6,2.

In G500 the 2,0, 4,0, and 6,0 terms are very well simulated by the model, while the 6,2 and 4,2 harmonics are overestimated in SLP. The 2,0 dominates in the M SLP and represents the largest "model climatology" error, because the above harmonic is not found in the C list. Also, the 7,1 is not among the leading harmonics in the M list, while 4,0, which dominates in C, is underestimated as is 3,1.

Table 7. Global mean values and the 8 largest harmonics $A_{n,m}$ for each field (T850, G500, SLP) for summer actual climatology (C) and summer model generated climatology (M) (Northern Hemisphere analysis). Code: n,m

$A_{n,m} / \beta_{n,m}$

T850	MEAN	1	2	3	4	5	6	7	8
C	287.4	2.0 20.8/180	4.0 6.5/180	1.1 5.4/ 54	5.1 3.2/208	3.3 3.2/ 87	2.2 3.1/152	6.0 3.0/ 0	4.2 3.0/173
M	289.1	2.0 22.4/180	4.0 16.2/180	4.2 8.6/173	1.1 8.2/ 63	2.2 6.4/156	3.1 5.2/ 73	5.1 4.5/222	8.2 4.2/359
G500	MEAN	1	2	3	4	5	6	7	8
C	5782.2	2.0 428.4/180	4.0 141.1/180	6.0 65.8/ 0	1.1 33.8/320	10.0 32.6/180	5.1 30.9/132	6.2 29.2/137	4.2 19.7/129
M	5769.1	2.0 424.1/180	4.0 228.9/180	5.1 24.4/147	9.5 21.4/221	3.1 18.7/114	7.5 18.1/241	8.2 17.7/357	5.3 17.0/ 83
SLP	MEAN	1	2	3	4	5	6	7	8
C	1011.8	1.1 11.7/275	2.2 6.3/356	5.1 5.9/ 80	4.2 4.8/ 38	6.2 4.5/149	7.1 3.7/236	3.1 2.9/282	4.0 2.6/180
M	1008.6	1.1 12.8/255	4.2 11.7/ 6	2.2 7.9/350	2.0 7.9/ 0	3.1 7.0/247	5.1 6.8/ 63	8.2 4.3/183	6.4 4.1/196

Table 8. Global mean values and the 8 largest harmonics $A_{n,m}$ for each field (T850, G500, SLP) for fall actual climatology (C) and fall model generated climatology (M) (Northern Hemisphere analysis)

Code: $A_{n,m} / \beta_{n,m}$

T850	MEAN	1	2	3	4	5	6	7	8
C	282.5	2.0 34.8/180	4.0 4.2/180	1.1 4.1/12	6.0 3.0/0	3.1 3.0/339	4.2 2.5/85	6.4 2.1/302	7.1 2.1/54
M	282.5	2.0 40.3/180	4.0 8.3/180	6.0 6.5/0	6.2 4.5/12	1.1 4.2/48	3.1 2.9/345	5.1 2.6/299	7.1 2.6/48
G500	MEAN	1	2	3	4	5	6	7	8
C	5707.1	2.0 699.3/180	4.0 153.1/180	6.0 88.9/0	3.1 63.4/6	6.2 46.0/95	4.2 34.6/97	1.1 33.0/352	7.3 28.8/18
M	5679.0	2.0 690.3/180	4.0 176.2/180	6.0 79.7/0	6.2 56.5/60	7.3 43.6/348	4.2 41.6/54	5.1 35.3/14	8.2 32.6/75
SLP	MEAN	1	2	3	4	5	6	7	8
C	1013.6	4.0 7.7/180	7.1 5.0/233	3.1 4.1/101	6.2 3.7/173	6.0 3.1/0	8.0 2.9/0	4.2 2.8/186	5.1 2.6/125
M	1011.9	2.0 17.5/0	5.1 4.4/93	6.2 4.3/165	3.1 3.6/145	4.0 3.3/180	1.1 3.2/241	6.4 2.8/177	6.0 2.7/180

Figures 13 and 14 illustrate the annual cycles of the components $A_{o,o}$ of T850, G500, and SLP for the global and hemispheric analyses respectively. The dashed curves represent the model-generated spectral components and the continuous curves correspond to the actual climatological data. The global means are related to $A_{o,o}$ through relations (9) and (5). Therefore, the annual cycle of $A_{o,o}$ in Figures 13 and 14 is proportional to the annual cycle of the global means for the above fields. The units for the amplitudes $A_{n,m}$ are degrees Celsius for T850, meters for G500, and millibars for SLP. To find the global or hemispherical mean values, the plotted $A_{o,o}$ values must be multiplied by $(4\pi)^{-\frac{1}{2}}$ or 0.28.⁴

In Figure 13 there is an annual cycle of the global mean C T850, with maximum in July and minimum in January, due to the large percentage of land in the Northern Hemisphere, which dominates the global annual temperature cycle. The climate model generates a similar annual cycle for the mean T850, but with a larger amplitude (overestimate in summer, underestimate in winter). This can be interpreted as a tendency of the model to overheat the continents in summer and overcool them in winter. This is also indicated by the annual cycle of 0,0 for T850 in the Northern Hemisphere (Figure 14), which, as expected, shows a larger amplitude than the global mean for both C and M. A similar annual cycle is observed for the mean G500. The model underestimates the winter mean values of G500 while it successfully captures the summer means.

There is virtually no annual cycle of the observed global mean SLP (Figure 13). This is correctly represented by the model with only a small difference in the winter.⁵ However, the distribution of mass

⁴For $A_{o,o}$ the units of SLP, G500 are mb - 1000, m - 5000, respectively.

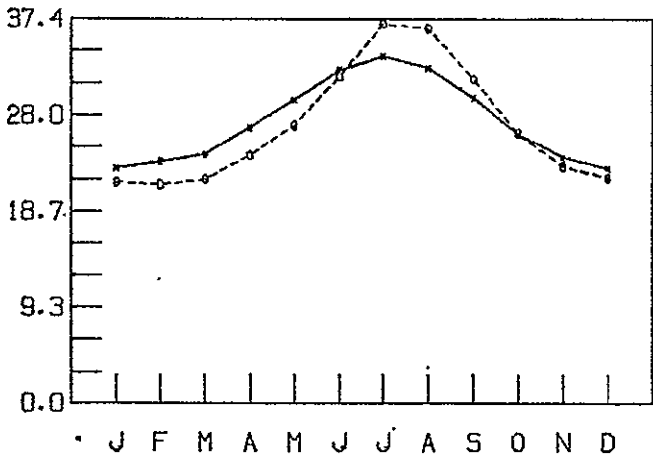
⁵The model is artificially corrected during the climate run to maintain constant global mass.

Figure 13.

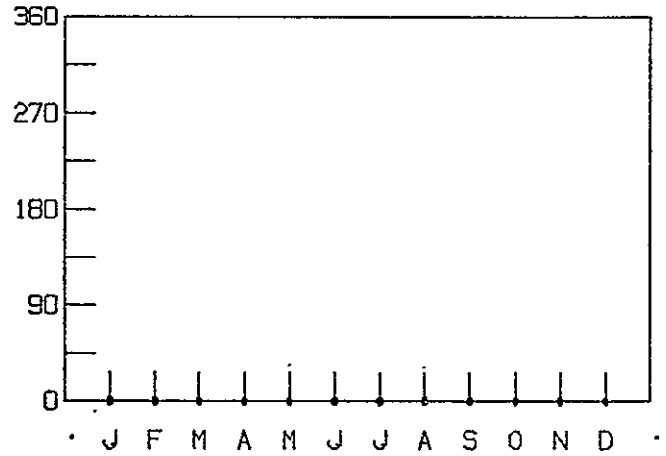
TIME SPECTRA FOR THE COMPONENT 0,0

T850

AMPLITUDES A .

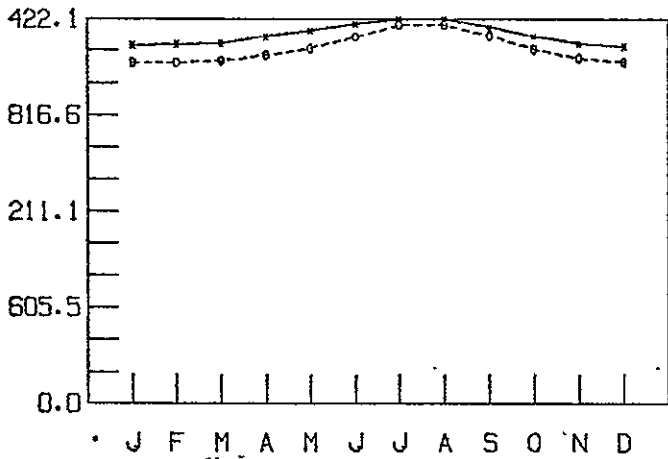


PHASES B .

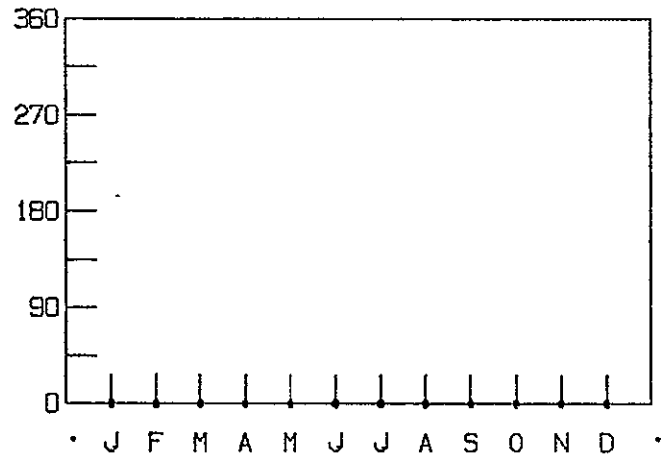


G500

AMPLITUDES A .

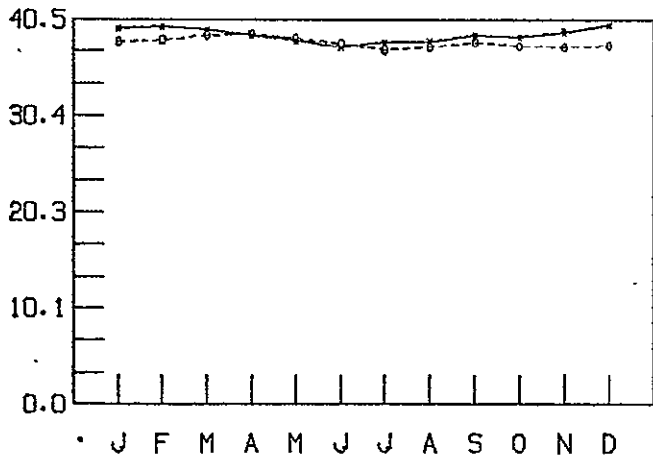


PHASES B .



SLP

AMPLITUDES A .



PHASES B .

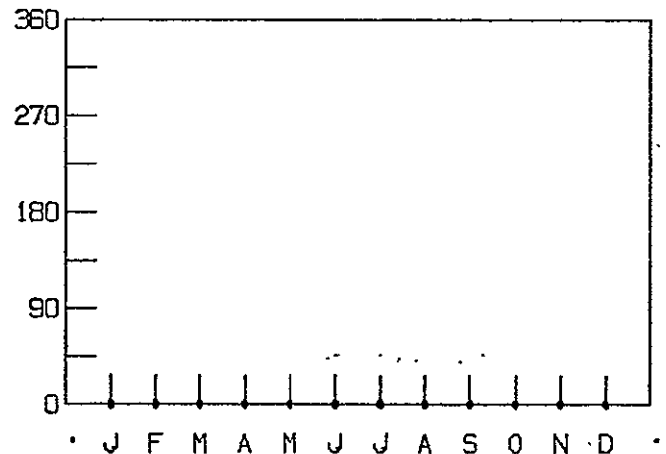


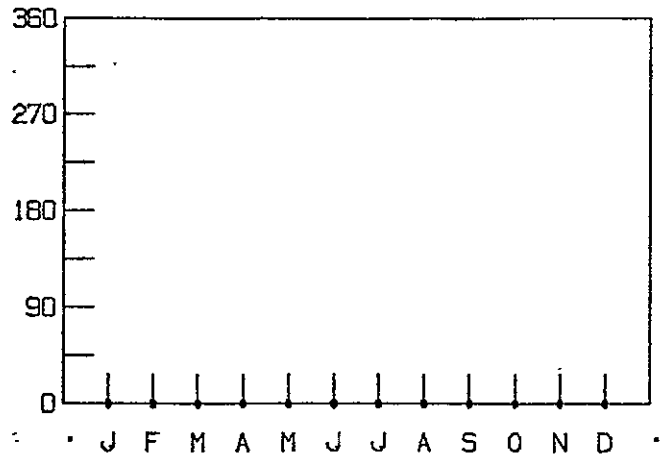
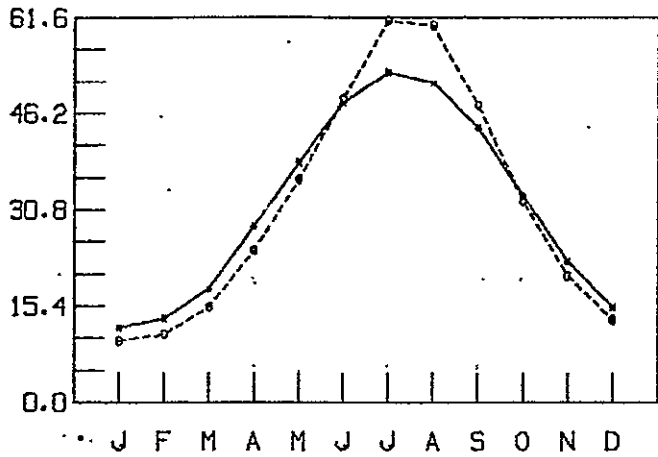
Figure 14.

TIME SPECTRA FOR THE COMPONENT 0.0

T850

AMPLITUDES A

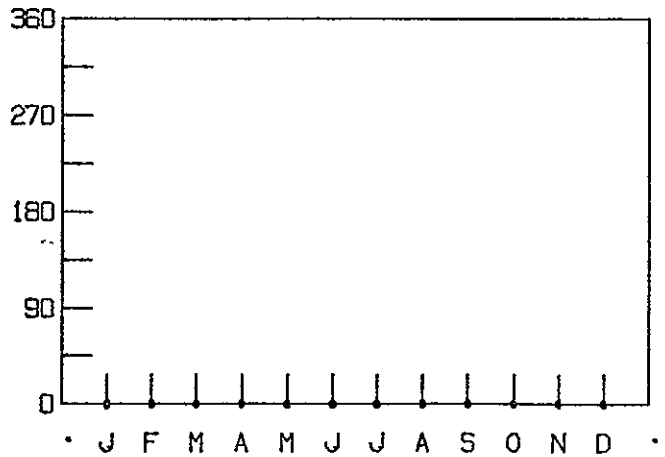
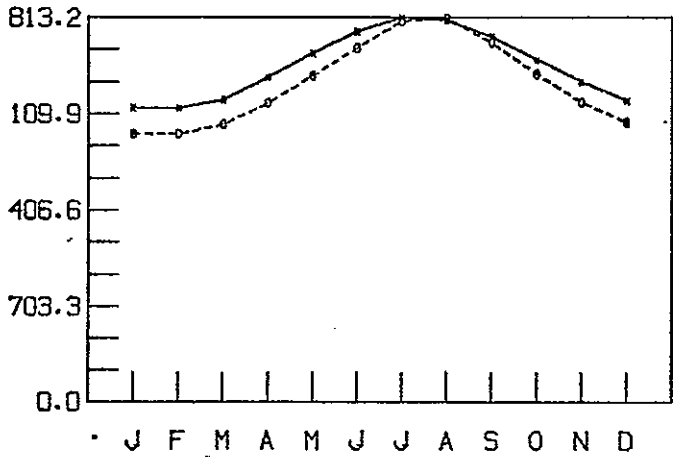
PHASES B



G500

AMPLITUDES A

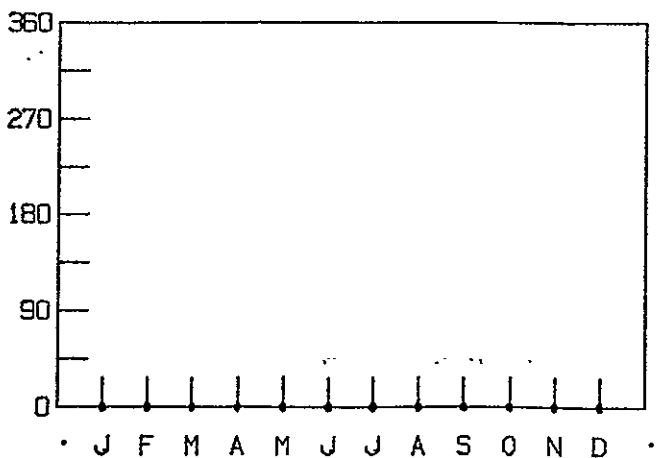
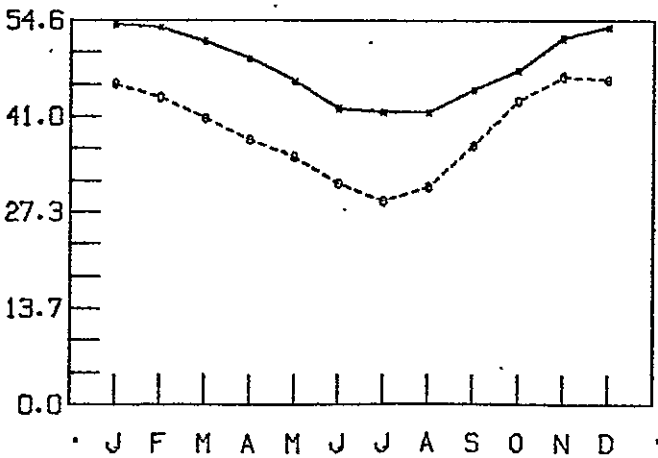
PHASES B



SLP

AMPLITUDES A

PHASES B



between the Northern and Southern Hemisphere is not correctly simulated by the model. This is indicated by the existence of a biased annual cycle in the mean SLP for the Northern Hemisphere (Figure 14). In the observed climatological SLP fields, the distribution of mass between the hemispheres is such that always the mean pressure is greater in the Northern Hemisphere. At least in winter this is associated with the large percentage of land in northern latitudes, which results in the generation of continental high pressure systems. The distribution of mass between the two hemispheres is indicated in Figure 15, where the 1,0 spectral component is plotted. The climatological C 1,0 harmonic shows that the Northern Hemisphere has maximum of mass in January and a minimum in July, with an excess of mass over the Northern Hemisphere all year, as shown by the constant phase angle $\beta_{1,0} = 0$. The model simulates the same minima and maxima in the 1,0 harmonic. However, from April through August the mean pressure in the model climatology is greater in the Southern Hemisphere, as indicated by the change of phase angle from 0° to 180° . This appears to be associated with excessively high pressures in the Antarctic in the Southern Hemisphere winter. The annual cycle of 1,0 for T850 (Figure 15), showing the seasonal temperature difference between the hemispheres reflected in the phase shift, is rather well simulated by the model but with a small phase delay in April and a temperature excess in the Northern Hemisphere in July and August, indicated by the large amplitude of the 1,0 harmonic in M. The same is observed for G500, with high geopotential values over the Northern Hemisphere in summer, which is correctly represented by the model.

Figures 16 and 17 represent the mean polar-equatorial differences, 2,0, for the globe and the Northern Hemisphere, respectively. For T850 and G500 the 2,0 harmonic is related to the distribution of insolation. In the 2,0 C global cycle (Figure 16) of T850, maximum and minimum

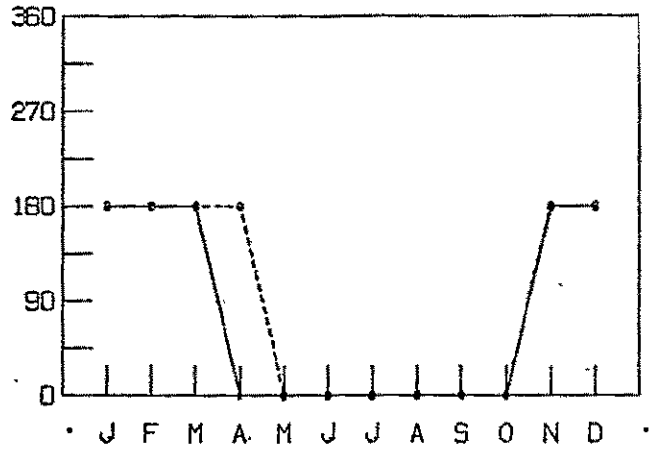
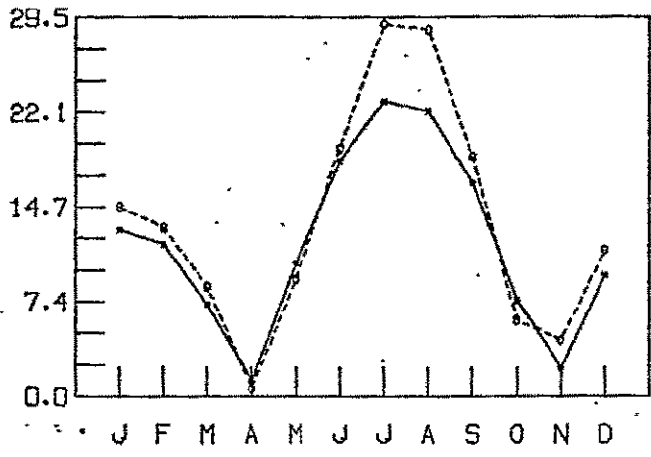
Figure 15.

TIME SPECTRA FOR THE COMPONENT 1.0

T850

AMPLITUDES A.

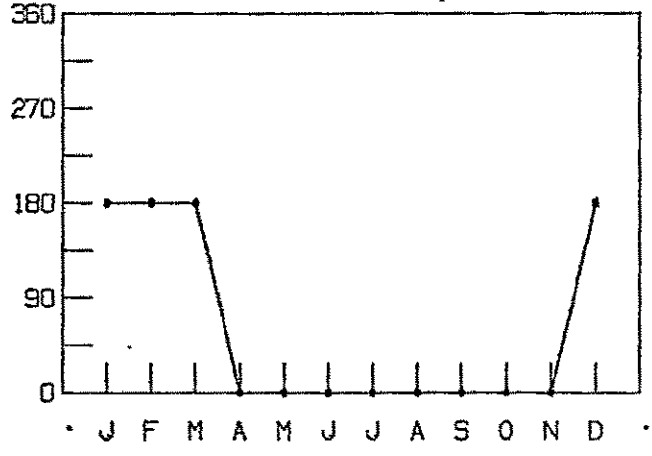
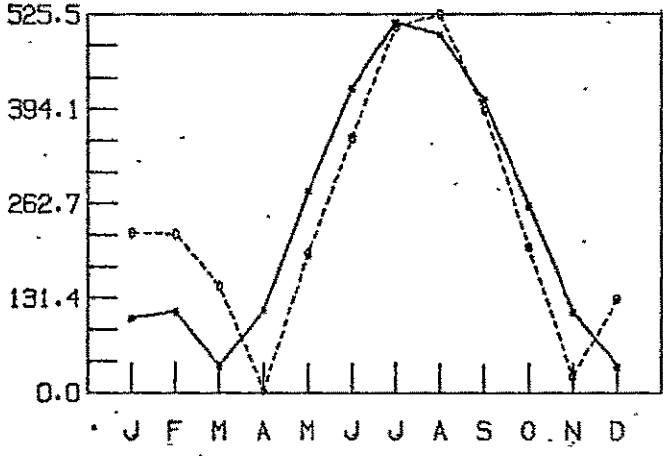
PHASES B.



G500

AMPLITUDES A.

PHASES B.



SLP

AMPLITUDES A.

PHASES B.

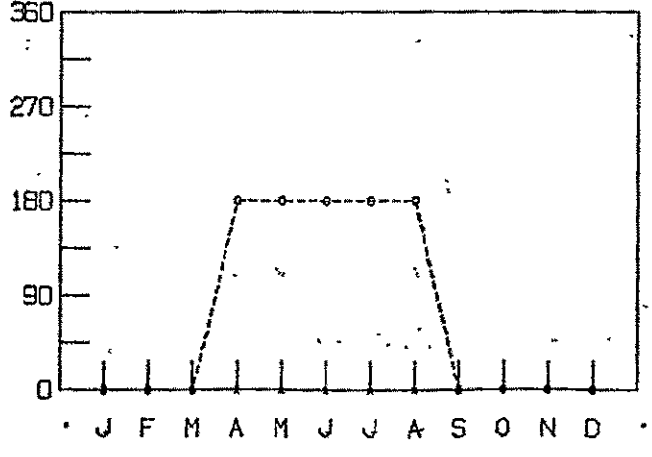
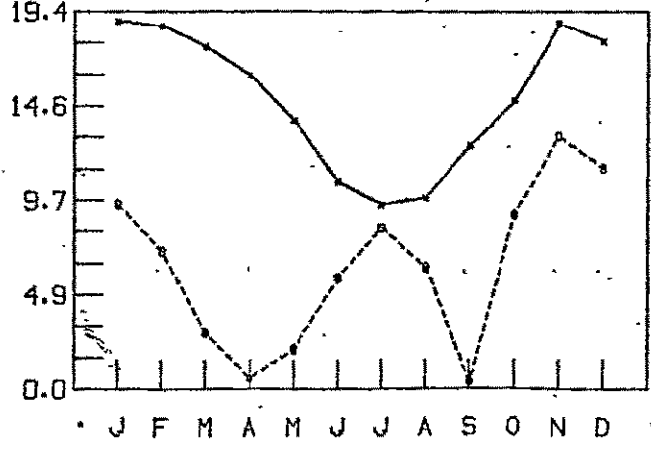
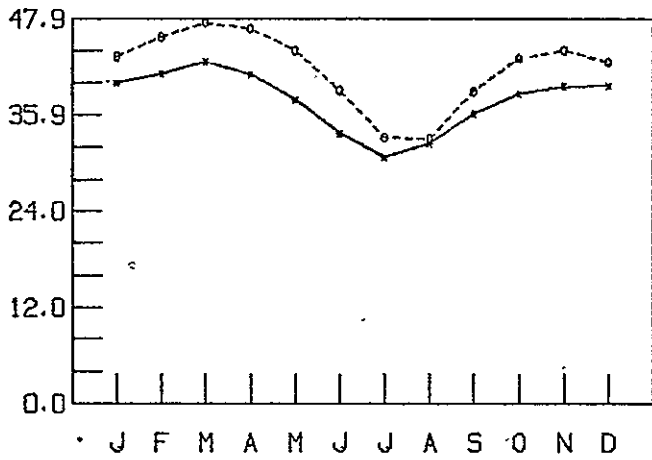


Figure 16.

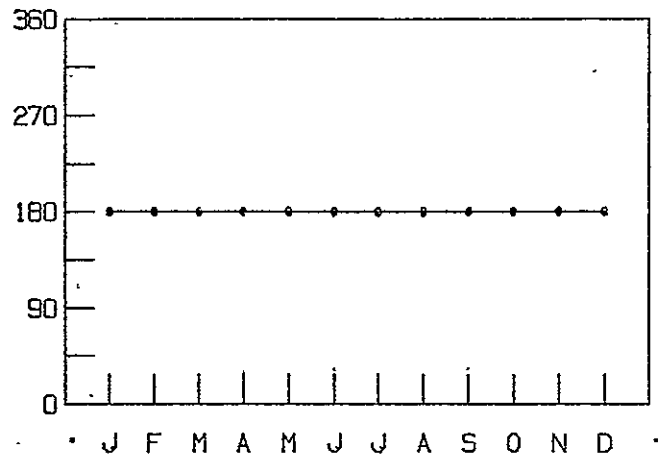
TIME SPECTRA FOR THE COMPONENT 2.0

T850

AMPLITUDES A ,

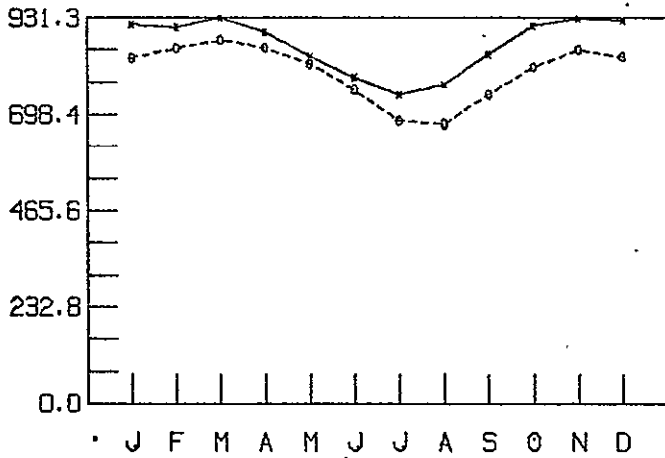


PHASES B ,

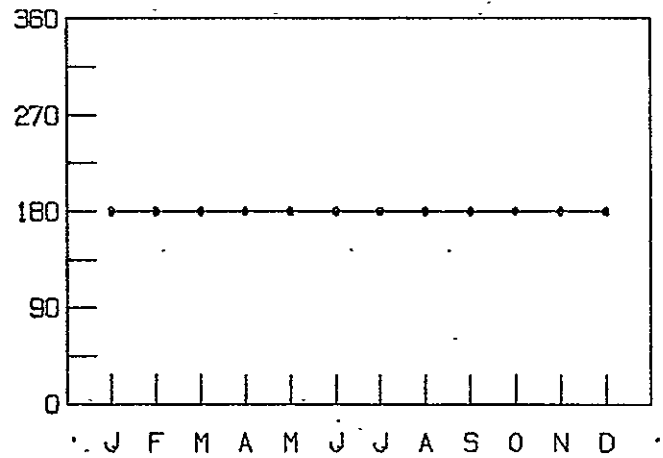


G500

AMPLITUDES A ,

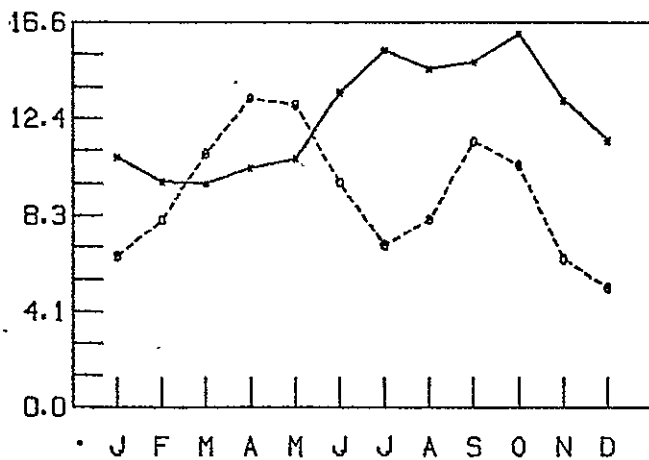


PHASES B ,



SLP

AMPLITUDES A



PHASES B ,

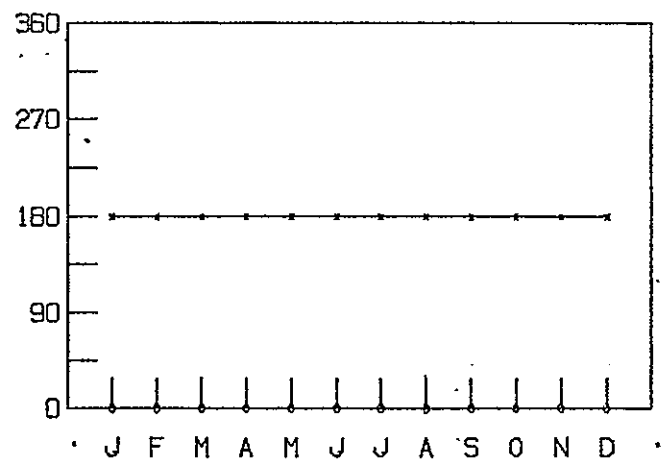


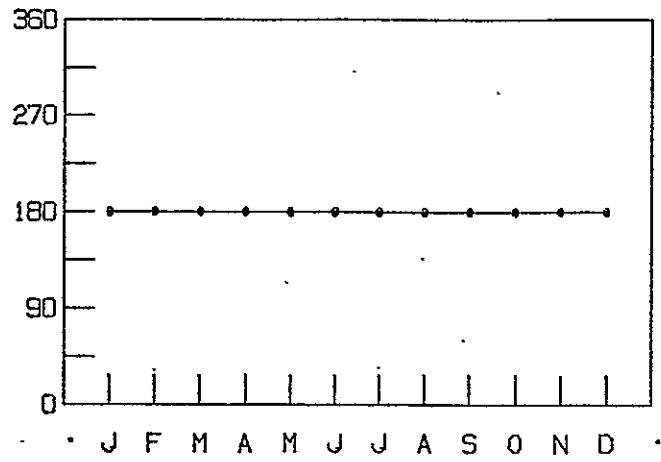
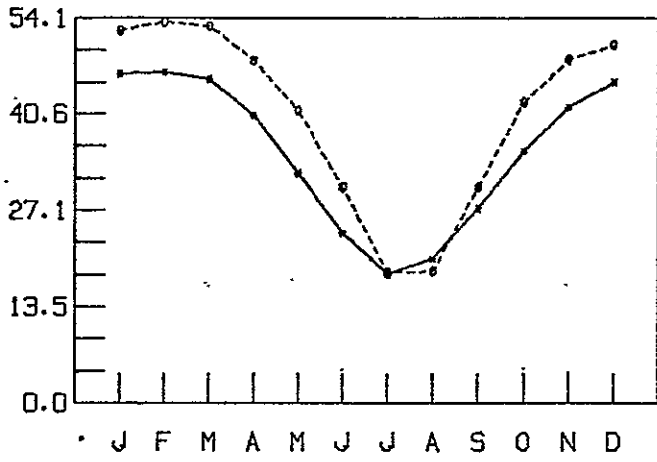
Figure 17.

TIME SPECTRA FOR THE COMPONENT 2.0

T850

AMPLITUDES A .

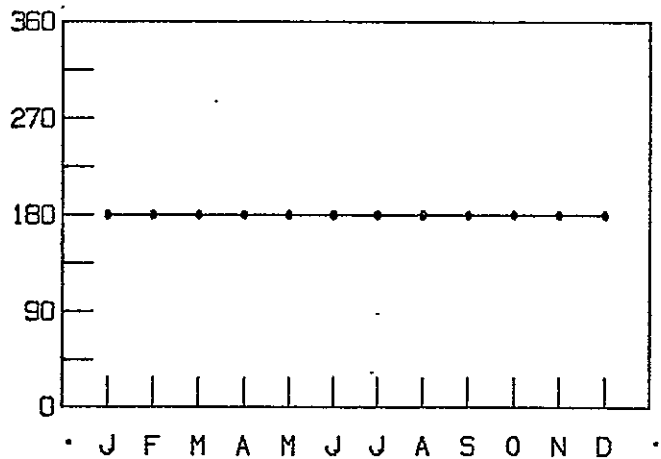
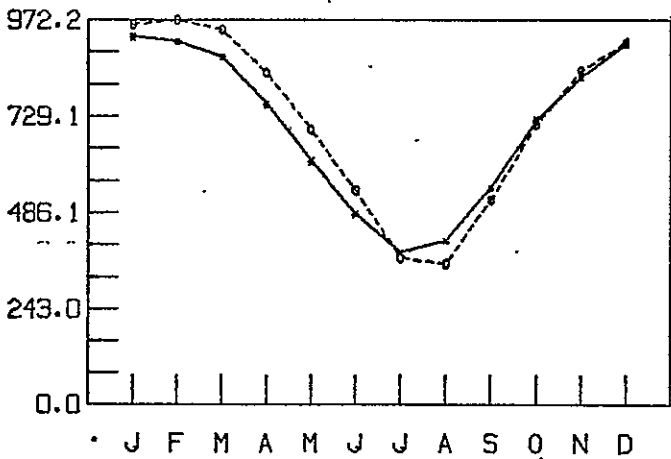
PHASES B .



G500

AMPLITUDES A .

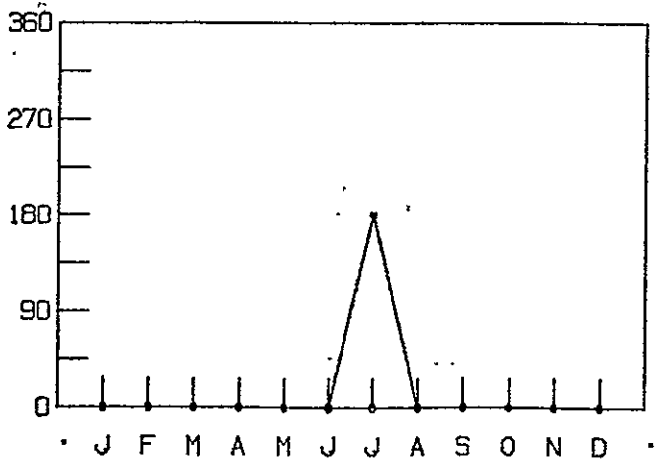
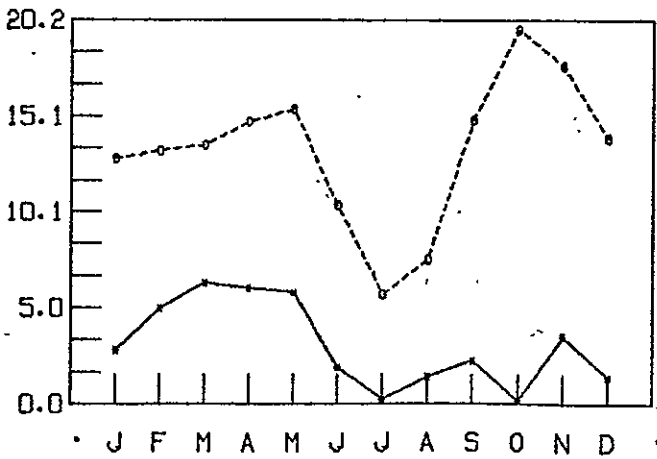
PHASES B .



SLP

AMPLITUDES A .

PHASES B .



amplitudes are found in March and July, respectively. The M cycle of 2,0 for T850 follows this pattern but with a high bias, including an overestimate of the maximum in March and a second maximum in November, indicating larger temperature differences between Poles and Equator. Similar cycles are observed in G500 but with a low bias in the global M cycle.

The C 2,0 annual cycle for the Northern Hemisphere (Figure 17) for T850 and G500 has one minimum (in July) and one maximum (in January). The model simulates these extrema with a lag of one month for both fields. As before, there is an overestimation of the maxima in winter, which results in too strong a meridional temperature gradient. In G500 the cycle of 2,0 for the Northern Hemisphere is very well estimated by the model. On the other hand, in the model simulation of the 2,0 harmonic of global SLP (Figure 17), the SLP cycle of 2,0 is correct in phase but positively biased in amplitude, notably in October. Apparently the Southern Hemisphere is mainly responsible for the global phase error.

The harmonics 3,0 and 5,0 (Figures 18 and 19) represent, like 1,0, the asymmetry of the hemispheres. The annual cycles of these harmonics for T850 are poorly represented by the model, with large phase and amplitude errors. For G500 the model annual cycle of 3,0 parallels that of the observed climatology but underestimates the amplitudes, while the 5,0 is reasonably well estimated by the model. In the C SLP there is a significant annual cycle of the 3,0 harmonic, which is not correctly represented by the model, indicating an inadequate exchange of mass between the hemispheres.

The annual cycle of the 4,0 harmonic is plotted in Figures 20 and 21. As mentioned before, the 4,0 term for T850 is related, like the 2,0, to the distribution of the insolation. For the global C cycle we have one minimum in January and one maximum in August. The latter lags

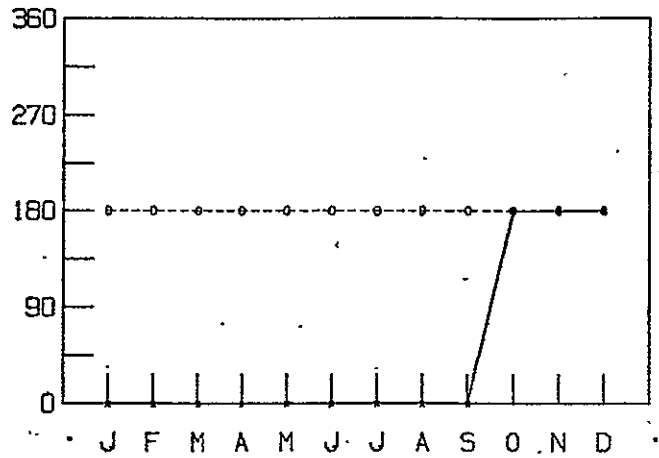
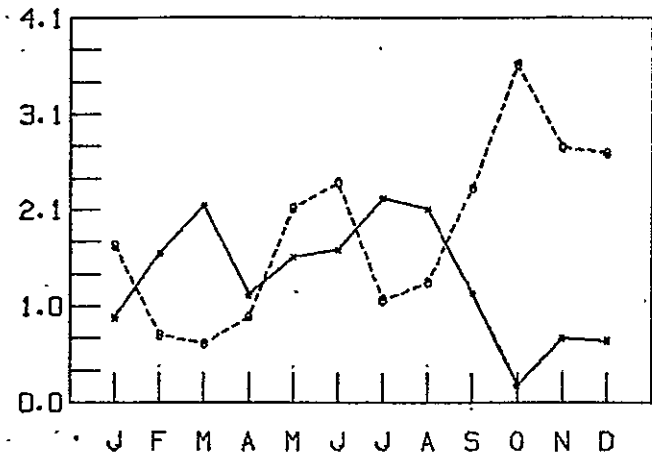
Figure 18.

TIME SPECTRA FOR THE COMPONENT 3.0

T850

AMPLITUDES A .

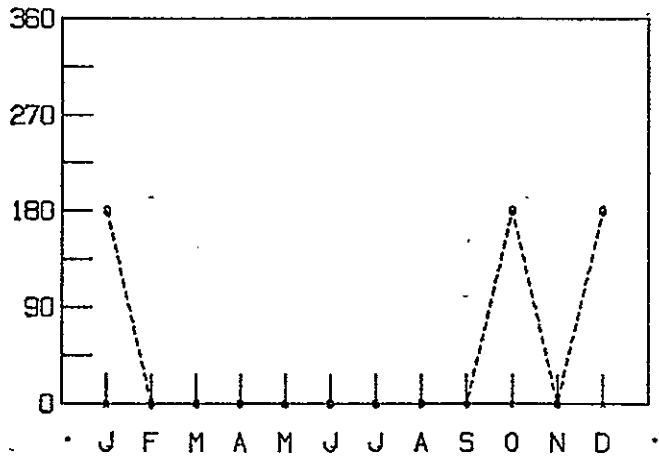
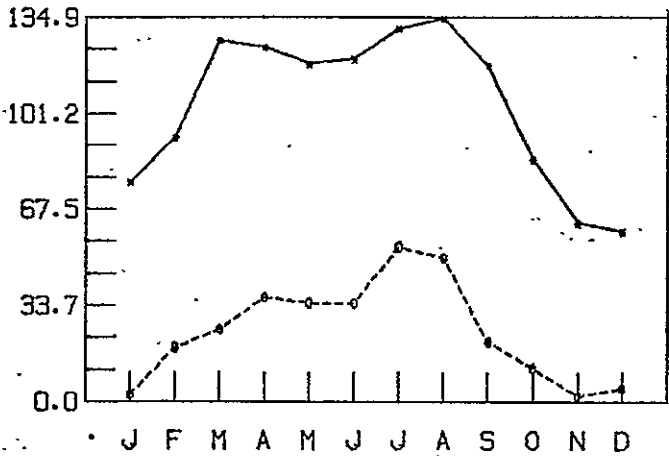
PHASES B .



G500

AMPLITUDES A .

PHASES B .



SLP

AMPLITUDES A .

PHASES B .

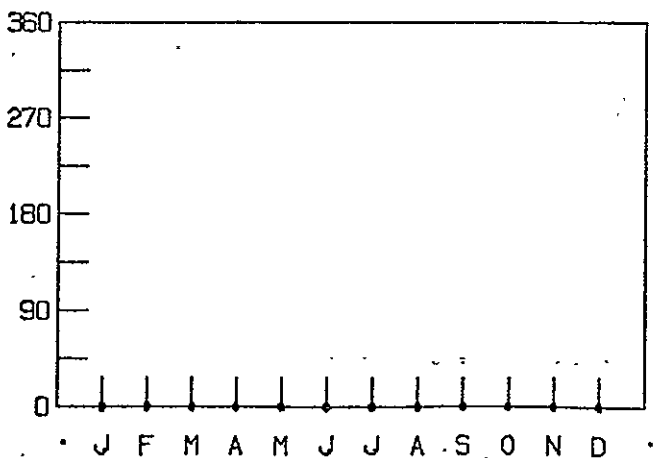
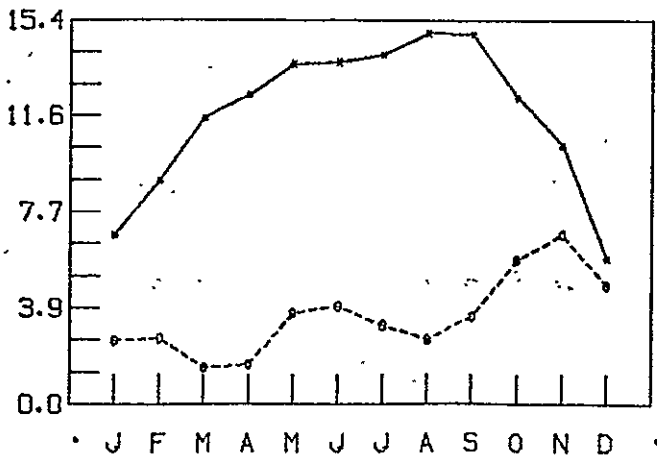
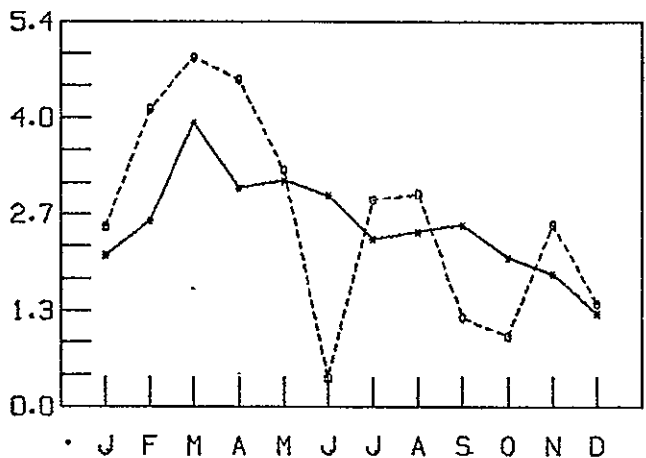


Figure 19.

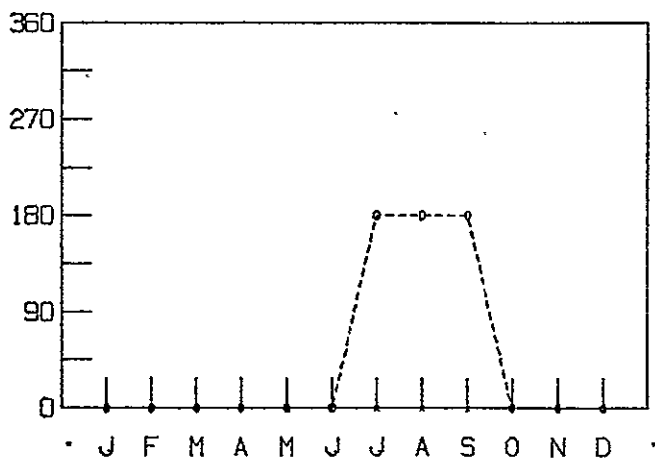
TIME SPECTRA FOR THE COMPONENT 5.0

T850

AMPLITUDES A.

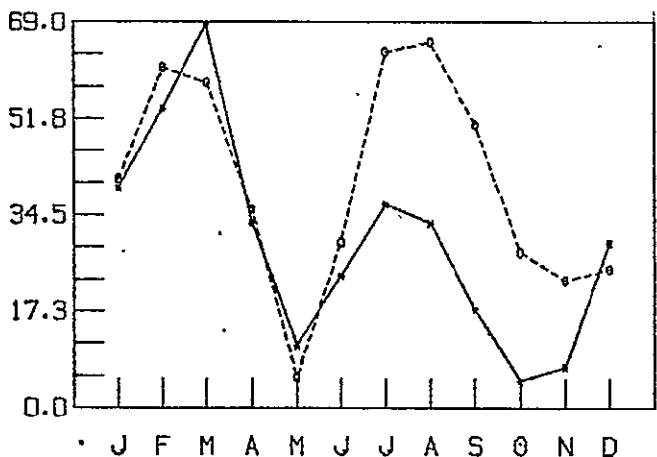


PHASES B.

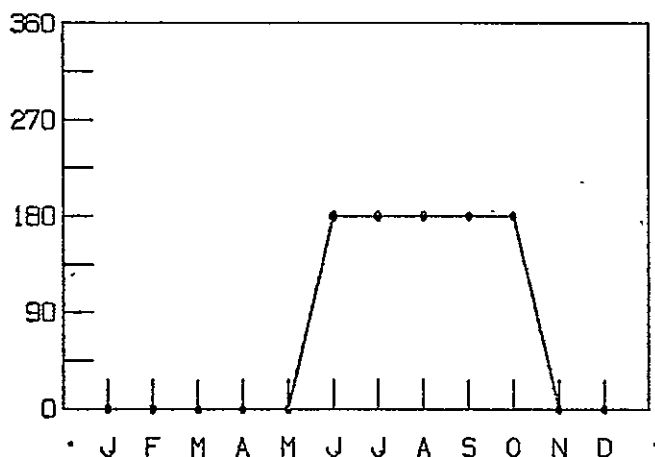


0500

AMPLITUDES A.

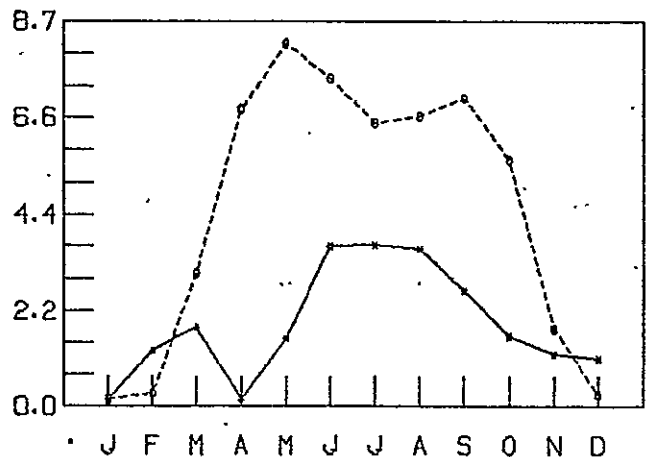


PHASES B.



SLP

AMPLITUDES A.



PHASES B.

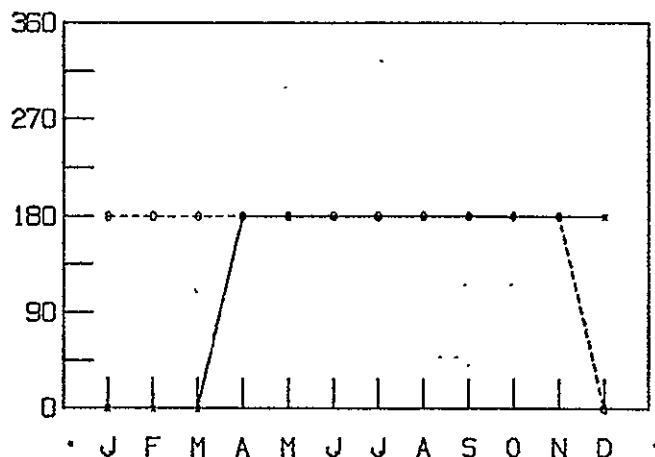
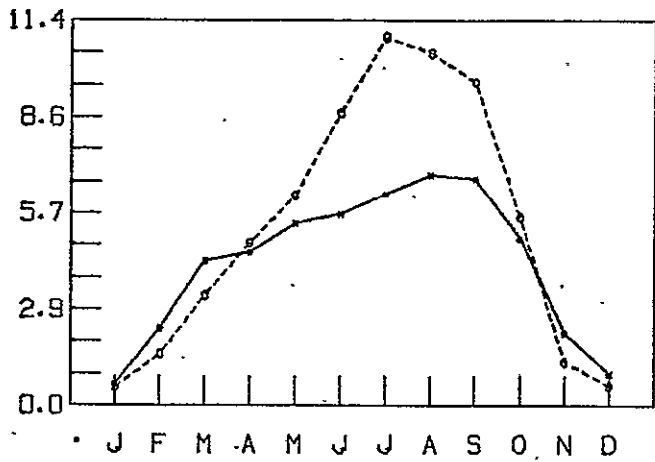


Figure 20.

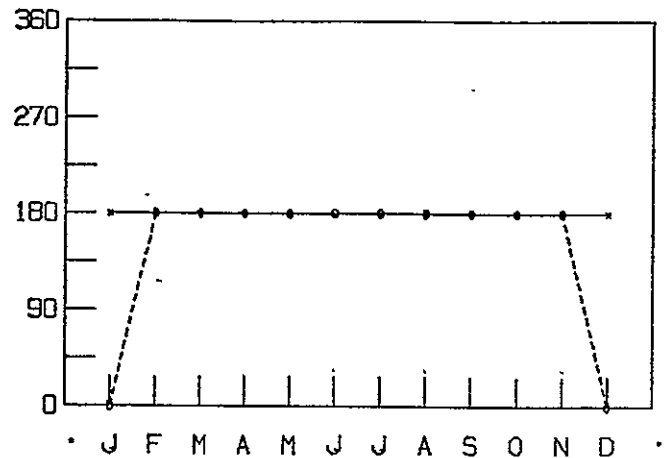
TIME SPECTRA FOR THE COMPONENT 4.0

T850

AMPLITUDES A.

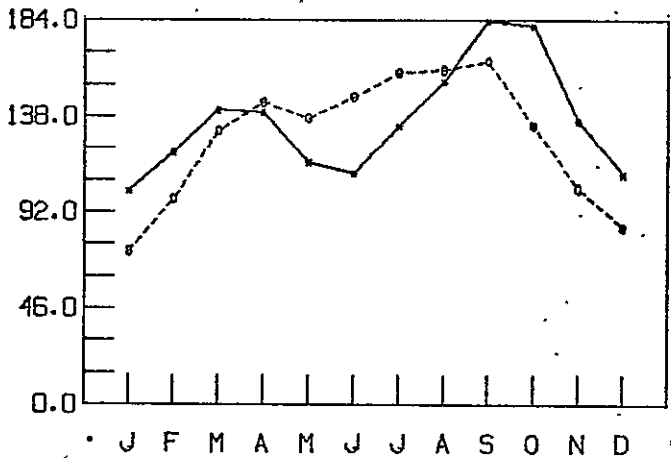


PHASES B.

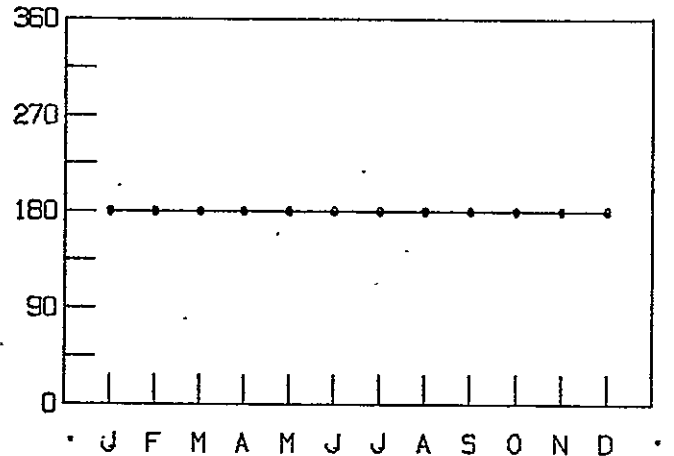


G500

AMPLITUDES A.

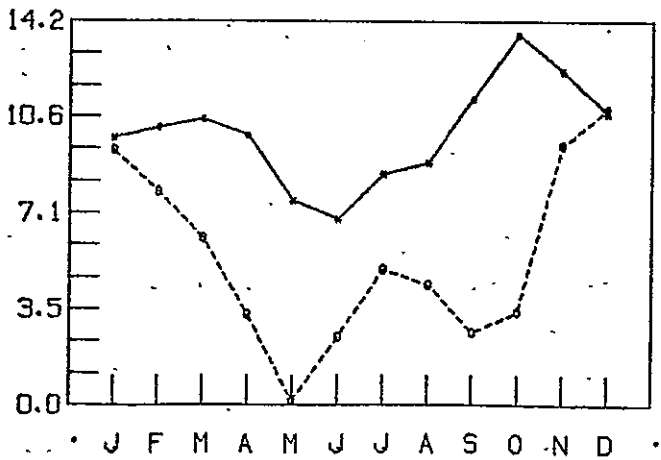


PHASES B.



SLP

AMPLITUDES A.



PHASES B.

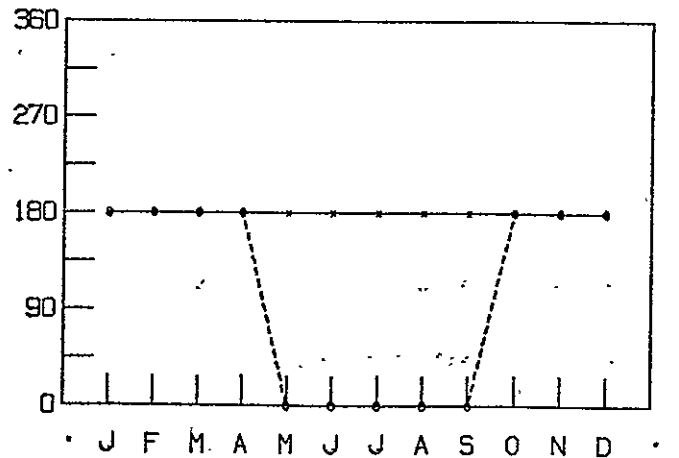


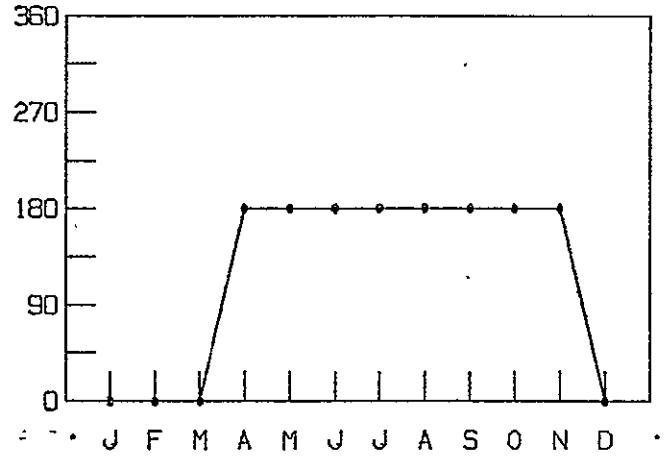
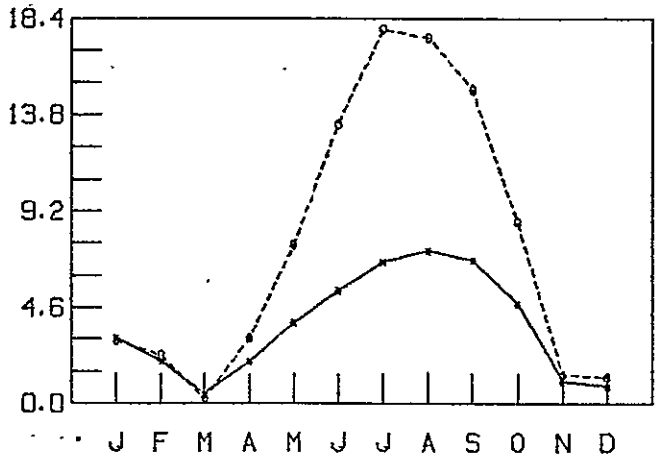
Figure 21.

TIME SPECTRA FOR THE COMPONENT 4,0

T850

AMPLITUDES A.

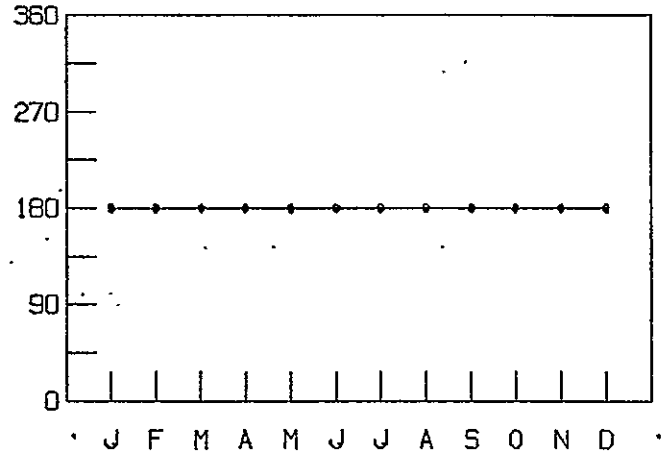
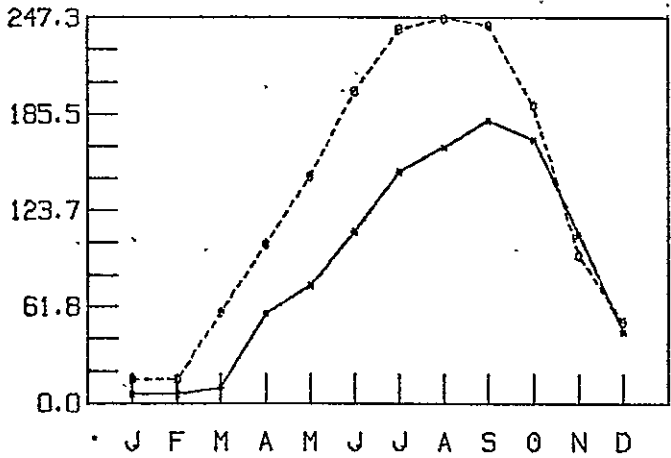
PHASES B.



G500

AMPLITUDES A.

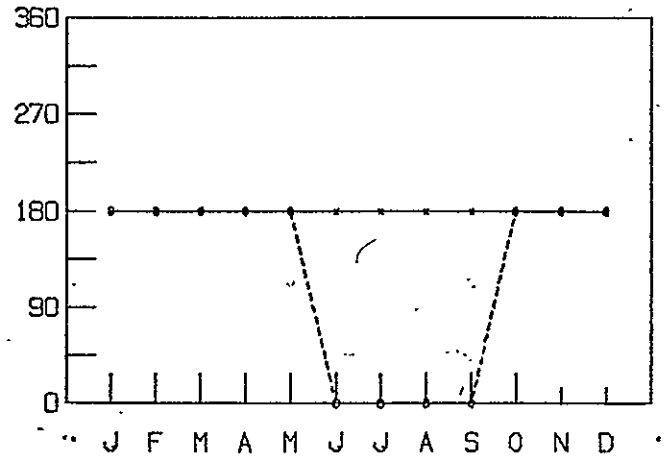
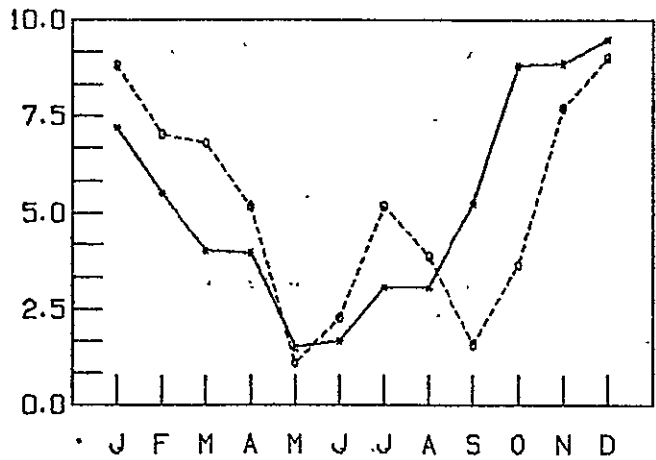
PHASES B.



SLP

AMPLITUDES A.

PHASES B.



behind the June solstice due to the thermal inertia of the earth's atmosphere. The model displays the same annual cycle, but the larger amplitude due to overheating of the continents in northern latitudes. Also, the maximum in the M T850 cycle occurs in July, which indicates too little thermal inertia in the model atmosphere. A similar cycle for 4,0 in T850 is observed for the Northern Hemisphere (Figure 21), with two maxima and two minima associated with phase shifts. This cycle is correlated with the annual insolation. The winter cycle of 4,0 for T850 is perfectly simulated by the model, while the summer cycle is overestimated. This result further illustrates the fact that the model artificially overheats the Northern Hemisphere in summer. This is also indicated by the large amplitudes of the model (4,0) of G500 in summer (Figure 21). For SLP, the amplitude of the global 4,0 harmonic (Figure 20) is underestimated, with incorrect phase from May through September, while in the Northern Hemisphere (Figure 21), the model more closely parallels the observed amplitude, although the phases are still shifted in summer.

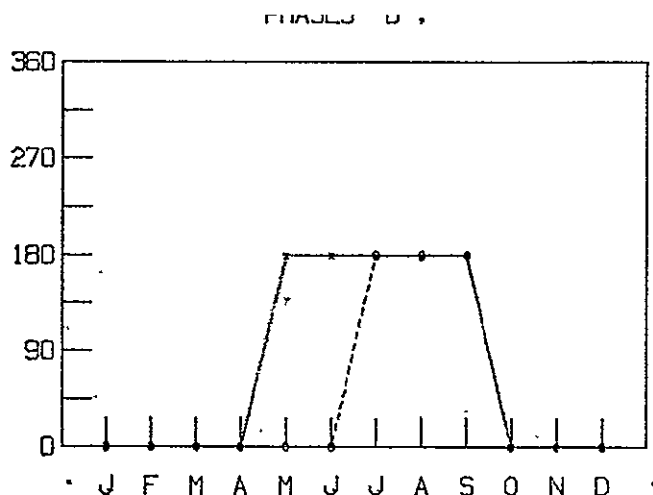
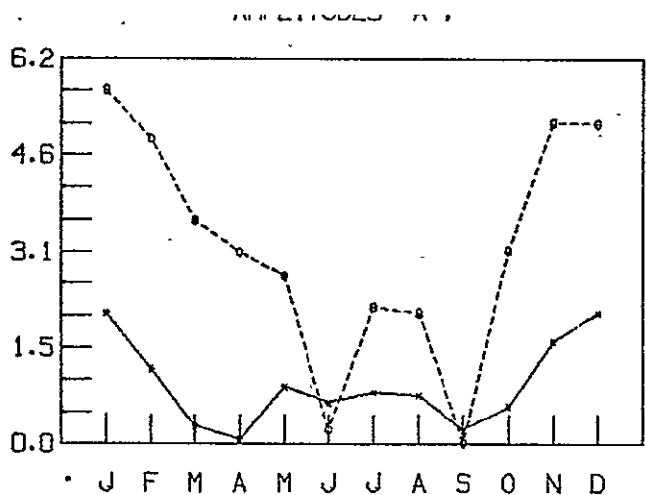
The 6,0 harmonic (Figures 22 and 23) is important as it represents the SLP meridional structure. However, in both the global and hemispheric analyses, the M annual cycle of 6,0 for SLP is very different from the corresponding C cycle. This may be due to the errors found over cold areas (Antarctic and Greenland), which appear to generate artificial high pressure systems. This results in a "squeezing" of the pressure systems in lower latitudes, with consequent meridional structure quite different than the one in Figure 12. For T850 and G500 the annual range of 6,0 is overestimated by the model.

From the annual cycles of the component 1,1 (Figures 24 and 25) it can be observed that the T850 cycle is overestimated in amplitude by the model, but with nearly correct phase. On the other hand, the model underestimates the amplitude of the 1,1 harmonic of G500, but

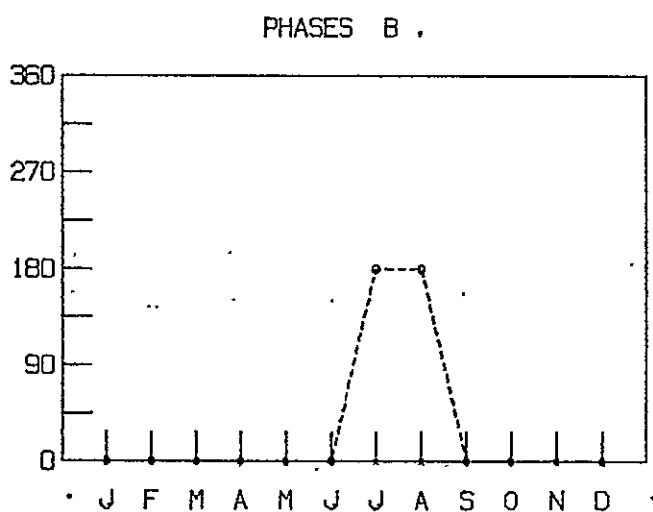
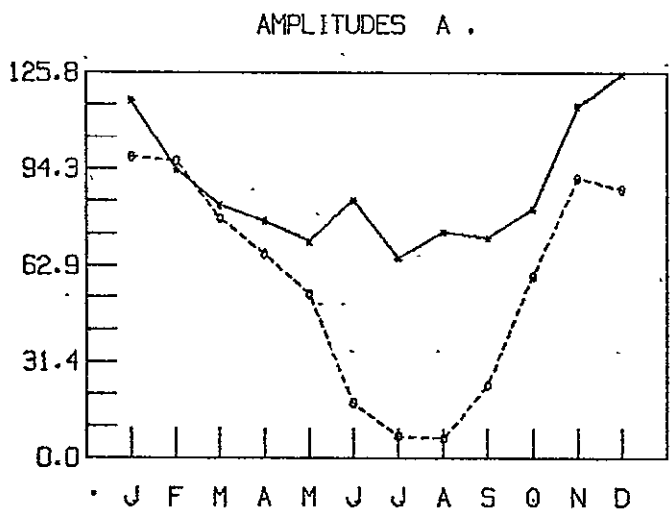
Figure 22.

TIME SPECTRA FOR THE COMPONENT 6,0

T850



G500



SLP

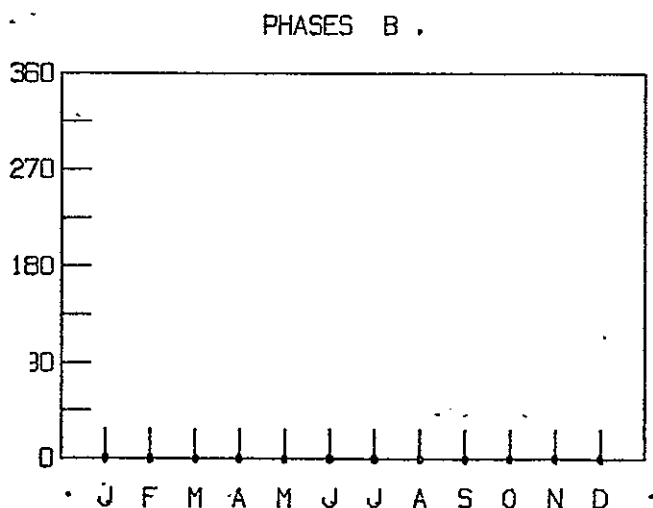
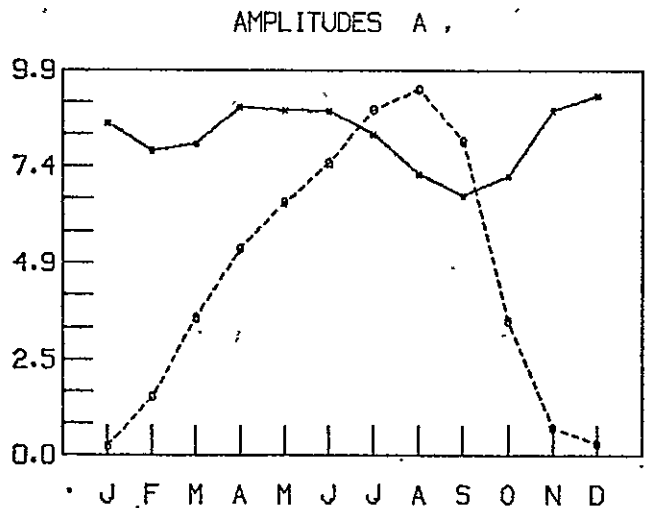
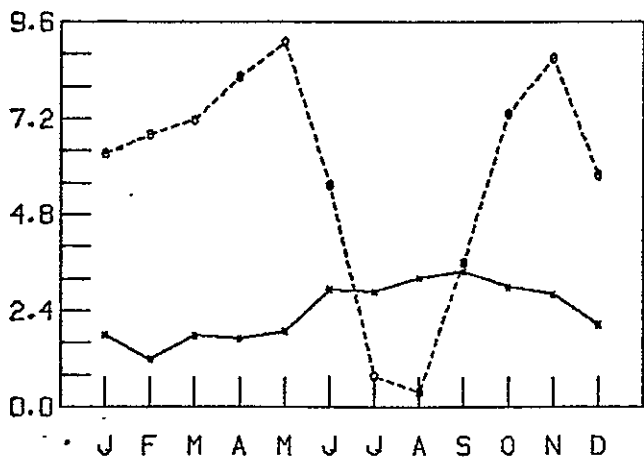


figure 23.

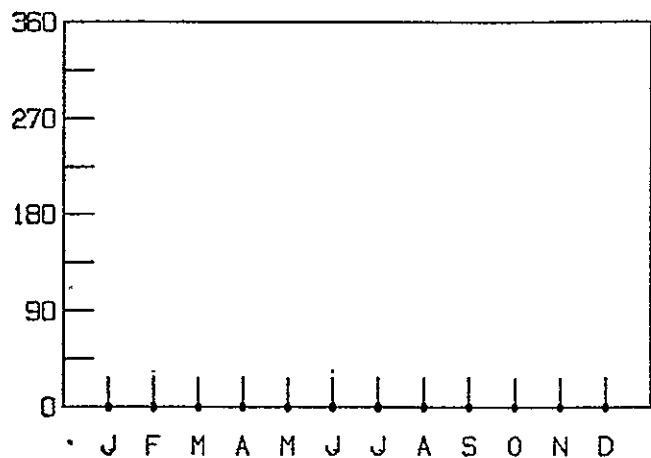
TIME SPECTRA FOR THE COMPONENT 6,0

T850

AMPLITUDES A .

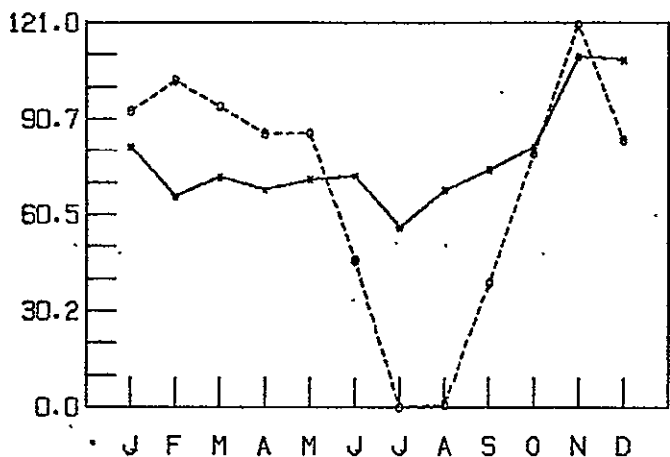


PHASES B .

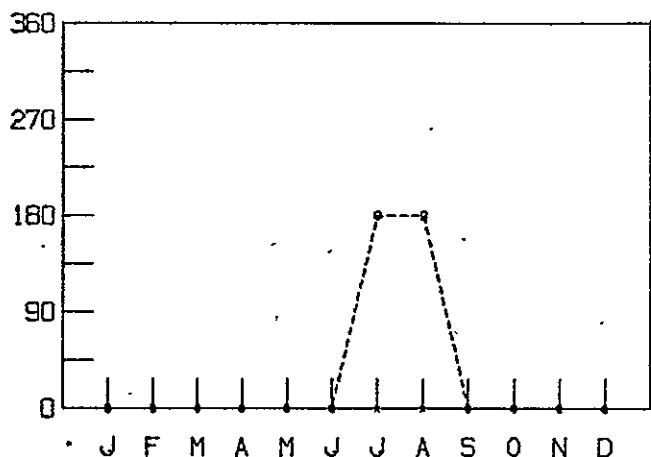


G500

AMPLITUDES A .

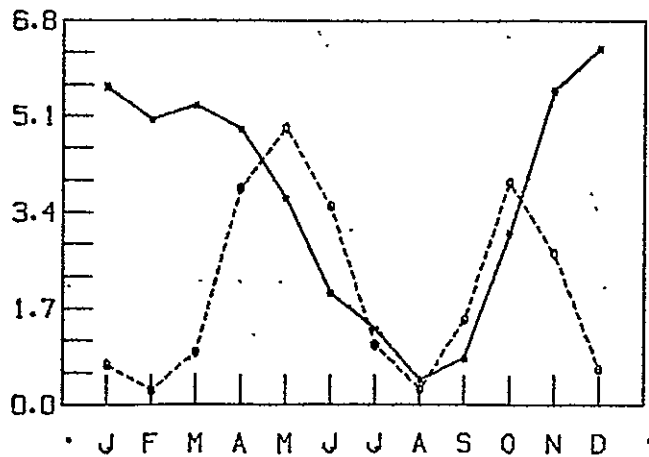


PHASES B .



SLP

AMPLITUDES A .



PHASES B .

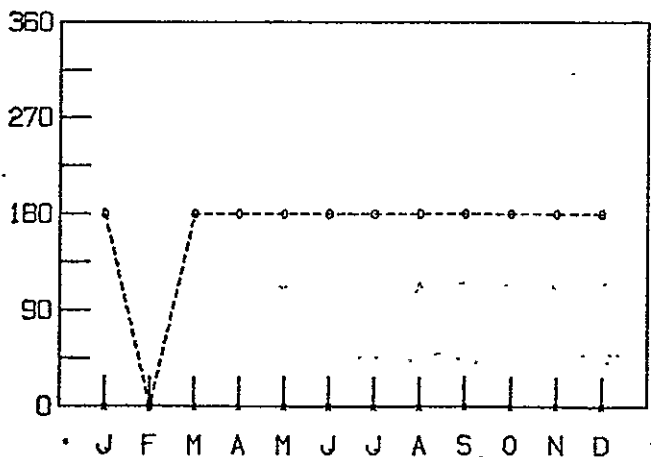


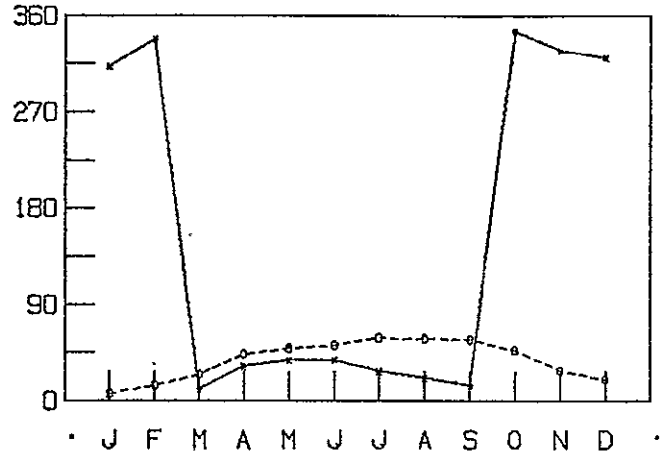
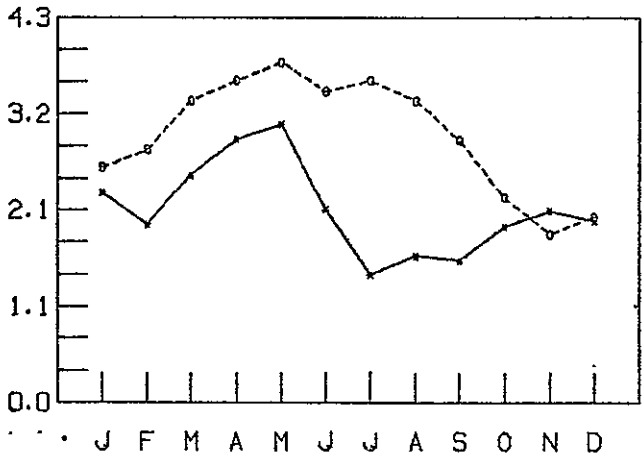
Figure 24.

TIME SPECTRA FOR THE COMPONENT 1,1

T850

AMPLITUDES A.

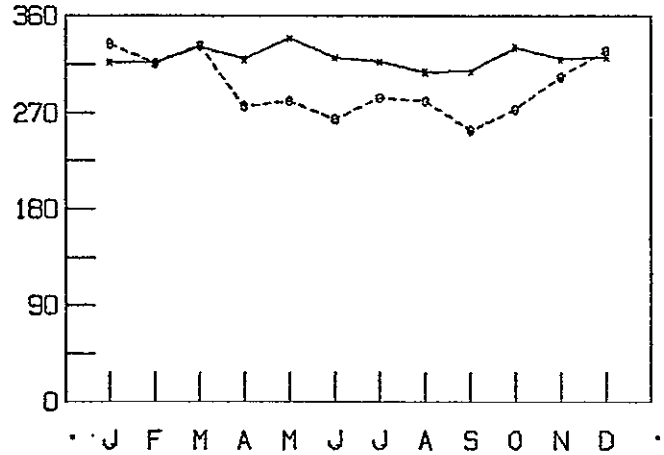
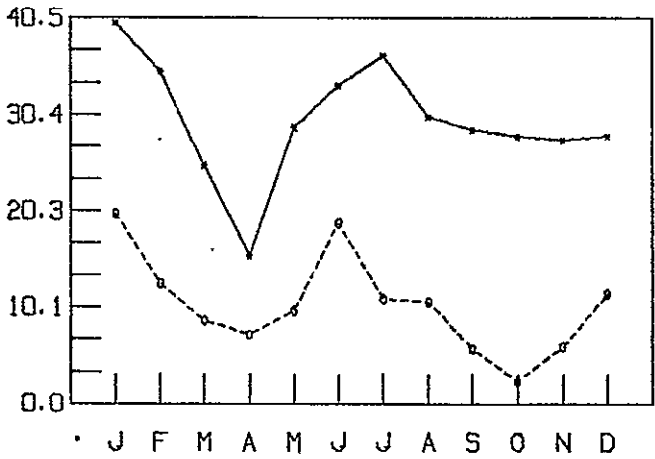
PHASES B.



G500

AMPLITUDES A.

PHASES B.



SLP

AMPLITUDES A.

PHASES B.

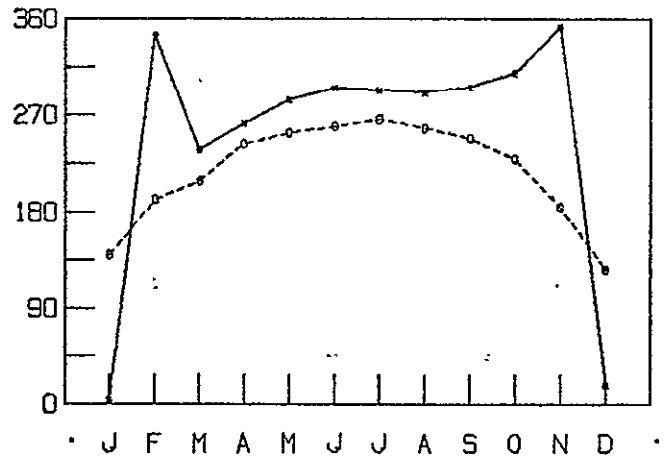
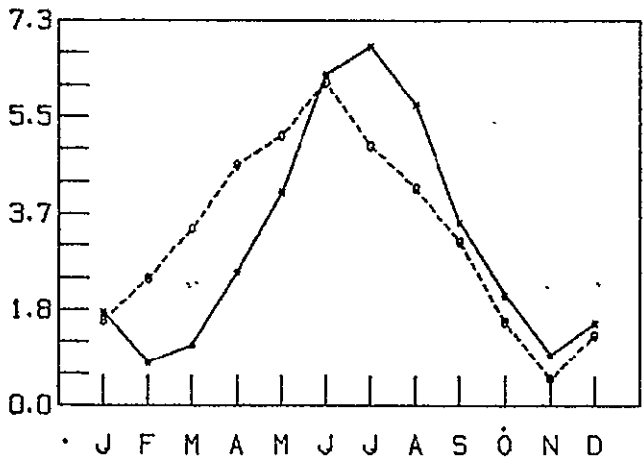
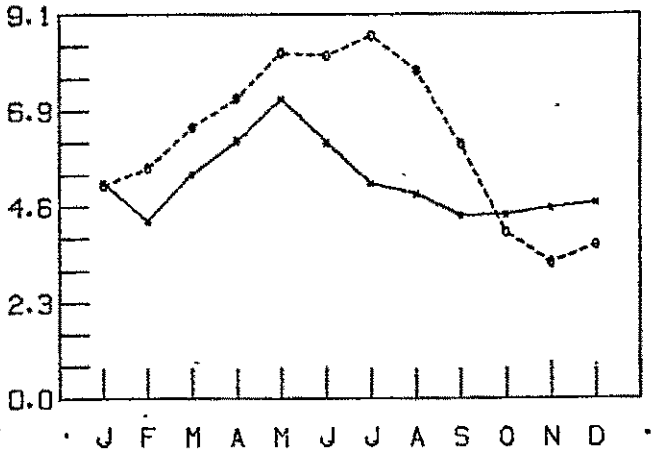


Figure 25.

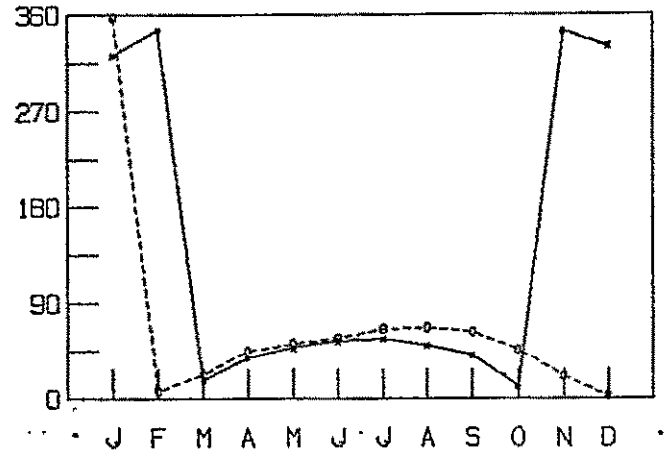
TIME SPECTRA FOR THE COMPONENT 1,1

T850

AMPLITUDES A .

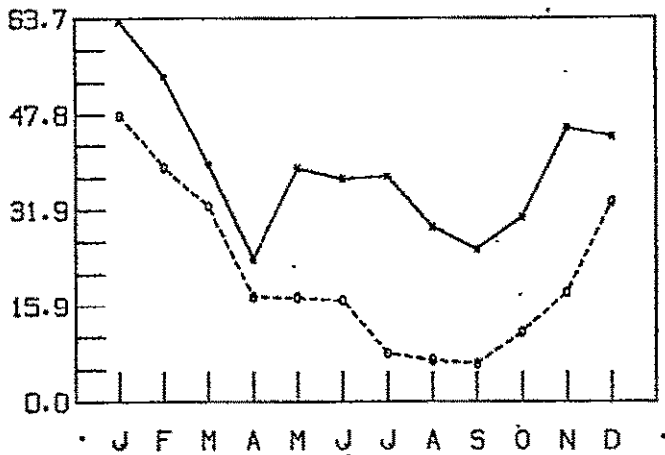


PHASES B .

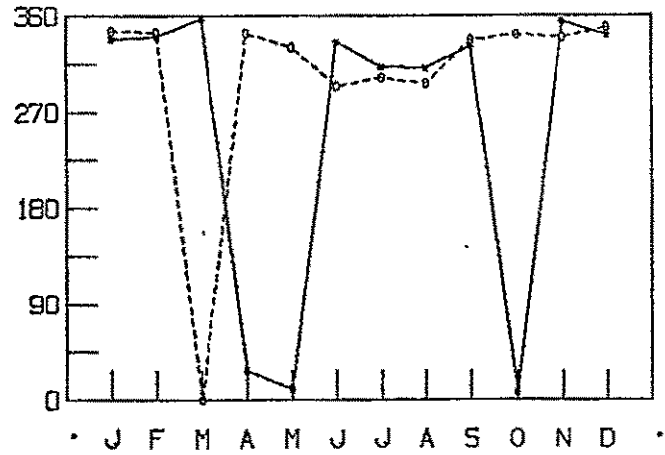


G500

AMPLITUDES A .

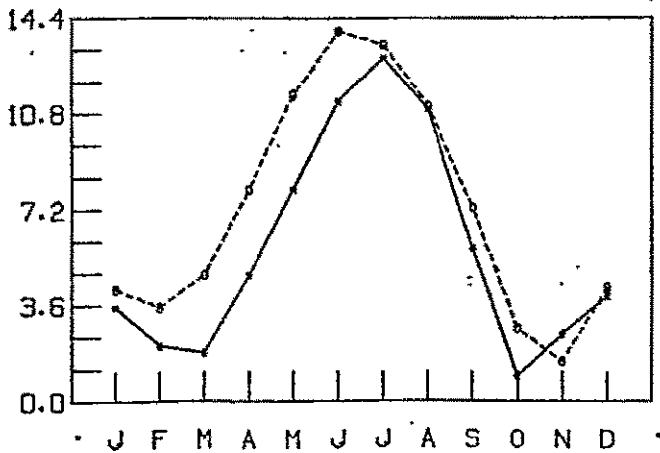


PHASES B .

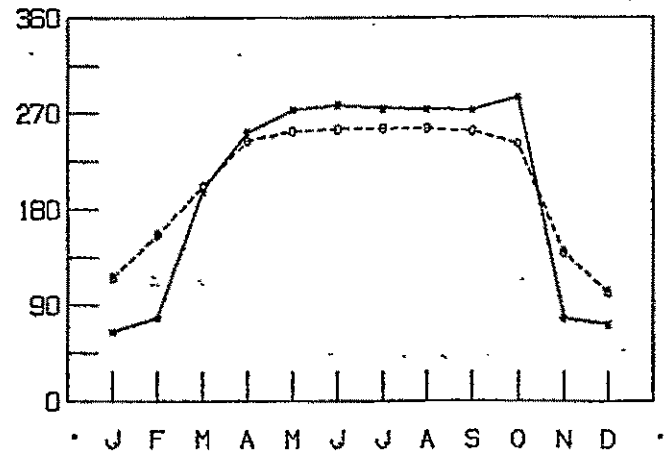


SLP

AMPLITUDES A .



PHASES B .



rather faithfully reproduces the global phase. It also produces reasonably close simulations of the 1,1 cycles of SLP. The Northern Hemisphere phase change (90° to 270°) from winter to summer (Figure 25) largely reflects the seasonal change in pressure over Asia.

The 2,1 harmonic (Figure 26) for the SLP represents mainly the difference between the Siberian anticyclone and the Canadian high in the Northern Hemisphere winter, as indicated by the 90° phase angle. The annual cycle of 2,1 is similar to 1,1, with an overestimation of the amplitude, notably in July, and a seasonal phase reversal reflecting the monsoonal pressure change over Asia. In T850 the 2,1 largely reflects the seasonal temperature differences between the hemispheres as well as the heating of the Asiatic continent in summer, as indicated by the maximum amplitude in July. The model correctly simulates the seasonal phase shift, but exaggerates the July amplitude, apparently due to over-heating of the Asiatic continent. For G500 the observed cycle of 2,1 is generally followed in phase and amplitude by the model.

In the SLP the cycle of 3,1 (Figures 27 and 28) is also dominated by the Siberian anticyclone during the winter, which is replaced by a low pressure system during summer. This is indicated, as in 2,1 and 1,1, by the seasonal phase shift. The above cycle is poorly represented by the model in the global analysis, while in the Northern Hemisphere the cycle is correct but overestimated, indicating some difficulty with the simulation of the Southern Hemisphere. The annual cycle of 3,1 for T850 is biased in amplitude for the Northern Hemisphere, while for the globe the summer cycle is not correctly represented in amplitude and phase.

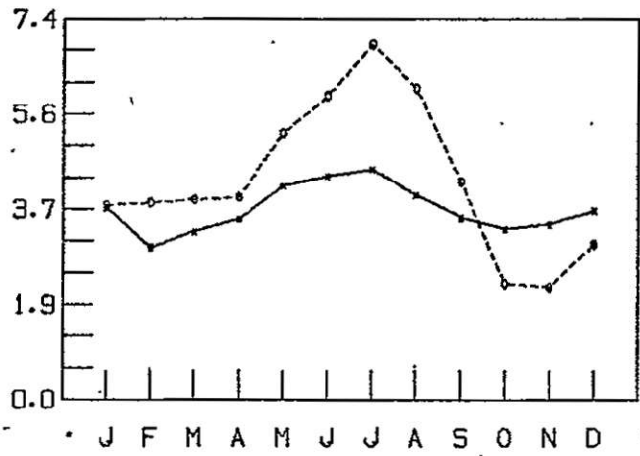
The component 2,2 (Figures 29 and 30) is related to the land-sea differences of temperature, geopotential and pressure. For all C fields similar annual cycles are observed, with two maxima and two minima. The model in July overestimates the amplitude of 2,2 in T850 and SLP, but

Figure 26.

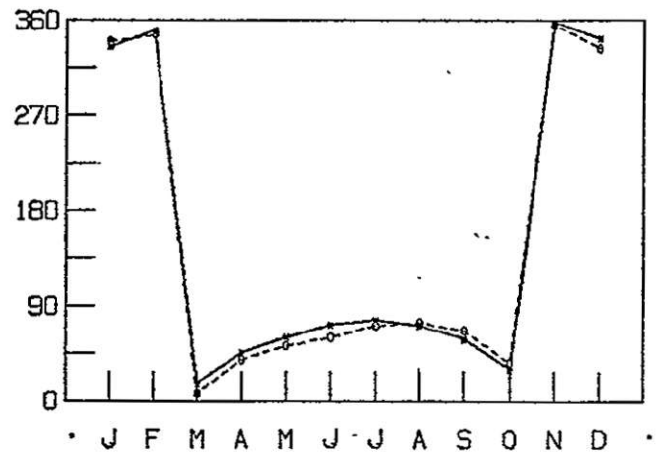
TIME SPECTRA FOR THE COMPONENT 2,1

T850

AMPLITUDES A .

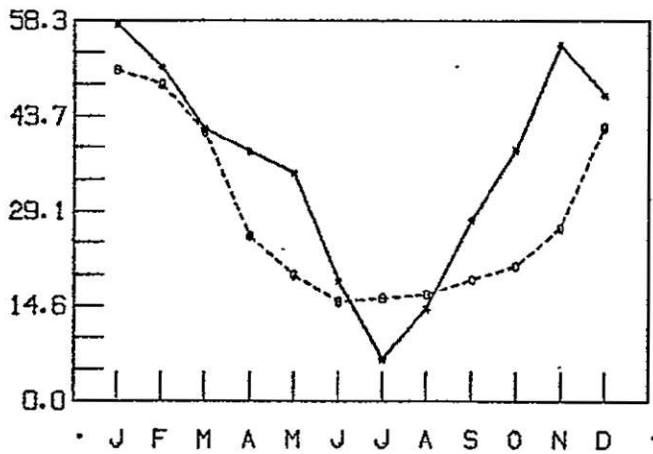


PHASES B .

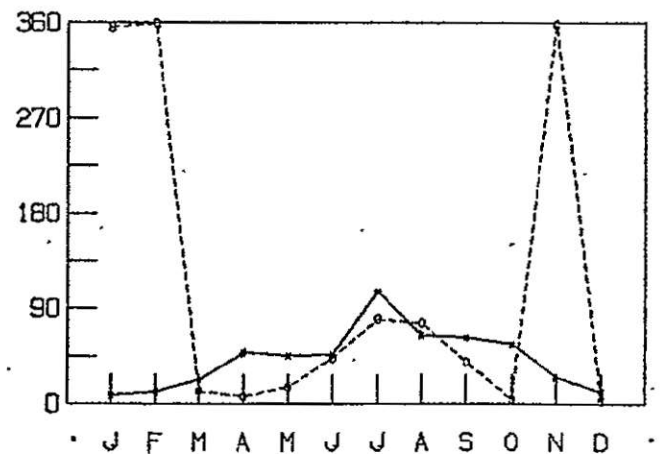


G500

AMPLITUDES A .

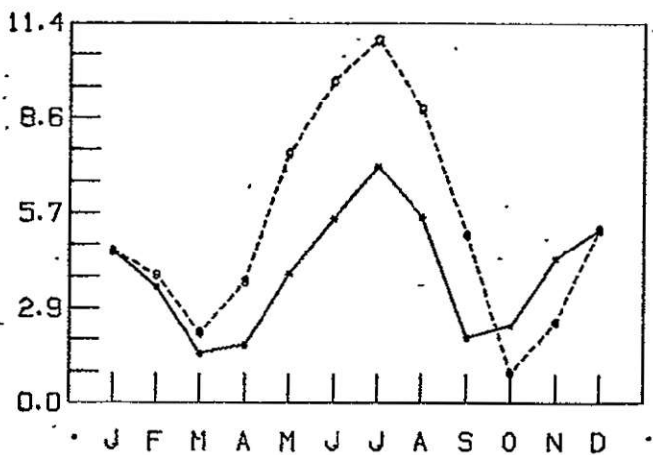


PHASES B .



SLP

AMPLITUDES A .



PHASES B .

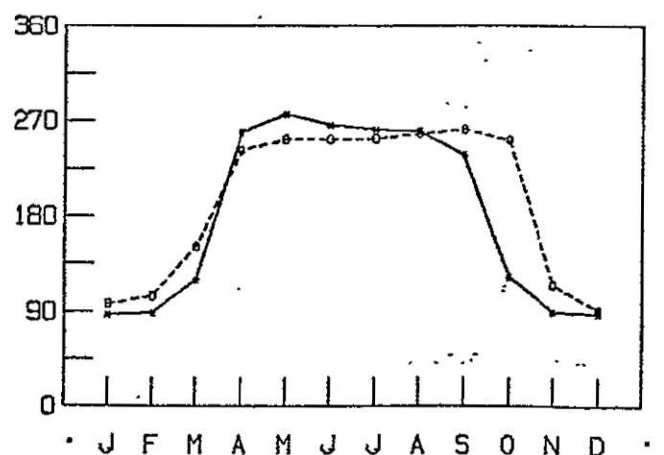


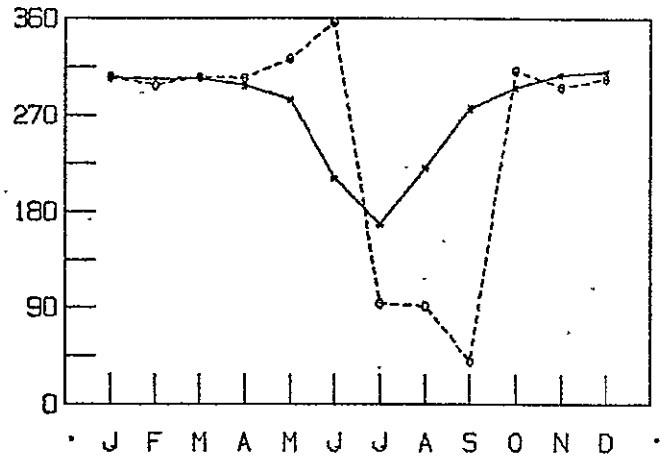
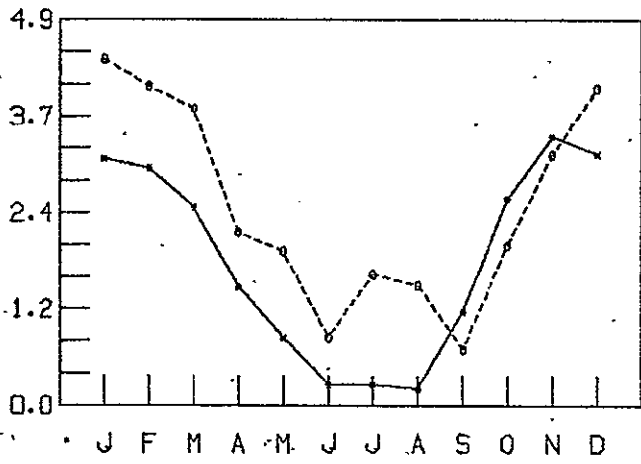
Figure 27.

TIME SPECTRA FOR THE COMPONENT 3,1

T850

AMPLITUDES A ,

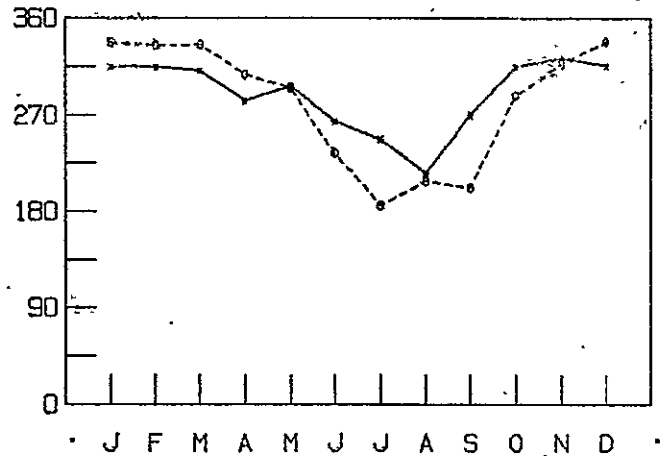
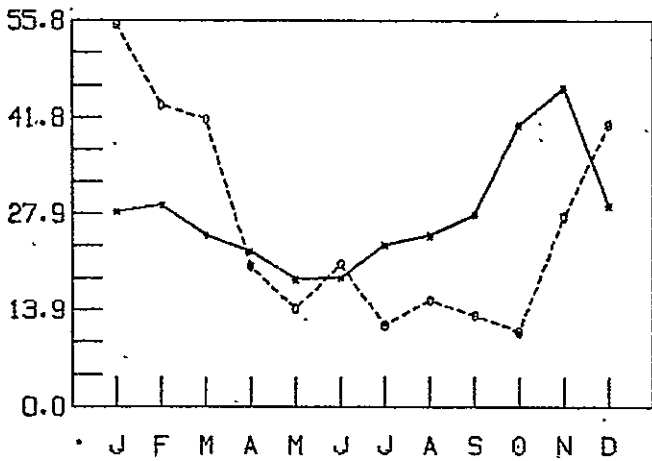
PHASES B ,



G500

AMPLITUDES A ,

PHASES B ,



SLP

AMPLITUDES A ,

PHASES B ,

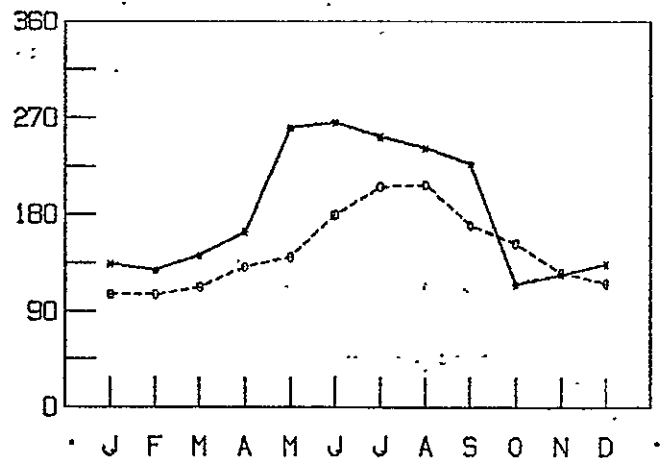
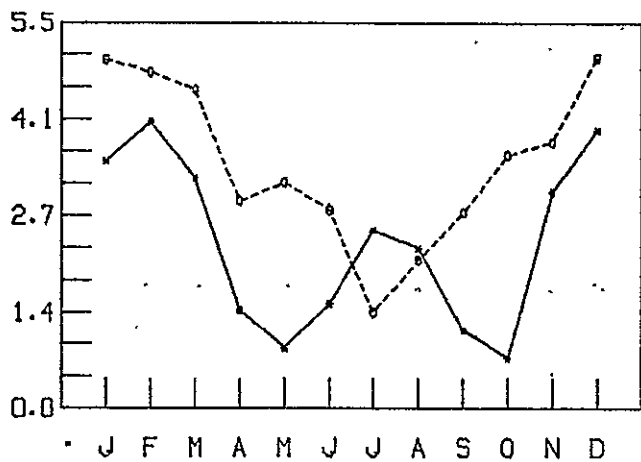
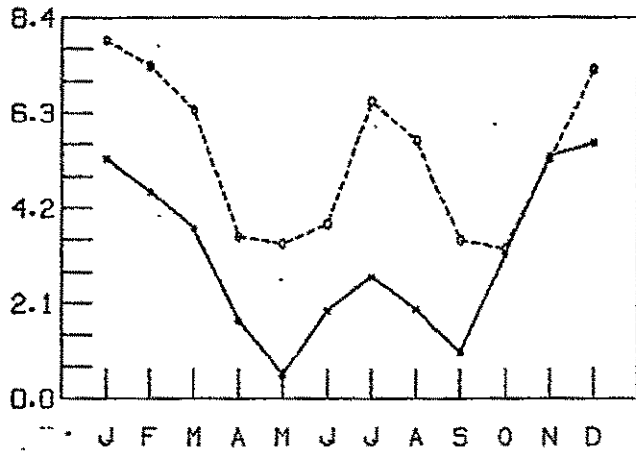


Figure 28.

TIME SPECTRA FOR THE COMPONENT 3,1

T850

AMPLITUDES A ,

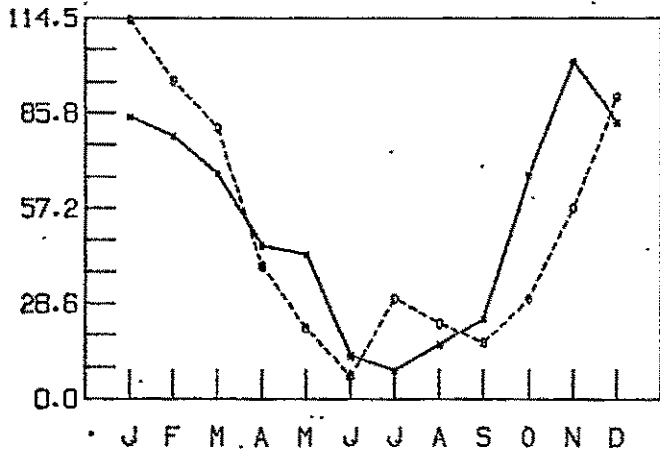


PHASES B ,

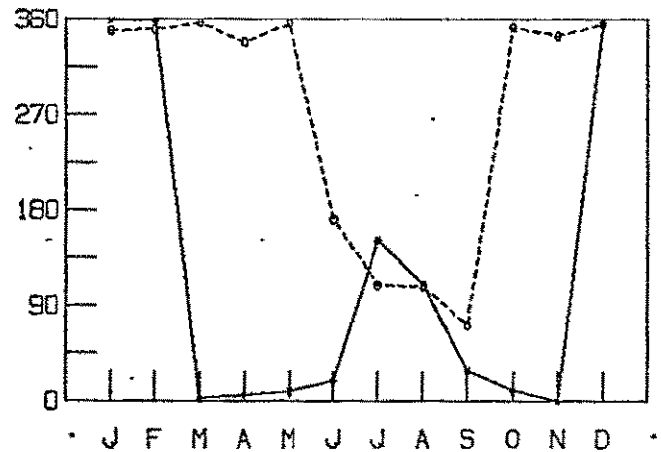


G500

AMPLITUDES A ,

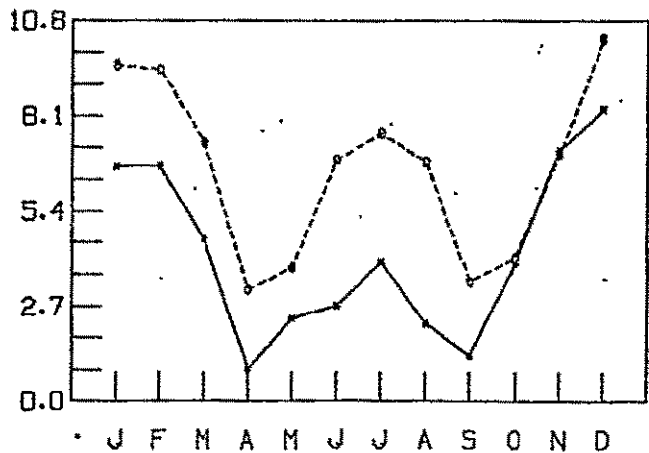


PHASES B ,



SLP

AMPLITUDES A ,



PHASES B ,

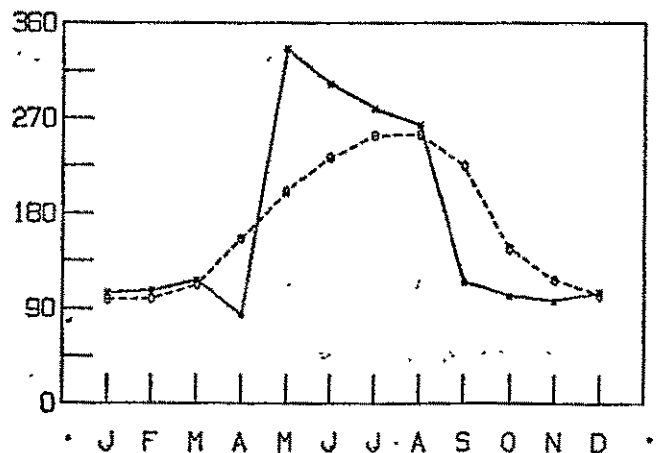


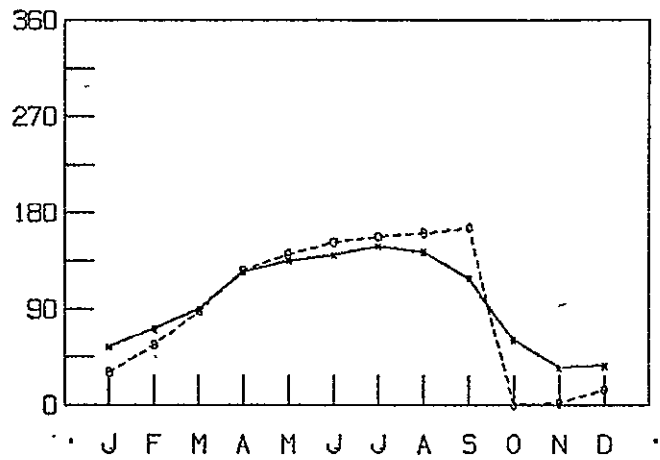
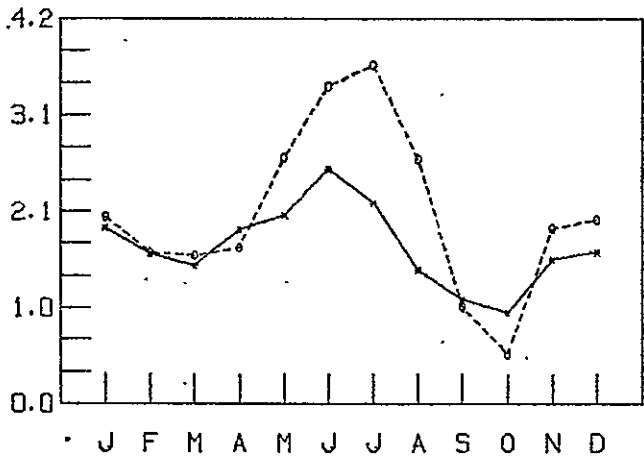
Figure 29.

TIME SPECTRA FOR THE COMPONENT 2,2

T850

AMPLITUDES A .

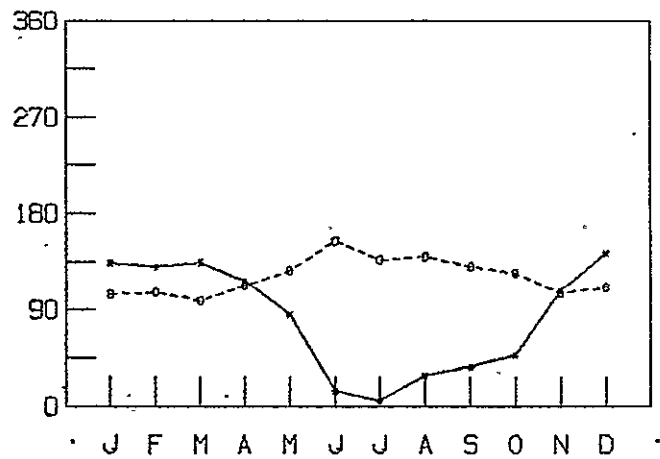
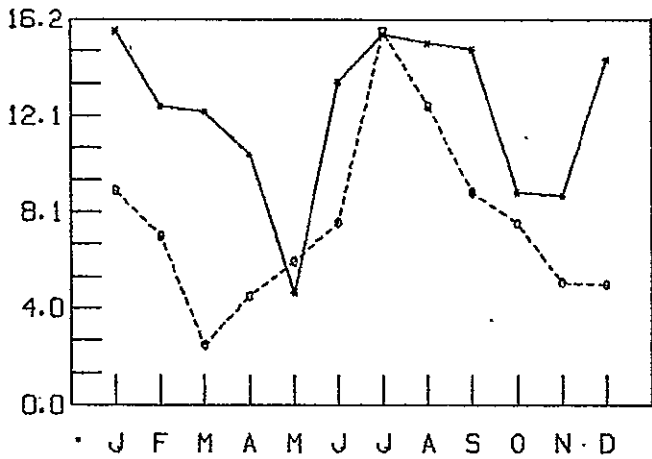
PHASES B .



G500

AMPLITUDES A .

PHASES B .



SLP

AMPLITUDES A .

PHASES B .

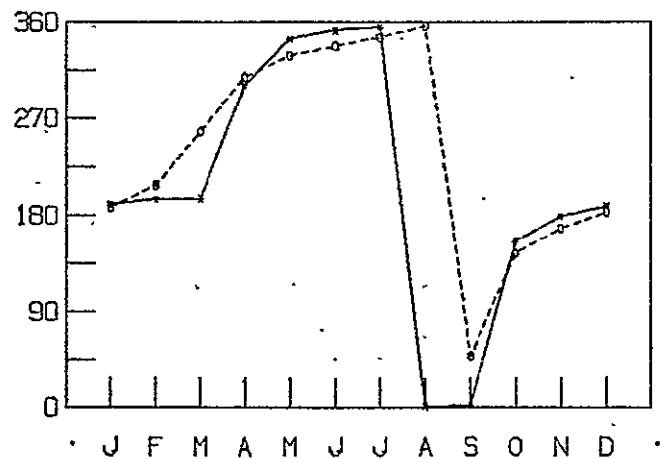
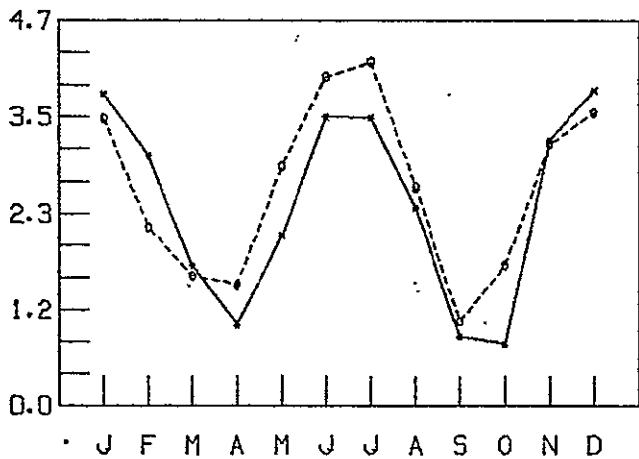


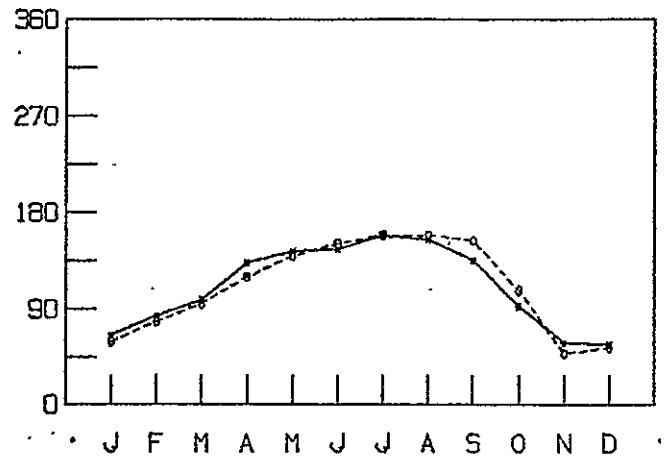
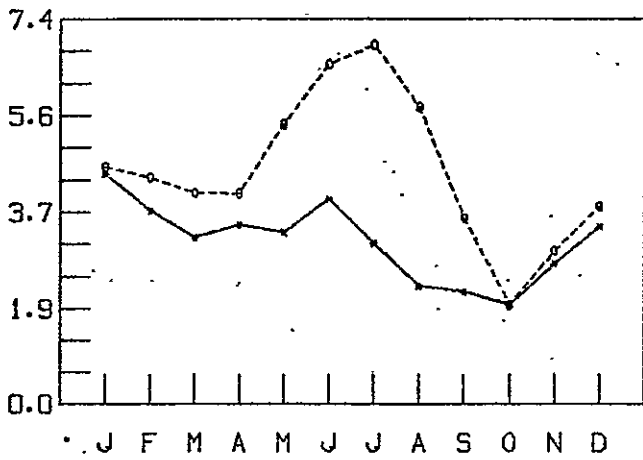
Figure 30.

TIME SPECTRA FOR THE COMPONENT 2.2

T850

AMPLITUDES A .

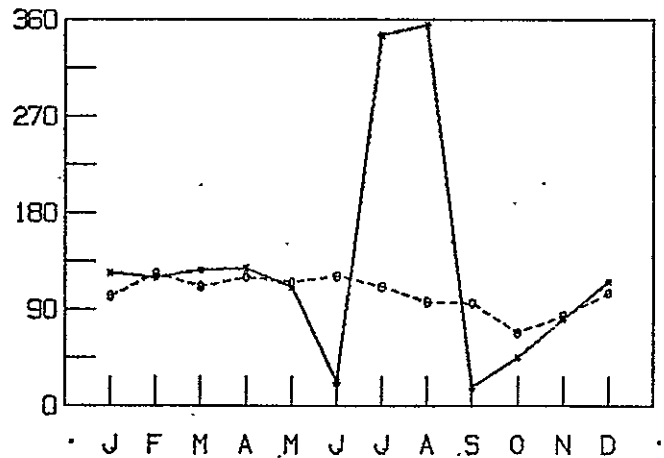
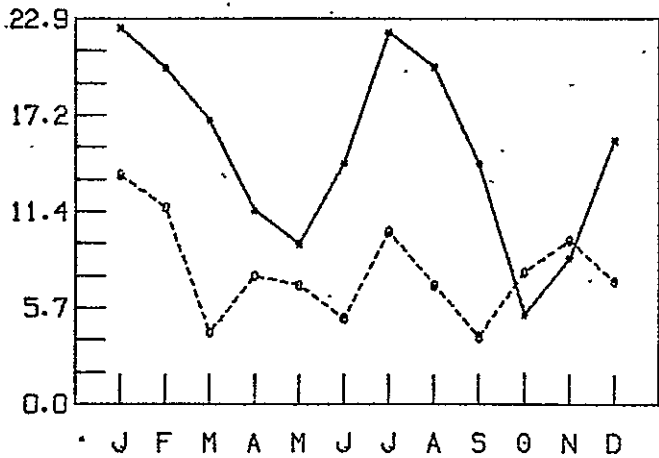
PHASES B .



G500

AMPLITUDES A .

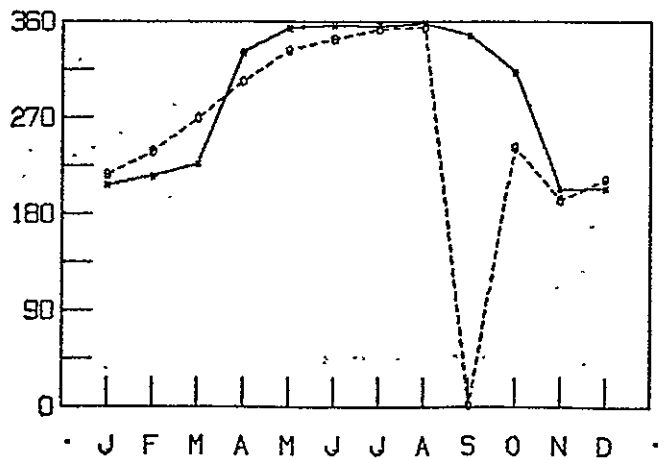
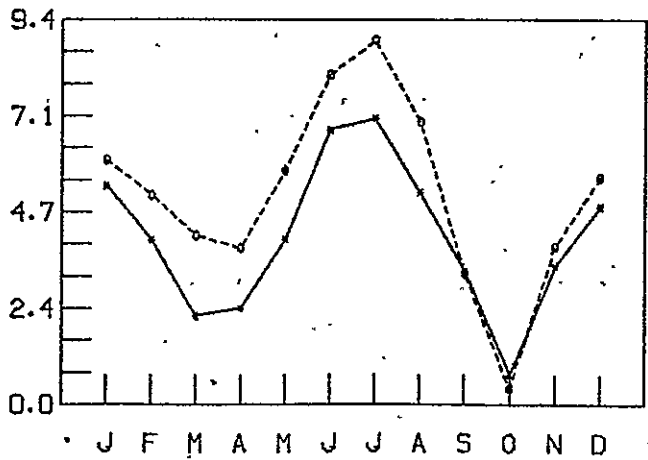
PHASES B .



SLP

AMPLITUDES A .

PHASES B .



the geographical positions of high and low values, as indicated by the phases, are well simulated.

The 3,2 component (Figure 31) reflects not only the longitudinal land-sea differences, but also the asymmetry between the hemispheres. The same characteristics are observed in the annual cycle of 3,2 for T850 and SLP as in 2,2. The G500 cycle is poorly simulated by the model. This is due to the zonal structure of the above field, which is well accounted for by the zonal harmonics, leaving only a small perturbation to be represented by the higher harmonics. Thus 3,2 is a relatively minor harmonic for G500.

The 4,2 component (Figures 32 and 33) ranks as a significant harmonic for all three fields. Additionally, for G500 4,2 corresponds to the zonal distribution of the major ridges and troughs of the quasi-stationary long wave pattern. The Northern Hemisphere annual cycles of 4,2 are similar to the global cycles, but with amplitudes twice as large. This indicates that either the Northern Hemisphere is a good reflection of the Southern Hemisphere or, more likely, the characteristics of the Northern Hemisphere dominate for all fields. As in the 3,2 harmonic, the M 4,2 component roughly parallels the annual cycle of the corresponding component for the actual climatology, with an overestimation of SLP and T850 in summer. The G500 cycle is fairly well simulated by the model in phases and amplitudes.

Very little additional information about the model simulations can be derived from the annual cycles of other spectral components. This is apparent from the mismatch of the M and C components for $n \geq 4$ and $m \geq 2$. These harmonics representing smaller scale features of the synoptic climatological patterns explain only a small part of the total variance of the three fields examined. However, it is possible to obtain further insight into the problem by comparing the observed and model climatologies as they are represented by their leading harmonics.

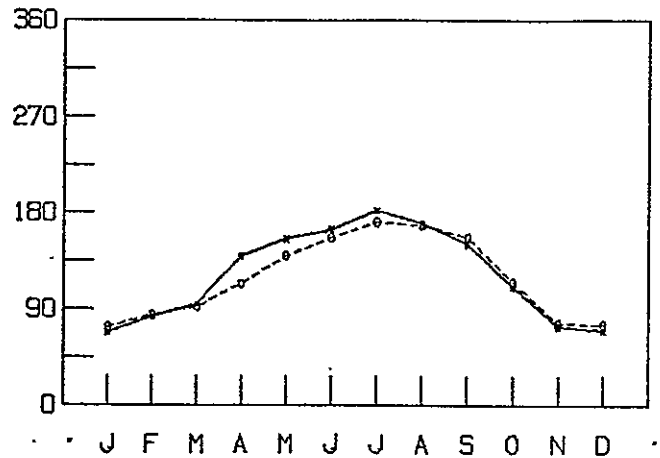
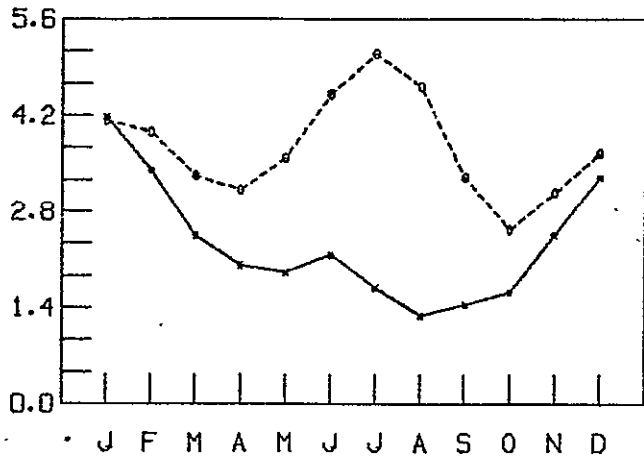
Figure 31.

TIME SPECTRA FOR THE COMPONENT 3.2

7850

AMPLITUDES A .

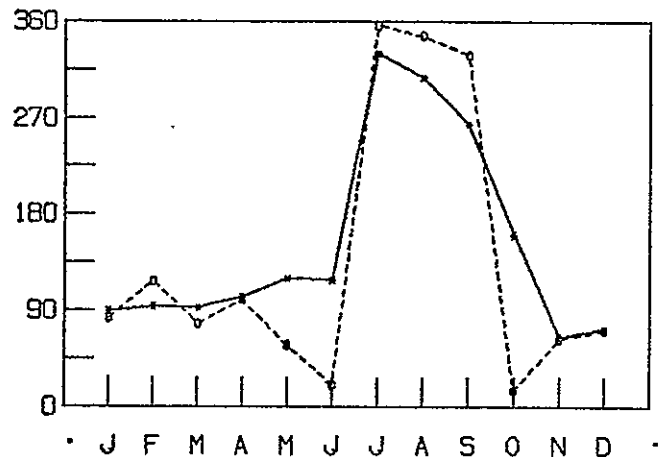
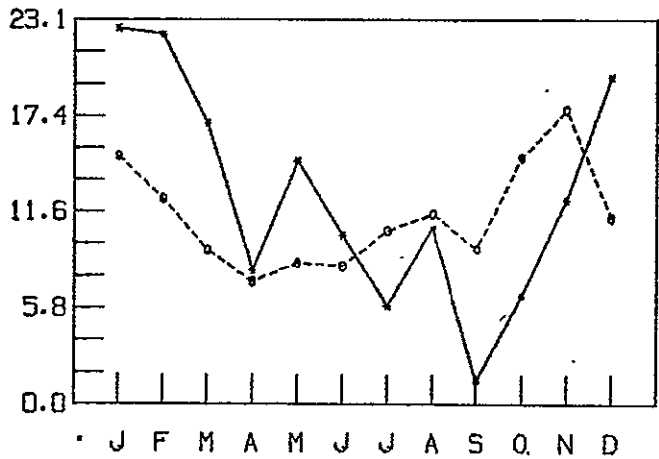
PHASES B .



6500

AMPLITUDES A .

PHASES B .



SLP

AMPLITUDES A .

PHASES B .

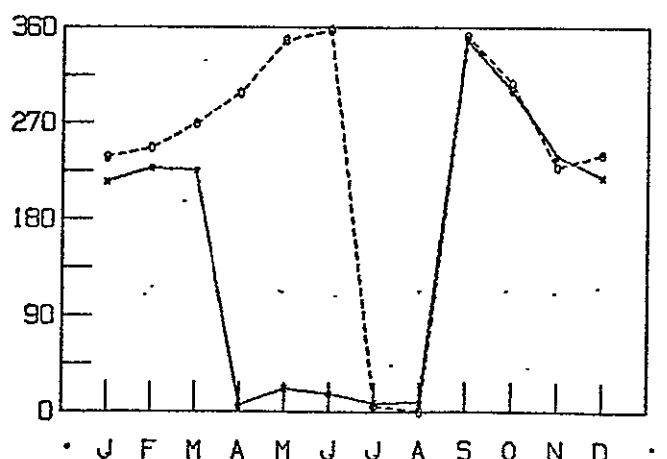
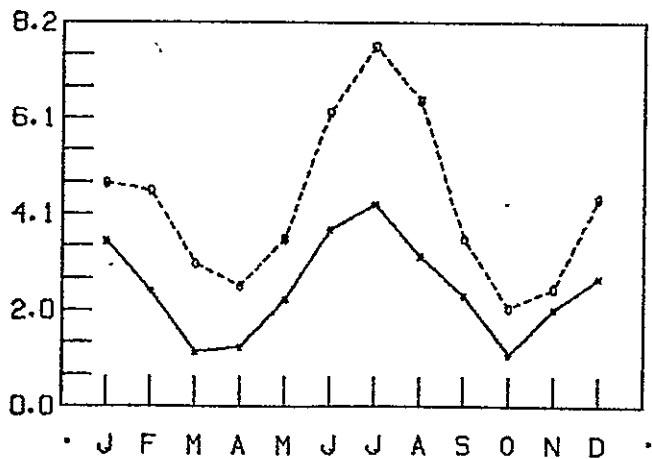


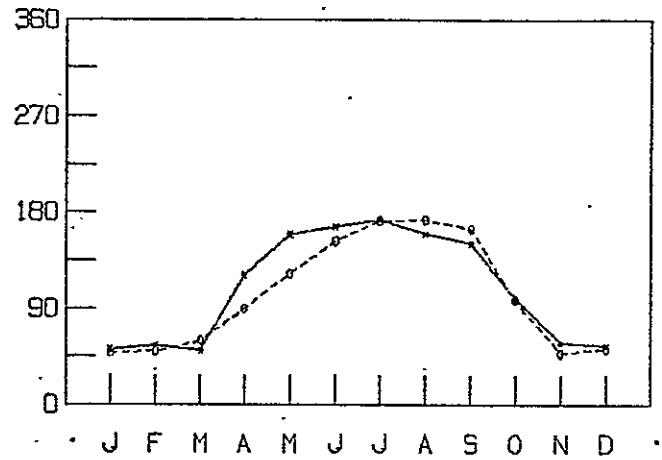
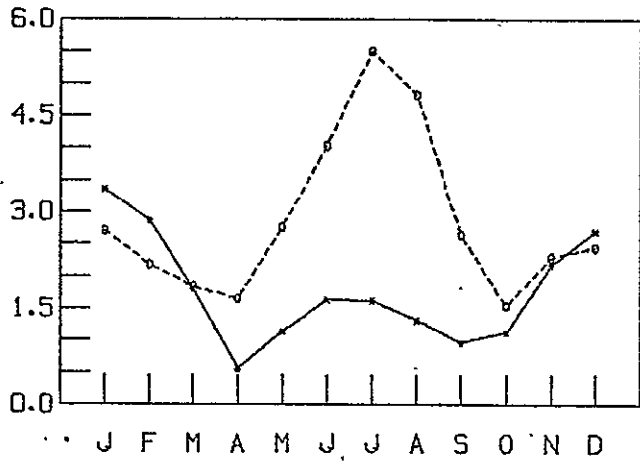
Figure 32.

TIME SPECTRA FOR THE COMPONENT 4.2

TB50

AMPLITUDES A .

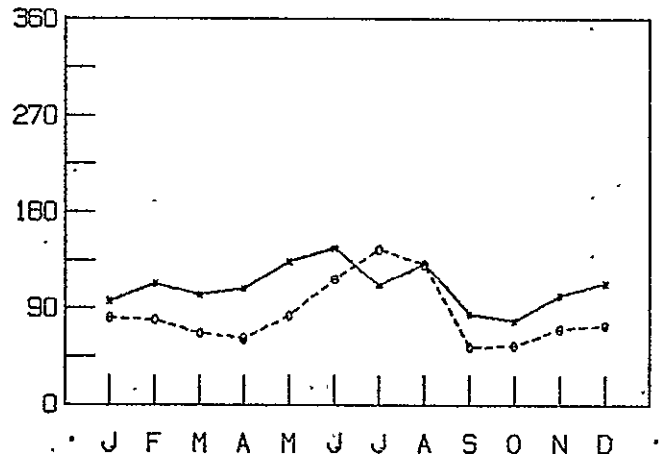
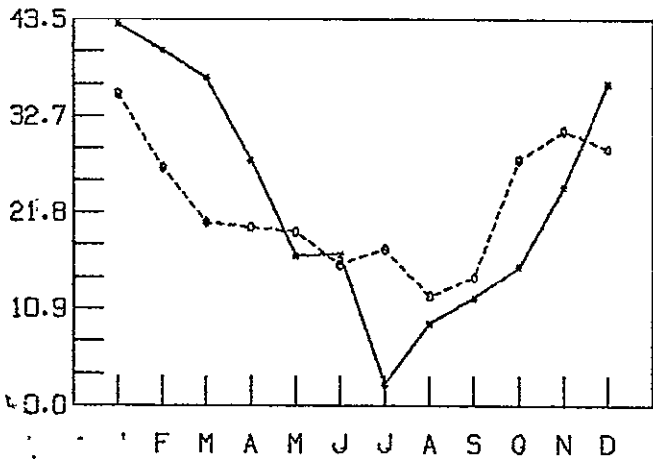
PHASES B .



6500

AMPLITUDES A .

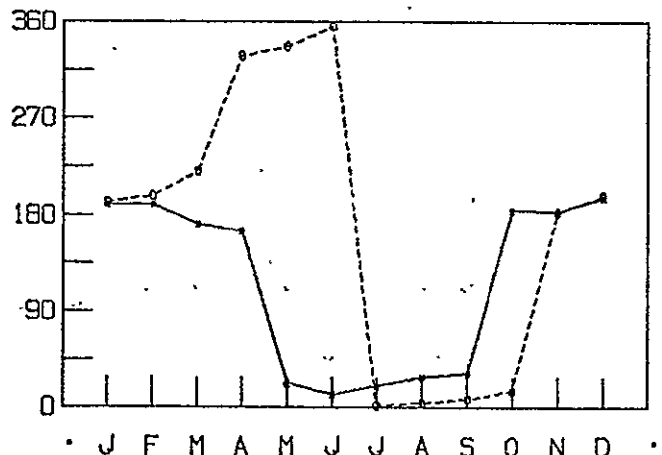
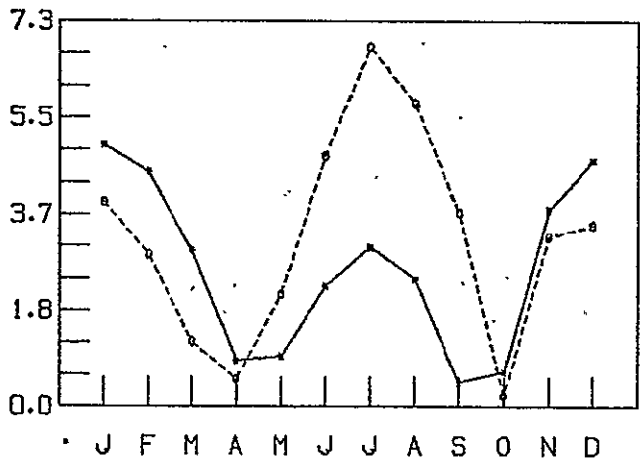
PHASES B .



SLP

AMPLITUDES A .

PHASES B .



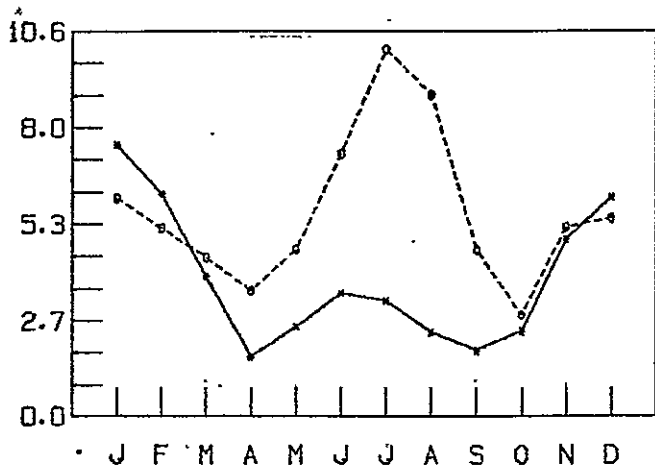
x—x—x OBSERVED o—o—o THEORY

Figure 33.

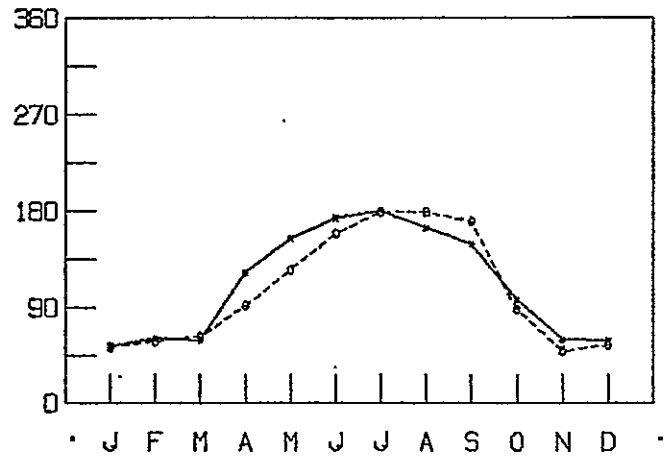
TIME SPECTRA FOR THE COMPONENT 4,2

T850

AMPLITUDES A ,

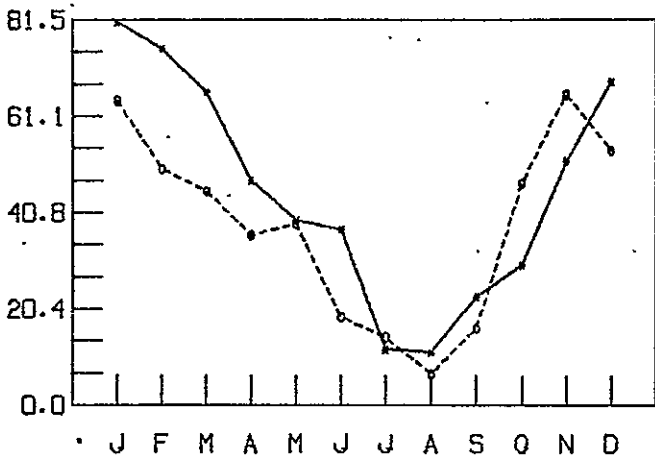


PHASES B ,

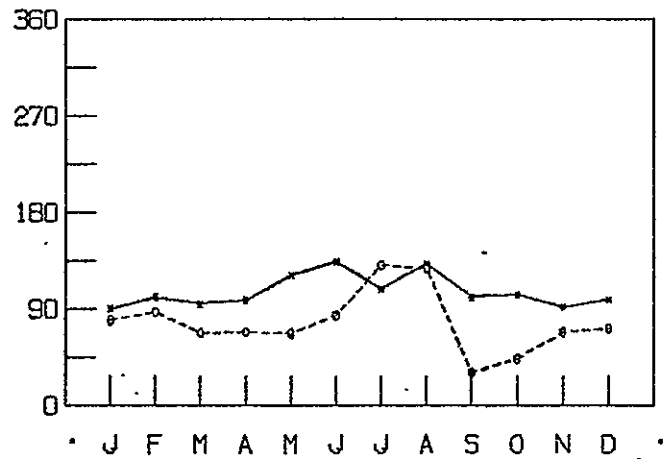


G500

AMPLITUDES A ,

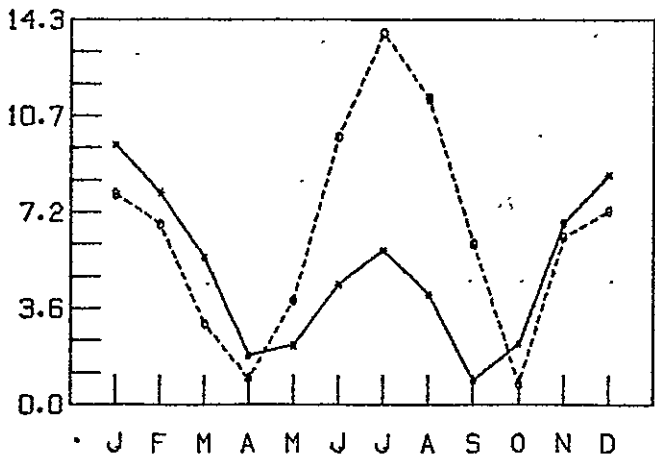


PHASES B ,

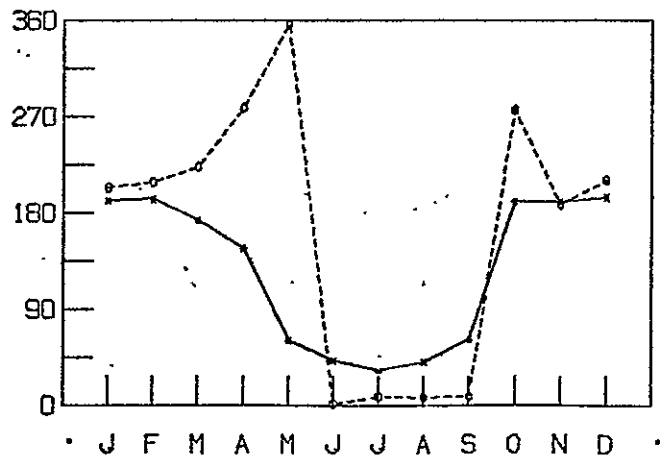


SLP

AMPLITUDES A ,



PHASES B ,



This permits an objective comparison to be made between the large-scale features of the two climatologies through the use of correlation analysis.

The following calculations were carried out:

1. Seasonal mean fields of T850, G500, and SLP were reproduced for C and M from their leading harmonics, ranked in descending order of amplitude, with the components accumulating, and correlation coefficients were computed between the corresponding reproduced fields.

2. A similar calculation was carried out using seasonal mean fields reproduced from harmonics ranked in ascending order of n and m .

In all cases, the mean value 0,0 was omitted, and, in the case of T850 and G500, the meridional structure term 2,0 was also taken out because it results in an artificially large correlation coefficient between the fields. The results obtained with both methods are displayed in Tables 9, 10, and 11 for T850, G500, and SLP respectively.

From the tables it is observed that, as the harmonics used to reproduce the fields accumulate, the correlation coefficient, r , either decreases or increases, depending on whether the fields were reproduced from the same or different dominant harmonics. For example, in Table 9, which lists the M and C T850 correlations, it is seen that when both fields are reproduced from the same single leading harmonic, the correlation coefficient is one. In spring when a second (mismatched) harmonic is added, the coefficient drops to 0.60, but when the third harmonics, which make up a set of three matching components, are added, the coefficient rises up to 0.99. The addition of weaker harmonics then degrades the correlation. The summer and winter correlations of reproduced T850 fields are quite high, while the spring and fall values are much lower. In Table 10, however, it is seen that the correlations between the fields of G500 reproduced from the leading harmonics are quite low in winter and spring, but high in summer and fall. The SLP

Table 9.

Correlation coefficients between the reproduced seasonal M and C fields from their: a) leading harmonics, b) harmonics ranked in ascending order of wavenumbers n,m. T850

a	WINTER			SPRING			SUMMER			FALL		
	C n,m	M n,m	r	C n,m	M n,m	r	C n,m	M n,m	r	C n,m	M n,m	r
	1, 0	1, 0	1.00	4, 0	4, 0	1.00	1, 0	1, 0	1.00	1, 0	1, 0	1.00
	3, 2	5, 0	0.89	2, 1	5, 0	0.60	4, 0	4, 0	1.00	4, 0	4, 0	0.99
	2, 1	5, 1	0.82	5, 0	2, 1	0.99	2, 1	2, 1	1.00	2, 1	7, 0	0.98
	3, 1	2, 1	0.90	1, 1	8, 0	0.82	5, 1	7, 0	0.98	5, 4	3, 0	0.79
	4, 2	2, 1	0.92	5, 4	7, 0	0.72	5, 0	4, 2	0.96	3, 1	5, 4	0.80
	5, 2	6, 0	0.87	8, 0	1, 1	0.87	7, 0	3, 2	0.96	5, 0	6, 0	0.75
	5, 4	6, 2	0.85	3, 2	6, 2	0.80	2, 2	1, 1	0.94	3, 3	8, 0	0.72
	6, 2	5, 2	0.85	2, 2	3, 2	0.82	3, 0	5, 1	0.95	7, 1	2, 1	0.75
	1, 1	5, 0	0.82	6, 2	6, 0	0.82	3, 3	2, 2	0.95	1, 1	3, 2	0.72
	5, 0	4, 1	0.85	3, 1	7, 2	0.78	5, 4	8, 2	0.94	8, 0	1, 2	0.75
	4, 1	5, 2	0.85	3, 0	5, 1	0.75	8, 0	5, 4	0.94	3, 2	6, 4	0.78
	6, 0	6, 1	0.87	6, 1	3, 1	0.76	7, 1	6, 4	0.94	7, 0	4, 4	0.78
	2, 2	1, 1	0.87	1, 0	5, 4	0.78	1, 1	7, 2	0.94	4, 2	8, 1	0.76
	5, 3	4, 2	0.90	5, 1	8, 1	0.79	3, 2	5, 2	0.95	5, 2	7, 2	0.75
	4, 4	7, 5	0.89	3, 3	16, 0	0.77	4, 1	3, 3	0.95	5, 1	5, 3	0.76
	7, 3	4, 5	0.90	7, 7	15, 0	0.76	4, 1	5, 0	0.94	6, 1	3, 3	0.76
	6, 3	4, 5	0.91	6, 3	12, 0	0.75	6, 2	6, 2	0.94	7, 3	7, 3	0.76
	7, 1	7, 5	0.92	16, 0	4, 2	0.75	5, 3	7, 1	0.94	8, 1	3, 1	0.78
	6, 1	4, 4	0.90	9, 2	2, 2	0.76	8, 2	3, 0	0.94	2, 2	5, 2	0.76
	4, 0	2, 2	0.92	18, 1	6, 2	0.76	9, 6	17, 2	0.93	4, 1	4, 2	0.76
	8, 0	6, 1	0.92	7, 2	10, 2	0.78	14, 0	4, 3	0.94	7, 2	4, 3	0.78
	8, 1	6, 1	0.92	14, 0	4, 1	0.77	16, 0	8, 0	0.94	6, 6	7, 1	0.79
	6, 6	4, 0	0.92	5, 2	8, 2	0.77	12, 1	16, 0	0.94	6, 2	13, 1	0.80
	8, 3	7, 2	0.91	7, 3	11, 2	0.76	6, 6	10, 2	0.94	6, 4	11, 3	0.79
	7, 0	5, 1	0.90	8, 1	7, 3	0.77	8, 6	4, 4	0.93	8, 2	8, 7	0.75
b	(C,M) n,m	r	(C,M) n,m	r	(C,M) n,m	r	(C,M) n,m	r				
	1, 0	1.00	1, 0	1.00	1, 0	1.00	1, 0	1.00				
	1, 1	0.99	1, 1	0.87	1, 1	1.00	1, 1	0.96				
	2, 1	0.99	2, 1	0.94	2, 1	1.00	2, 1	0.96				
	2, 2	0.99	2, 2	0.94	2, 2	1.00	2, 2	0.96				
	3, 3	0.97	3, 3	0.84	3, 3	0.98	3, 3	0.89				
	4, 4	0.94	4, 4	0.86	4, 4	0.97	4, 4	0.89				
	5, 5	0.94	5, 5	0.88	5, 5	0.96	5, 5	0.87				
	6, 6	0.92	6, 6	0.84	6, 6	0.95	6, 6	0.85				
	7, 7	0.92	7, 7	0.82	7, 7	0.94	7, 7	0.84				
	8, 8	0.90	8, 8	0.81	8, 8	0.94	8, 8	0.83				
	9, 9	0.90	9, 9	0.80	9, 9	0.94	9, 9	0.82				
	10, 10	0.89	10, 10	0.79	10, 10	0.94	10, 10	0.82				
	11, 11	0.89	11, 11	0.78	11, 11	0.93	11, 11	0.82				
	12, 12	0.89	12, 12	0.77	12, 12	0.93	12, 12	0.81				
	13, 13	0.89	13, 13	0.76	13, 13	0.93	13, 13	0.81				
	14, 14	0.88	14, 14	0.76	14, 14	0.93	14, 14	0.81				
	15, 15	0.88	15, 15	0.76	15, 15	0.93	15, 15	0.81				
	16, 16	0.87	16, 16	0.76	16, 16	0.93	16, 16	0.80				
	17, 17	0.87	17, 17	0.76	17, 17	0.92	17, 17	0.80				
	18, 18	0.87	18, 18	0.76	18, 18	0.92	18, 18	0.80				

Table 10.

Correlation coefficients between the reproduced seasonal M and C fields from their: a) leading harmonics, b) harmonics ranked in ascending order of wavenumbers n,m. G 500

WINTER			SPRING			SUMMER			FALL		
C	n,m	r	C	n,m	r	C	n,m	r	C	n,m	r
6, 0	1, 0	0.60	4, 0	4, 0	1.00	1, 0	1, 0	1.00	1, 0	1, 0	1.00
4, 0	6, 0	0.31	3, 0	4, 0	0.50	4, 0	4, 0	1.00	4, 0	4, 0	1.00
1, 0	4, 0	0.88	1, 0	6, 0	0.54	3, 0	5, 0	0.96	6, 0	6, 0	1.00
3, 0	4, 1	0.79	6, 0	7, 2	0.63	6, 0	3, 0	0.97	3, 0	7, 0	0.98
7, 0	2, 1	0.74	4, 1	5, 1	0.81	9, 0	7, 0	0.97	4, 1	7, 2	0.92
2, 1	5, 1	0.75	5, 0	5, 2	0.59	4, 1	4, 1	0.96	2, 1	7, 3	0.92
4, 1	5, 0	0.76	2, 1	5, 0	0.60	8, 1	9, 0	0.97	8, 1	6, 2	0.91
6, 3	6, 2	0.74	8, 1	3, 0	0.67	1, 1	7, 1	0.98	3, 1	7, 1	0.90
8, 1	5, 1	0.71	7, 0	2, 1	0.68	5, 0	10, 0	0.97	9, 0	4, 1	0.91
5, 2	5, 2	0.72	5, 2	8, 1	0.69	5, 1	9, 1	0.96	5, 2	8, 3	0.90
5, 0	6, 3	0.78	4, 2	3, 1	0.68	3, 1	9, 3	0.96	1, 1	5, 2	0.90
6, 1	5, 3	0.74	0, 3	6, 3	0.68	5, 2	5, 1	0.96	6, 3	4, 2	0.89
4, 2	4, 2	0.74	9, 0	4, 1	0.70	9, 1	8, 2	0.96	7, 2	6, 3	0.90
5, 3	7, 7	0.74	1, 1	7, 8	0.69	7, 1	6, 1	0.96	7, 1	2, 1	0.91
1, 1	5, 5	0.73	3, 1	4, 2	0.71	12, 1	8, 0	0.96	6, 2	5, 1	0.91
6, 2	7, 3	0.74	5, 1	7, 1	0.71	6, 3	11, 0	0.96	4, 2	5, 0	0.91
4, 3	6, 1	0.73	9, 1	11, 0	0.71	4, 3	7, 3	0.96	16, 1	8, 0	0.90
3, 1	5, 0	0.74	0, 2	13, 0	0.71	2, 2	2, 1	0.96	9, 2	11, 0	0.90
9, 2	7, 1	0.73	6, 1	8, 2	0.70	5, 3	3, 1	0.96	6, 1	8, 1	0.90
3, 2	4, 3	0.74	16, 1	8, 1	0.70	16, 1	4, 2	0.96	9, 1	9, 2	0.90
7, 2	7, 0	0.75	3, 2	1, 0	0.74	9, 2	6, 2	0.96	8, 3	9, 1	0.90
16, 1	8, 1	0.75	7, 2	7, 0	0.73	7, 2	15, 0	0.96	4, 3	13, 1	0.90
8, 2	9, 3	0.75	6, 4	5, 3	0.73	12, 0	12, 3	0.96	5, 4	9, 0	0.90
7, 3	10, 4	0.75				2, 1	1, 1	0.96	3, 3	5, 3	0.90
6, 4	15, 0	0.75				6, 2	6, 4	0.96	12, 1	9, 3	0.90

(C,M)	n,m	r	(C,M)	n,m	r	(C,M)	n,m	r	(C,M)	n,m	r
	1, 0	1.00		1, 0	1.00		1, 0	1.00		1, 0	1.00
	1, 1	0.95		1, 1	0.95		1, 1	1.00		1, 1	1.00
	2, 1	0.92		2, 1	0.70		2, 1	1.00		2, 1	0.99
	2, 2	0.91		2, 2	0.70		2, 2	1.00		2, 2	0.99
	3, 3	0.76		3, 3	0.79		3, 3	0.98		3, 3	0.94
	4, 4	0.79		4, 4	0.79		4, 4	0.98		4, 4	0.95
	5, 5	0.79		5, 5	0.78		5, 5	0.98		5, 5	0.95
	6, 6	0.80		6, 6	0.80		6, 6	0.97		6, 6	0.94
	7, 7	0.78		7, 7	0.77		7, 7	0.96		7, 7	0.92
	8, 8	0.76		8, 8	0.75		8, 8	0.96		8, 8	0.91
	9, 9	0.75		9, 9	0.74		9, 9	0.96		9, 9	0.90
	10, 10	0.75		10, 10	0.73		10, 10	0.96		10, 10	0.90
	11, 11	0.74		11, 11	0.73		11, 11	0.95		11, 11	0.90
	12, 12	0.74		12, 12	0.72		12, 12	0.95		12, 12	0.90
	13, 13	0.74		13, 13	0.72		13, 13	0.95		13, 13	0.89
	14, 14	0.74		14, 14	0.72		14, 14	0.95		14, 14	0.89
	15, 15	0.73		15, 15	0.71		15, 15	0.95		15, 15	0.89
	16, 16	0.73		16, 16	0.71		16, 16	0.95		16, 16	0.89
	17, 17	0.73		17, 17	0.71		17, 17	0.95		17, 17	0.89
	18, 18	0.73		18, 18	0.71		18, 18	0.95		18, 18	0.89

Table 11.

Correlation coefficients between the reproduced seasonal M and C fields from their: a) leading harmonics, b) harmonics ranked in ascending order of wavenumbers n,m. SLP

a	WINTER			SPRING			SUMMER			FALL		
	C	n,m	r	C	n,m	r	C	n,m	r	C	n,m	r
	1, 0	4, 0	0.00	1, 0	2, 0	0.00	2, 0	2, 1	0.00	1, 0	2, 0	0.00
	2, 0	1, 0	0.61	3, 0	3, 0	0.00	3, 0	7, 0	0.01	2, 0	1, 0	-0.09
	4, 0	2, 0	0.56	2, 0	7, 0	-0.33	1, 0	6, 0	0.01	3, 0	7, 0	-0.07
	6, 0	5, 1	0.53	4, 0	5, 0	-0.28	6, 0	2, 0	-0.11	4, 0	8, 0	-0.05
	3, 0	8, 0	0.47	6, 0	8, 1	-0.26	4, 0	5, 1	-0.10	6, 0	3, 0	0.10
	7, 0	3, 2	0.44	7, 0	6, 0	-0.08	1, 1	5, 0	-0.08	8, 0	5, 0	0.16
	4, 2	2, 1	0.42	8, 0	5, 1	-0.03	2, 1	3, 2	0.03	8, 1	8, 1	0.18
	2, 1	4, 1	0.44	8, 1	1, 1	0.01	4, 1	1, 0	0.08	4, 1	6, 0	0.24
	5, 2	4, 2	0.46	4, 1	10, 1	0.01	7, 0	8, 1	0.02	7, 0	5, 1	0.27
	6, 1	4, 2	0.48	5, 2	11, 1	0.01	3, 2	8, 0	0.02	5, 2	4, 0	0.34
	3, 1	5, 4	0.50	1, 1	9, 1	0.02	5, 0	4, 2	0.05	5, 4	5, 4	0.35
	8, 1	2, 0	0.53	5, 4	2, 1	0.02	8, 1	9, 1	0.08	6, 1	3, 1	0.35
	3, 2	7, 2	0.54	6, 1	3, 1	0.02	2, 2	1, 1	0.14	1, 1	10, 1	0.34
	5, 4	3, 3	0.57	6, 1	16, 0	0.02	2, 2	11, 1	0.14	5, 0	7, 2	0.35
	3, 2	4, 4	0.58	9, 0	12, 1	0.02	5, 2	10, 1	0.13	2, 1	5, 2	0.36
	6, 1	7, 1	0.58	9, 2	14, 0	0.02	4, 2	7, 1	0.15	9, 2	4, 4	0.36
	9, 0	6, 3	0.58	4, 3	4, 0	0.06	4, 3	4, 0	0.11	4, 4	9, 1	0.36
	4, 1	7, 0	0.59	4, 3	7, 2	0.06	5, 1	12, 1	0.12	6, 3	3, 3	0.36
	6, 2	8, 1	0.60	3, 1	5, 4	0.08	3, 1	14, 0	0.12	16, 1	11, 1	0.35
	5, 3	8, 4	0.61	2, 1	13, 1	0.09	5, 4	2, 2	0.13	4, 2	12, 1	0.35
	7, 1	9, 0	0.62	7, 1	6, 2	0.10	9, 1	5, 4	0.15	5, 1	6, 1	0.36
	3, 3	9, 4	0.62	16, 1	6, 1	0.10	6, 3	16, 0	0.15	6, 5	7, 1	0.36
	5, 3	9, 0	0.62	7, 4	3, 2	0.10	10, 1	3, 0	0.20	7, 1	16, 0	0.35
	7, 1	7, 5	0.63	9, 1	10, 0	0.11	6, 2	13, 1	0.20	7, 3	6, 3	0.35
	12, 1	1, 1	0.62	8, 2	9, 0	0.12	9, 2	7, 2	0.20	3, 3	16, 1	0.36
b	(C,M)	n,m	r	(C,M)	n,m	r	(C,M)	n,m	r	(C,M)	n,m	r
		1, 0	1.00		1, 0	1.0		1, 0	-1.00		1, 0	1.00
		1, 1	0.97		1, 1	0.15		1, 1	-0.41		1, 1	0.98
		2, 0	0.41		2, 0	-0.47		2, 0	-0.73		2, 0	-0.09
		2, 1	0.44		2, 1	-0.43		2, 1	-0.54		2, 1	-0.09
		2, 2	0.46		2, 2	-0.42		2, 2	-0.29		2, 2	-0.09
		3, 3	0.53		3, 3	-0.23		3, 3	-0.04		3, 3	0.15
		4, 4	0.63		4, 4	-0.11		4, 4	0.06		4, 4	0.24
		5, 5	0.64		5, 5	-0.06		5, 5	0.03		5, 5	0.28
		6, 6	0.62		6, 6	0.06		6, 6	0.14		6, 6	0.33
		7, 7	0.62		7, 7	0.12		7, 7	0.18		7, 7	0.34
		8, 8	0.63		8, 8	0.19		8, 8	0.22		8, 8	0.39
		9, 9	0.63		9, 9	0.20		9, 9	0.23		9, 9	0.39
		10, 10	0.62		10, 10	0.20		10, 10	0.23		10, 10	0.39
		11, 11	0.62		11, 11	0.20		11, 11	0.22		11, 11	0.39
		12, 12	0.62		12, 12	0.20		12, 12	0.22		12, 12	0.39
		13, 13	0.62		13, 13	0.20		13, 13	0.22		13, 13	0.39
		14, 14	0.62		14, 14	0.20		14, 14	0.22		14, 14	0.38
		15, 15	0.62		15, 15	0.20		15, 15	0.22		15, 15	0.38
		16, 16	0.62		16, 16	0.20		16, 16	0.22		16, 16	0.38
		17, 17	0.62		17, 17	0.20		17, 17	0.22		17, 17	0.38
		18, 18	0.62		18, 18	0.20		18, 18	0.22		18, 18	0.38

correlations, shown in Table 11, are universally low, as expected, again indicating that the model fails to reproduce this field adequately.

Summary and Conclusions

Spherical harmonic analysis has been applied to global and Northern Hemispheric monthly mean observed (C) and model-generated (M) climatological fields of 850 mb temperature (T850), 500 mb geopotential height (G500), and sea-level pressure (SLP) for the purpose of evaluating the atmospheric simulations produced by the GISS climate model. All three fields were found to be adequately represented by wave numbers $n, m \leq 8$, and, indeed, by a relatively small group of dominant harmonics for each field. Thus, the method of spherical harmonic analysis does appear to be applicable, at least to the coarse-mesh (8° latitude by 10° longitude) data sets employed.

The C and M fields were first compared by ranking the dominant harmonics of both for each season in order of decreasing amplitude. The 0,0 harmonics, representing the global mean values, were found to be generally similar for the corresponding C and M fields. The model also successfully simulates the dominant 2,0 harmonics of T850 and G500, which represent the mean meridional gradients (i.e., the differences between Poles and Equator), although it does overestimate the amplitude of the temperature gradient as well as the global mean value, apparently due to overheating of the continents in summer. On the other hand, the model simulation of SLP is less satisfactory in terms of the leading harmonics. The 1,0 harmonics, representing the mean pressure difference between the hemispheres, are opposite in phase for C and M summer, indicating an incorrect mass distribution, while the 2,0 harmonics reflect a tendency of the model to build high pressure over the Antarctic and low pressure at the Equator.

Monthly spherical harmonic analyses for both the globe and the Northern Hemisphere were obtained for the M and C fields. Then the annual cycles of the C leading components were compared with the

corresponding M harmonics in terms of amplitude and phase differences. The annual cycles of the global mean values were generally correctly simulated by the model, while for the Northern Hemisphere the hemispheric mean values for T850 were overestimated in summer. Also, the hemispheric means for SLP were low biased for all months. This was reflected in the M annual cycle of the 1,0 harmonic, with a phase shift of 180° from April through August, indicating, as before, an incorrect pressure distribution between the hemispheres. The M 2,0 annual cycles of T850 and G500 were parallel to those of C, while for SLP the same term was incorrectly simulated in phase and amplitude by the model. The M 4,0 annual cycles of T850 and G500 were overestimated in summer, especially for the Northern Hemisphere, due to the overheating of the continents. This becomes more apparent from the annual cycles of the M 2,2, 3,2, 4,2 terms, which represent the continent-ocean temperature differences for T850 (overestimated in summer). The simulated temperature distributions resulted in overestimations (underestimations) in the amplitude of the zonal pressure distributions for summer (winter). This was interpreted as a failure of the model to simulate the four basic pressure systems of the Northern Hemisphere with the correct intensities. The annual cycle of the M meridional pressure distribution, 6,0, was not similar to the climatological one (Figure 12). This indicates the false meridional structure of the predicted SLP field.

An objective comparison of the large-scale features of the two climatologies was obtained by correlating the reproduced seasonal M and C fields from their components. The results taken from this method generally confirm the subjective comparison of the C and M leading harmonics for the same fields. Also, they indicate the fact that G500 and T850 were successfully simulated by the model (especially for the summer), while the SLP was poorly simulated for all seasons.

Acknowledgments

This research was supported by the National Aeronautics and Space Administration (NASA), Goddard Space Flight Center, through Grant No. NGR 33-013-086 to the City College (Prof. Jerome Spar, Principal Investigator), and the work was carried out almost entirely at the Goddard Institute for Space Studies (GISS) in New York. The author gratefully acknowledges the support and assistance of the GISS staff under Dr. Robert Jastrow, Director, and Dr. James Hansen, head of the climate research group, and their permission to use the GISS climate model and computer system for this investigation. A special thanks and acknowledgment is extended to the author's research advisor, Dr. Jerome Spar, for his help and suggestions on style and his continuous guidance, encouragement, and understanding, which made this study possible and enjoyable. Also, special acknowledgments are due to J. Notario for his help and suggestions on programming and to R. Klugman, who prepared the data and aided in all phases of this study.

APPENDIX A.

Normalization of the spherical harmonic functions

If $P_{n,m}(\sin\phi)$ are the unnormalized Legendre associated functions, and

$$\bar{P}_{n,m}(\sin\phi) = (\cos\phi)^m \frac{d^m P_n(\sin\phi)}{d(\sin\phi)^m},$$

where $P_n(\sin\phi)$ are the Legendre polynomials defined as

$$P_n(\sin\phi) = \frac{1}{2^n n!} \frac{d^n (\cos\phi)^{2n}}{d(\sin\phi)^n},$$

then the mean square value of the spherical harmonic function

$$\left[P_{n,m}(\sin\phi) \begin{Bmatrix} \cos m\lambda \\ \sin m\lambda \end{Bmatrix} \right]$$

over the surface of a sphere of radius α is,

$$\begin{aligned} \overline{\left[P_{n,m}(\sin\phi) \begin{Bmatrix} \cos m\lambda \\ \sin m\lambda \end{Bmatrix} \right]^2} &= \frac{1}{4\pi\alpha^2} \int_0^{2\pi} \int_{-\pi/2}^{\pi/2} \left[P_{n,m} \begin{Bmatrix} \cos m\lambda \\ \sin m\lambda \end{Bmatrix} \right]^2 \cdot d(\alpha\sin\phi) \cdot d(\alpha\lambda) = \\ &= \frac{1}{4\pi} \int_0^{2\pi} \left[\begin{Bmatrix} \cos m\lambda \\ \sin m\lambda \end{Bmatrix} \right]^2 d\lambda \cdot \int_{-\pi/2}^{\pi/2} \left[P_{n,m}(\sin\phi) \right]^2 \cdot \cos\phi \cdot d\phi = \left[\frac{\delta_m}{2(2n+1)} \cdot \frac{(n+m)!}{(n-m)!} \right] \end{aligned}$$

because

$$\left\{ \begin{aligned} \int_{-1}^1 \left[P_{n,m}(x) \right]^2 \cdot dx &= \left[\frac{2}{2n+1} \frac{(n+m)!}{(n-m)!} \right] \\ \int_0^{2\pi} \left[\begin{Bmatrix} \cos my \\ \sin my \end{Bmatrix} \right]^2 \cdot dy &= \pi\delta_m \end{aligned} \right\} \quad \text{where } \delta_m = \begin{cases} 1 & \text{if } m \neq 0 \\ 2 & \text{if } m = 0 \end{cases}$$

Thus the complete normalizing factor for this function, in order for it's mean square value over a sphere to be unity, is

$$\left[\frac{2(2n+1)}{\delta_m} \frac{(n-m)!}{(n+m)!} \right]^{\frac{1}{2}}$$

To normalize the sperical harmonic function to $(4\pi)^{-1}$, we use the following set of harmonic functions:

$$\begin{cases} Y_{n,m}^{(\ominus)} \\ Y_{n,m}^{(\odot)} \end{cases} = \left[\frac{(2n+1)}{2\pi} \frac{(n-m)!}{(n+m)!} \right]^{\frac{1}{2}} \cdot \begin{cases} \cos m\lambda \\ \sin m\lambda \end{cases} \cdot P_{n,m}(\sin\phi) \quad , \quad n \geq m > 0$$

$$Y_n = \left[\frac{2n+1}{4\pi} \right]^{\frac{1}{2}} \cdot P_n(\sin\phi) \quad m = 0$$

APPENDIX B

Evaluation of the expansion coefficients.

The observed field, $Q(\phi, \lambda)$, is represented by the series,

$$\widehat{Q}(\phi, \lambda) = \sum_{n,m} \sum (C_{n,m} \cdot Y_{n,m}^{(e)} + S_{n,m} \cdot Y_{n,m}^{(o)})$$

Multiplying both sides by $Y_{i,j}^{(k)}$ and integrating over the domain of $Q(\phi, \lambda)$, (i.e. the domain of the observations of $Q(\phi, \lambda)$ as gridded), we get,

$$\int_{\mathbf{s}} Q(\phi, \lambda) \cdot Y_{i,j}^{(k)} \cdot d\Omega = \sum_{n,m} \sum \int_{\mathbf{s}} (C_{n,m} \cdot Y_{n,m}^{(e)} \cdot Y_{i,j}^{(k)} + S_{n,m} \cdot Y_{n,m}^{(o)} \cdot Y_{i,j}^{(k)}) \cdot d\Omega$$

where $d\Omega = \cos\phi d\phi d\lambda$ and $\pi/2 \leq \phi \leq \pi/2$, $0 \leq \lambda \leq 2\pi$ and \mathbf{s} is a spherical surface. If the superscript (k) indicates evenness of the $Y_{n,m}$, it follows that

$$\int_{\mathbf{s}} Q(\phi, \lambda) \cdot Y_{i,j}^{(e)} \cdot d\Omega = \sum_{n,m} \sum C_{n,m} \cdot \int_{\mathbf{s}} Y_{n,m}^{(e)} \cdot Y_{i,j}^{(e)} \cdot d\Omega + 0.$$

Expanding the summations and taking into account the orthonormality property of the spherical harmonic functions,

$$\int_{\mathbf{s}} Q(\phi, \lambda) \cdot Y_{i,j}^{(e)} \cdot d\Omega = C_{i,j} \cdot \int_{\mathbf{s}} Y_{i,j}^{(e)} \cdot Y_{i,j}^{(e)} \cdot d\Omega = C_{i,j} \cdot 1 \text{ and}$$

$$C_{i,j} = \int_{\mathbf{s}} Q(\phi, \lambda) \cdot Y_{i,j}^{(e)} \cdot d\Omega$$

An analogous relation is derived for $S_{i,j}$ if we let (k) denote oddness of the $Y_{n,m}$.
 Finally,

$$\begin{Bmatrix} C_{n,m} \\ S_{n,m} \end{Bmatrix} = \int_0^{2\pi} \int_{-\pi/2}^{\pi/2} Q(\phi, \lambda) \cdot \begin{Bmatrix} Y_{n,m}^{(e)} \\ Y_{n,m}^{(o)} \end{Bmatrix} \cdot \cos\phi \, d\phi \, d\lambda$$

If $Q(\phi, \lambda) = Q(-\phi, \lambda)$, which states that Q is an even function of latitude ϕ , then

$$\begin{Bmatrix} C_{n,m} \\ S_{n,m} \end{Bmatrix} = N \cdot \int_0^{2\pi} \begin{Bmatrix} \cos m\lambda \\ \sin m\lambda \end{Bmatrix} d\lambda \cdot \int_{-\pi/2}^{\pi/2} Q(\phi, \lambda) \cdot P_{n,m}(\sin\phi) \, d\phi$$

where N is the normalization factor. The second integral above has symmetrical limits, for $(n-m) = \text{odd}$, the function $P_{n,m}(\sin\phi)$ is odd, $\cos\phi$ is even and therefore the quantity $Q(\phi, \lambda) \cdot P_{n,m}(\sin\phi) \cdot \cos\phi$ is an odd function of latitude ϕ , and

$$\begin{Bmatrix} C_{n,m} \\ S_{n,m} \end{Bmatrix} = 0$$

If the data Q are also functions of time (form a time series), then

$$\begin{Bmatrix} C_{n,m}(t) \\ S_{n,m}(t) \end{Bmatrix} = \int_S Q(\phi, \lambda, t) \cdot \begin{Bmatrix} Y_{n,m}^{(e)} \\ Y_{n,m}^{(o)} \end{Bmatrix} \cdot d\Omega$$

When averaged over a time period T , the last equation becomes.

$$\left\{ \begin{array}{c} \overline{C_{n,m}(t)} \\ \overline{S_{n,m}(t)} \end{array} \right\} = \int_{\mathbf{s}} \overline{Q(\phi, \lambda, t)} \cdot \left\{ \begin{array}{c} Y_{n,m}^{(e)} \\ Y_{n,m}^{(o)} \end{array} \right\} \cdot d\Omega$$

where $\overline{(\quad)} = \frac{1}{T} \int_{T_i}^{T_j} (\quad) dt$ and $T_j - T_i = T$.

Thus we may either average the fields Q over time, and apply spherical harmonic analysis to Q , or apply the harmonic analysis to each field Q and average the expansion coefficients; $S_{n,m}$, $C_{n,m}$.

References

- Belousov, S. L., 1962: Tables of Normalized Associated Legendre Polynomials (translated by D.E. Brown). New York: Pergamon Press. 379 pp.
- Blackmon, M. L., 1976: A climatological spectral study of the 500 mb geopotential height of the Northern Hemisphere. J. Atmos. Sci., 33, 1607-1623.
- Boyd, J. P., 1978: The choice of spectral functions on a sphere for boundary and eigenvalue problems: a comparison of Chebyshev, Fourier and associate Legendre expansions. Mon. Wea. Rev., 106, 1184-1191.
- Chapman, S. and J. Bartels; 1962: Geomagnetism (Vol. II, corrected edition).. London: Oxford University Press. 1049 pp. (First edition, 1940)
- Christidis, Z. and J. Spar, 1979: Spherical harmonic analysis for verification of a global atmospheric model. (Technical report)
- Critchfield, H. J., 1974: General Climatology. 3rd ed. Englewood Cliffs, N.J.: Prentice-Hall, Inc. 446 pp.
- Davis, P. J. and P. Rabinowitz, 1967: Numerical Integration. Waltham, Mass.: Blaisdell Publishing Co. 230 pp.
- Eliassen, E. and B. Machenhauer, 1965: A study of the fluctuations of the atmospheric planetary flow patterns represented by spherical harmonics. Tellus, 17, 220-228.
- Hansen, J. and Collaborators, 1979: An efficient three-dimensional global model for climate studies. Goddard Institute for Space Studies (GISS). (Unpublished)
- Hobson, E. W., 1955: Theory of Spherical and Ellipsoidal Harmonics. New York: Chelsea Publishing Co. 500 pp.
- Krulov, V. J., 1956: Approximate Calculation of Integrals (translated by A. H. Stroud). New York: Macmillan Co. 360 pp.
- Leith, C. E., 1974: Spectral statistical-dynamic forecast experiment. International Symposium on Spectral Methods of Numerical Weather Prediction, Copenhagen, August 1974. GARP Rep. No. 7.
- Merilees, P. E., 1973: An alternative scheme for the summation of a series of spherical harmonics. J. Appl. Meteor., 12, 224-227.

- North, G. R. and J. A. Coakley, 1979: Differences between seasonal and mean annual energy balance model calculations of climate and climate sensitivity. J. Atmos. Sci., 36, 1189-1204.
- Somerville, R. C. J., P. H. Stone, M. Halem, J. E. Hansen, J. S. Hogan, L. M. Druyan, G. Russell, A. A. Lacis, W. J. Quirk and J. Tenenbaum, 1974: The GISS model of the global atmosphere. J. Atmos. Sci., 31, 84-117.
- Spar, J.; 1950: On the theory of annual pressure variations. J. Meteor., 7, 167-180.
- _____, 1965: Earth, Sea and Air. 2nd ed. Reading, Mass.: Addison-Wesley Publishing Co., Inc. 156 pp.
- _____, 1979: Prediction experiments with a coarse-mesh global model. Climate Diagnostic Workshop, Madison, Wisc. 16-18 October 1979.